

Naval Surface Warfare Center

Carderock Division

West Bethesda, MD 20817-5700

NSWCCD-70-TR-2001/098 June 2001

Signatures Directorate

Research and Development Report

Induced Changes in the Impedance of a Master Oscillator Due to Coupling to a Set of Satellite Oscillators: Linear Analysis

by

G. Maidanik and K. J. Becker

20010720 071



Approved for public release; Distribution is unlimited.

REPORT DOCUMENTATION PAGEForm Approved
OMB No. 0704-0188

Public reporting burden for this collection of information is estimated to average 1 hour per response, including the time for reviewing instructions, searching existing data sources, gathering and maintaining the data needed, and completing and reviewing this collection of information. Send comments regarding this burden estimate or any other aspect of this collection of information, including suggestions for reducing this burden to Department of Defense, Washington Headquarters Services, Directorate for Information Operations and Reports (0704-0188), 1215 Jefferson Davis Highway, Suite 1204, Arlington, VA 22202-4302. Respondents should be aware that notwithstanding any other provision of law, no person shall be subject to any penalty for failing to comply with a collection of information if it does not display a currently valid OMB control number. PLEASE DO NOT RETURN YOUR FORM TO THE ABOVE ADDRESS.

1. REPORT DATE (DD-MM-YYYY)

25-Jun-2001

2. REPORT TYPE

Final

3. DATES COVERED (From - To)

-

4. TITLE AND SUBTITLE

Induced Changes in the Impedance of a Master Oscillator Due to Coupling to a Set of Satellite Oscillators: Linear Analysis

5a. CONTRACT NUMBER**5b. GRANT NUMBER****5c. PROGRAM ELEMENT NUMBER****5d. PROJECT NUMBER****5e. TASK NUMBER****5f. WORK UNIT NUMBER****6. AUTHOR(S)**

G. Maidanik and K. J. Becker

7. PERFORMING ORGANIZATION NAME(S) AND ADDRESS(ES) AND ADDRESS(ES)

Naval Surface Warfare Center
Carderock Division
9500 Macarthur Boulevard
West Bethesda, MD 20817-5700

8. PERFORMING ORGANIZATION REPORT NUMBER

NSWCCD-70-TR-2001/098

9. SPONSORING / MONITORING AGENCY NAME(S) AND ADDRESS(ES)**10. SPONSOR/MONITOR'S ACRONYM(S)****11. SPONSOR/MONITOR'S REPORT NUMBER(S)****12. DISTRIBUTION / AVAILABILITY STATEMENT**

Approved for public release; Distribution is unlimited.

13. SUPPLEMENTARY NOTES**14. ABSTRACT**

The influence of a set of satellite oscillators on the response behavior of a master oscillator, to which the set is coupled, is of fundamental significance to structural acoustics and beyond. The focus is largely on the term that modifies the impedance of the master oscillator due to that coupling. The real and imaginary parts of this term are dubbed the induced reactive factor and the induced loss factor, respectively. For a passive set of satellite oscillators the induced reactive factor may be either positive (mass-like) or negative (stiffness-like) whereas the induced loss factor is invariably positive definite. The behavior of both induced factors as functions of frequency is explored, especially in the range of frequency spanning the resonance frequencies of the satellite oscillators. The resonance frequency of the master oscillator in isolation is placed centrally in this frequency range. The phenomenon of the "suppression of undulations", in the induced reactive factor and in the induced loss factor, as the modal overlap parameter approaches and exceeds unity, is demonstrated. Also demonstrated and defined is the phenomenon of "erosion" in these induced factors, again, as the modal overlap parameter approaches and increases beyond unity.

15. SUBJECT TERMS**16. SECURITY CLASSIFICATION OF:****a. REPORT**

UNCLASSIFIED

b. ABSTRACT

UNCLASSIFIED

c. THIS PAGE

UNCLASSIFIED

17. LIMITATION OF ABSTRACT

SAR

18. NUMBER OF PAGES

0

19a. NAME OF RESPONSIBLE PERSON

G. Maidanik

19b. TELEPHONE NUMBER (include area code)

301-227-1292

Contents

	Page
Abstract.....	2
I. Introduction.....	3
II. Elaborated Coupling Forms	16
III. Resonance Frequency Distribution and Assignment of Individual Loss Factors to the Satellite Oscillators	24
IV. Revisiting the Results Presented in Reference 1	30
V. Various Coupling Forms and Coupling Strengths.....	35
VI. Replacing a Summation by an Integration.....	40
VII. Typical Member of an Ensemble of Complexes Supporting Various Parametric Combinations.....	47
Appendix A.....	53
References.....	56
Figures.....	60

Abstract

The influence of a set of satellite oscillators on the response behavior of a master oscillator, to which the set is coupled, is of fundamental significance to structural acoustics and beyond. The focus is largely on the term that modifies the impedance of the master oscillator due to that coupling. The real and imaginary parts in this term are dubbed the induced *reactive factor* and the induced *loss factor*, respectively. For a passive set of satellite oscillators the induced reactive factor may be either positive (mass-like) or negative (stiffness-like) whereas the induced loss factor is invariably positive definite. The behavior of both induced factors as functions of frequency is explored, especially in the range of frequency spanning the resonance frequencies of the satellite oscillators. The resonance frequency of the master oscillator in isolation is placed centrally in this frequency range. The phenomenon of the "suppression of undulations", in the induced reactive factor and in the induced loss factor, as the modal overlap parameter approaches and exceeds unity, is demonstrated. Also demonstrated and defined is the phenomenon of "erosion" in these induced factors, again, as the modal overlap parameter approaches and increases beyond unity.

I. Introduction

Harmonic oscillators are simple structural elements that are helping to model structural complexes. The models are then analyzed in terms of these coupled harmonic oscillators. The result of the analysis is interpreted to yield information of the sensitivity of the response behavior of the complex to parameters that define it. The sensitivity may then reveal which parameters need to be modified in order to achieve, for example, noise control goals for the complex. The scheme of this analysis is initiated by casting the structural complex in terms of structural components. This division of the structural complex yields a matrix equation of motion in the form

$$\int \underline{\underline{z}}(\underline{x} | \underline{x}', t) d\underline{x}' \underline{v}(\underline{x}', t) = \underline{p}_e(\underline{x}, t); \quad \int \underline{\underline{z}}(\underline{x} | \underline{x}', t) d\underline{x}' = \left(\int z_{\alpha\gamma}(x_\alpha | x'_\gamma, t) dx'_\gamma \right), \quad (\text{I.1})$$

$$z_{\alpha\alpha}(x_\alpha | x'_\alpha, t) = z_\alpha(x_\alpha, t) \delta(x_\alpha - x'_\alpha); \quad \underline{v}(\underline{x}, t) = \{v_\alpha(x_\alpha, t)\};$$

$$\underline{p}_e(\underline{x}, t) = \{p_{e\alpha}(x_\alpha, t)\}; \quad \underline{x} = \{x_\alpha\}; \quad d\underline{x} = (d\alpha_\alpha \delta_{\alpha\gamma}), \quad (\text{I.2})$$

and (t) is the temporal variable. In Eqs. (I.1) and (I.2) the quantity $z_{\alpha\gamma}(x_\alpha | x'_\gamma, t)$ is the element in the impedance matrix operator $\underline{\underline{z}}(\underline{x} | \underline{x}', t)$ that is due to the $(\gamma)th$ structural component influence on the $(\alpha)th$ structural com-

ponent. The diagonal elements are typically defined by the self-impedance operator $z_\alpha(x_\alpha, t)$ and the off-diagonal elements are typically defined by the coupling impedance operator $z_{\alpha\gamma}(x_\alpha | x'_\gamma, t)$ between the $(\gamma)th$ and the $(\alpha)th$ structural components with $\alpha \neq \gamma$; there is no coupling between these structural components if $z_{\alpha\gamma}(x_\alpha | x'_\gamma, t)$ is identically equal to zero. Further in these equations, $v_\alpha(x_\alpha, t)$ and $p_{e\alpha}(x_\alpha, t)$ are, respectively, the response and the external drive for the $(\alpha)th$ structural component and (x_α) is the *vector* that spans the spatial dimensionality of the $(\alpha)th$ structural component. The rank of the matrix equation of motion is equal to (N) , the number of structural components in the complex. Each structural component is selected in a manner that admits its equation of motion to a modal analysis; i.e., the impedance operator $z_\alpha(x_\alpha, t)$ is selected to be an eigenoperator in the spatial domain. [This selection is not necessarily unique; there may be a number of choices for selecting $z_\alpha(x_\alpha, t)$. Of course, each choice may determine a different set for $z_{\alpha\gamma}(x_\alpha | x'_\gamma, t)$ with $\alpha \neq \gamma$.] The modal analysis is characterized by eigenfunctions (mode shapes), typically $\phi_{\alpha j}(x_\alpha)$, and by eigenvalues, typically $z_{\alpha j}(t)$, of the eigenoperator $z_\alpha(x_\alpha, t)$; namely

$$z_\alpha(x_\alpha, t) \phi_{\alpha j}(x_\alpha) = z_{\alpha j}(t) \phi_{\alpha j}(x). \quad (I.3)$$

The mode shapes may be collated into a mode shape vector

$$\underline{\phi}(\underline{x}) = \{\underline{\phi}_\alpha(x_\alpha)\}; \quad \underline{\phi}_\alpha(x_\alpha) = \{\phi_{\alpha j}(x_\alpha)\}, \quad (\text{I.4})$$

and the mode shapes are by definition, orthogonal and closed

$$\int dx_\alpha \phi_{\alpha j}(x_\alpha) \phi_{\alpha k}(x_\alpha) = \delta_{jk}; \quad \sum_j^{N_\alpha} \phi_{\alpha j}(x_\alpha) \phi_{\alpha j}(x'_\alpha) = \delta(x_\alpha - x'_\alpha), \quad (\text{I.5})$$

respectively, where (N_α) enumerates the modes in the $(\alpha)th$ structural component. In Eq. (I.3)-(I.5) the subscripts (α) and (j) designate the $(\alpha)th$ structural component and the $(j)th$ mode in that structural component, respectively. The modes are then employed to remove the spatial dependence from the matrix equation of motion for the complex, yielding, in its place, a modal matrix equation of motion in the form

$$\underline{\underline{z}}(t) \underline{v}(t) = \underline{p}_e(t), \quad (\text{I.6})$$

where $\underline{\underline{z}}(t)$ is the modal impedance matrix operator, $\underline{v}(t)$ is the modal response vector and $\underline{p}_e(t)$ is the modal external drive vector. In some details

$$\underline{\underline{z}}(t) = (\underline{\underline{z}}_{\alpha\alpha} \delta_{\alpha\gamma} - \underline{\underline{z}}_{\alpha\gamma}^c (1 - \delta_{\alpha\gamma})); \quad \underline{\underline{z}}_{\alpha\alpha} = (z_{\alpha j} \delta_{jk}); \quad z_{\alpha j} = \sum_{\gamma}^N \sum_q^{N_\gamma} z_{\gamma q \alpha j};$$

$$z_{\alpha j \alpha i} \equiv 0 \text{ for } j \neq i; \quad \underline{\underline{z}}_{\alpha\alpha}^c = (z_{\alpha j \gamma q});$$

$$z_{\alpha j \gamma q} = \int dx_\alpha \phi_{\alpha j}(x_\alpha) z_{\alpha\gamma}(x_\alpha | x'_\gamma, t) dx'_\gamma \phi_{\gamma q}(x'_\gamma), \quad (\text{I.7a})$$

$$\underline{v} = \{v_\alpha\}; \quad v_\alpha = \{v_{\alpha j}\}; \quad v_{\alpha j} = \int dx_\alpha v_\alpha(x_\alpha, t) \phi_{\alpha j}(x_\alpha), \quad (\text{I.7b})$$

$$\underline{p}_e = \{p_{e\alpha}\}; \quad p_{e\alpha} = \{p_{e\alpha j}\}; \quad p_{e\alpha j} = \int dx_\alpha p_{e\alpha}(x_\alpha, t) \phi_{\alpha j}(x_\alpha), \quad (\text{I.7c})$$

where occasionally, the dependence of quantities on the temporal variable is obvious and, as such, is suppressed. The particular division of the structure into components, each of which admits to a modal decomposition, defines the nature of the couplings among the components. Clearly, the orthogonality of the modes in a structural component assures that modes that belong to that component are not coupled to each other; i.e., $\underline{z}_{\alpha\alpha}$, in Eq. (I.7a), is a diagonal matrix operator. Moreover, the modal impedance operator is equivalently that of a harmonic oscillator. The coupling between two structural components is then defined in terms of coupling between a mode of one component to that in another; $\underline{z}_{\alpha\gamma}^c (1 - \delta_{\alpha\gamma})$ accounts for off-diagonal elements only. For example, the off-diagonal element $z_{\alpha j \gamma q}$ pertains to the coupling element between the $(q)th$ mode in the $(\gamma)th$ structural component and the $(j)th$ mode in the $(\alpha)th$ structural component with $\alpha \neq \gamma$. The rank of the modal equation of motion is equal to $\sum_{\alpha}^N N_{\alpha}$ where (N_{α}) is the number of viable modes in the $(\alpha)th$ structural component. Naturally, the rank of Eq. (I.6) usually far exceeds that of Eq. (I.1); that increase in rank is the penalty that is paid for the removal of the spatial dependence from the latter equation. The penalty is partially relieved by

the fact that the modal matrix impedance operator in Eq. (I.6) harbors elements that are much simpler than those usually characterizing the matrix impedance operator in Eq. (I.1). However, the increase in rank is not the only penalty. If spatial information in the response of the structure is significant, to reconstitute this information one requires, in addition to the derivation of $\underline{v}(t)$, the construction of the scalar product

$$v_{\alpha}(x_{\alpha}, t) = \underline{v}_{\alpha}^T(t) \cdot \underline{\phi}_{\alpha}(x_{\alpha}); \quad \underline{v}(\underline{x}, t) = \{v_{\alpha}(x_{\alpha}, t)\}, \quad (\text{I.8})$$

where $\underline{v}(\underline{x}, t)$, $\underline{\phi}_{\alpha}(x_{\alpha})$, $\underline{v}(t)$ and $\underline{v}_{\alpha}(t)$ are defined Eqs. (I.2), (I.4), (I.6) and (I.7b), respectively, and the superscript (T) indicates the transpose of the quantity. The availability and storage of the mode shape vector $\underline{\phi}(\underline{x})$, as stated in Eq. (I.4), is a tall order that can seldom be satisfactorily met. Whether the penalty for circumventing Eq. (I.1) via Eqs. (I.6) and (I.8) is advantageous, is difficult to assess without clear statements of goals and requirements. Often such statements can be made only when the analysis is completed; a catch (22), to be sure. Excluded from these arguments are situations in which the analyzed complex ideally lacks a priori spatial dependence and yet the constituent components can be represented by sets of harmonic oscillators. In this case Eq. (I.6) is the whole shebang.

In this thesis a modest part, in this grand scheme of providing descriptions to the behavior of structural complexes, is pursued. The modal matrix equation of motion is assumed given. The aim is to seek answers to questions such as: How is one to draw relevant information that lies within the modal equation of motion? And how is one to interpret this information in seeking to beneficially modify the parameters that specify the complex that is at the core of this equation of motion? Moreover, the thesis deals with a highly simplified complex composed of a single master oscillator coupled to a set of satellite oscillators. The satellite oscillators in the set are uncoupled to each other. Several papers and theses are found in the open literature with a largely similar aim in sight, employing basically a similar complex [1-11]. What is then new in the present effort? For one, most of these cited papers deal with satellite oscillators that are essentially sprung-masses as depicted in Fig. 1a. The coupling in this case are stiffness control and they are strong. In the present thesis other forms of couplings are also introduced, in particular, mass and gyroscopically controlled couplings [12, 13]. In addition, the coupling strengths are moderated so that the influences of moderate and weak couplings may be defined and analyzed. The modal equation of motion is stated for the complex as depicted in Fig. 1b. Mass,

stiffness and gyroscopic coupling parameters are defined and employed to establish the equation of motion for a complex that harbors such forms of couplings.

Assuming that the complex is stationary in the temporal domain, it is convenient to express the modal matrix equation of motion, hereto defined in the time domain, also in the frequency domain. In the frequency domain Eqs. (I.6) and (I.7) take the forms

$$\underline{\underline{Z}}(\omega) \underline{\underline{V}}(\omega) = \underline{\underline{P}}_e(\omega), \quad (\text{I.9})$$

$$\underline{\underline{Z}}(\omega) = (\underline{\underline{Z}}_{\alpha\alpha}(\omega) \delta_{\alpha\gamma} - \underline{\underline{Z}}_{\alpha\gamma}^c(\omega) (1 - \delta_{\alpha\gamma})); \quad \underline{\underline{Z}}_{\alpha\alpha} = (Z_{\alpha j} \delta_{jk});$$

$$Z_{\alpha j} = \sum_{\gamma}^N \sum_q^{N_\gamma} Z_{\gamma q \alpha j}; \quad \underline{\underline{Z}}^c = (Z_{\alpha j \gamma q}); \quad Z_{\alpha j \alpha i} \equiv 0 \text{ for } j \neq i;$$

$$z_{\alpha j}(t) f(t) = Z_{\alpha j}(\omega) f(t); \quad z_{\alpha j \gamma q}(t) f(t) = Z_{\alpha j \gamma q}(\omega) f(t), \quad (\text{I.10a})$$

$$\underline{\underline{V}} = \{\underline{\underline{V}}_\alpha\}; \quad \underline{\underline{V}}_\alpha = \{V_{\alpha j}\}; \quad V_{\alpha j}(\omega) = \int dt v_{\alpha j}(t) f(t), \quad (\text{I.10b})$$

$$\underline{\underline{P}}_e = \{\underline{\underline{P}}_{e\alpha}\}; \quad \underline{\underline{P}}_{e\alpha} = \{P_{e\alpha j}\}; \quad P_{e\alpha j}(\omega) = \int dt p_{e\alpha j}(t) f(t) \quad (\text{I.10c})$$

where the Fourier function $f(t)$ is defined

$$f(t) = (2\pi)^{-(1/2)} \exp(-i\omega t), \quad (\text{I.11})$$

and, again, occasionally the dependence of quantities on the frequency variable is obvious and, as such, is suppressed. The choice of the frequency domain versus the temporal domain is, with caution, largely a matter of convenience and

preference; again with caution, the two domains are merely related by a Fourier transformation [14]. One recalls that the modal matrix equation of motion is defined in terms of a matrix impedance operator that describes the behavior of a complex composed of coupled harmonic oscillators. In the model of the complex here considered, a master oscillator is coupled to a set of satellite oscillators; the satellite oscillators are not coupled to one another. [cf. Fig 1b.]

The modification in the matrix element that describes the impedance operator of the master oscillator, induced by the coupling to the set of satellite oscillators, is of particular interest. This modification is characterized by a reactive part $S(y)$ and by a real part $\eta_s(y)$, where (y) is the normalized frequency variable; $y = (\omega/\omega_o)$, with (ω_o) the resonance frequency of the master oscillator in isolation. A positive value for the induced reactive factor $S(y)$ contributes a mass control term, a negative value contributes a stiffness control term. For the passive complex here analyzed, the induced loss factor $\eta_s(y)$ is positive definite.

The natures of $S(y)$ and of $\eta_s(y)$ and their modifications to variations in the parameters that specify the complex are recorded and interpreted. Some of these variations are locally imposed by pseudo-statistical means e.g., the resonance

frequency and the modal overlap parameters that are assigned to each individual satellite oscillator are picked pseudo-statistically, either separately or in unison.

A companion report that deals only with the induced loss factor $\eta_s(y)$ has been recently issued; in that report the induced reactive factor $S(y)$ is not investigated [15]. Indeed, the present report is largely issued in order to rectify this omission. In the present report it is noted that the induced reactive factor $S(y)$ may be of significance only when the coupling strengths are strong. In these cases at the edges of the frequency range spanned by the resonance frequency distribution of the satellite oscillators, the absolute value of the induced reactive factor $S(y)$ may approach and exceed unity. On the other hand, even at the edges of this frequency range, for moderate coupling strengths the values of $|S(y)|$ are insignificant and for weak coupling strengths the values of $|S(y)|$ are negligible compared with unity.

A loss factor is basically an energetic quantity, and, therefore, one may inquire whether the induced loss factor $\eta_s(y)$, as just determined via the linear impedance analysis (LIA) may be estimated via an energy analysis (EA). In this vein in another companion report, the analysis of the complex performed herein and in Reference 15 is repeated [16]. In Reference 16, however, instead of using

a linear impedance analysis: e.g., as stated in Eq. (I.9), an alternative approach is used. In this approach the stored energy $E_o(y)$ in the master oscillator, the stored energy $E_r(y)$ in the $(r)th$ satellite oscillator and the stored energy $E_{cr}(y)$ in the coupling of this satellite oscillator to the master oscillator are estimated in terms of the sum of the kinetic and potential stored energies in each category. Distinguishing between the kinetic and potential stored energies renders it possible to determine the Lagrangians for the complex. Applying the Lagrangian equations, the linear equation of motion are yielded [12, 16]. This procedure provides a check that the equation of motion in the linear impedance analysis (LIA) are compatible with the equation of motion in the energy analysis (EA). This check is successfully performed [12, 16]. In terms of the stored energies, $E_o(y)$, $E_r(y)$ and $E_{cr}(y)$, the dissipated power $\Pi_o(y)$ in the master oscillator, the dissipated power $\Pi_r(y)$ in the $(r)th$ satellite oscillator and the dissipated power $\Pi_{cr}(y)$ in the coupling between these two oscillators are estimated, respectively, using the loss factors η_o , η_r and η_{cr} that are assigned to the master oscillator, to the $(r)th$ satellite oscillator and to the coupling between them, respectively. Also estimated is the external input power $\Pi_e(y)$ into the master oscillator by an external drive. Under the prevailing assumptions that only the

master oscillator is driven, $\Pi_e(y)$ is the total power input into the complex from an external drive. Invoking the conservation of energy (or the balance of power) one may equate

$$\begin{aligned}\Pi_e(y) &= \Pi_o(y) + \Pi_{os}(y); \quad \Pi_{or}(y) = \Pi_r(y) + \Pi_{cr}(y); \\ \Pi_{os}(y) &= \sum_{r=1}^N \Pi_{or}(y),\end{aligned}\tag{I.12a}$$

where (N) is the number of satellite oscillators in the complex. From Eq. (I.12a) the loss factor $\eta_o^e(y)$ of the master oscillator and the induced loss factor $\eta_s^e(y)$ may be estimated; namely

$$(y^2/2)[\Pi_o(y)/\omega E_{oK}(y)] = \eta_o^e(y) \equiv \eta_o,\tag{I.12b}$$

$$(y^2/2)[\Pi_{os}(y)/\omega E_{oK}(y)] = \eta_s^e(y),\tag{I.12c}$$

where $E_{oK}(y)$ is the kinetic energy stored in the master oscillator, as a function of (y) . The superscript (e) is introduced to distinguish between the loss factor η_o of the master oscillator and the induced loss factor $\eta_s(y)$, as assigned and determined for the master oscillator, respectively, via the linear impedance analysis (LIA), and the loss factor $\eta_o^e(y)$ and the induced loss factor $\eta_s^e(y)$, as determined via the energy analysis (EA), respectively. The equality of the loss factors η_o and $\eta_o^e(y)$ is obvious and is stated as such in Eq. (I.12b). On the other hand, the comparison between the two induced loss factors; $\eta_s(y)$ and

$\eta_s^e(y)$, is computationally performed and it is found that, by and large, they are identical [16].

Finally, and in addition, in Reference 16 the relationship of (EA) to the statistical energy analysis (SEA) is established. In particular, it is found that (SEA) may underestimate the ratio $\Xi_o^s(y)$ of the energy $E_{os}(y)$ stored in the satellite oscillators and in the couplings to the energy $E_o(y)$ stored in the master oscillator; namely

$$\begin{aligned} \Xi_o^s(y) &= [E_{os}(y)/E_o(y)]; & E_{os}(y) &= \sum_{r=1}^N E_{or}(y); \\ E_{or}(y) &= E_r(y) + E_{cr}(y); & E_o(y) &= E_{oK}(y) + E_{oP}(y), \end{aligned} \quad (\text{I.13a})$$

where (N) , again, is the number of satellite oscillators and $E_{oP}(y)$ is the potential energy stored in the master oscillator, as functions of (y) . [cf. Eq. (I. 12).]

The ratio $\Xi_o^s(y)$ is a measure of the global coupling strength in the milieu of (SEA); it is related to the modal coupling strength $\zeta_o^s(y)$ in the form

$$\Xi_o^s(y) = [n_o(y)/n_s(y)] \zeta_o^s(y), \quad (\text{I.13b})$$

where $n_o(y)$ and $n_s(y)$ are the modal densities in the master oscillator and in the set of satellite oscillators, respectively. (A modal density is the average number of modes per unit frequency [12].) A tenet in (SEA) is that the modal coupling strength $\zeta_o^s(y)$ can never exceed unity. It transpires, nonetheless, that for the stronger coupling strengths, the modal coupling strength $\zeta_o^s(y)$ estimated via (EA) may exceed unity when the typical modal overlap parameter (b), assigned

to the satellite oscillators, falls below a threshold value. Thus a discrepancy between the modal coupling strengths, as estimated via (EA) and via (SEA), may ominously emerge. However, for modal overlap parameters that exceed the threshold value, the validation of (SEA) is not challenged by (EA) [16].

II. Elaborated Coupling Forms

In a companion paper, designated as Reference 1, the complex is specified in terms of the impedance $Z_o^o(\omega)$ of the isolated master oscillator, the impedance $(i\omega m_r)$ of the (r) th isolated satellite "oscillator" and the coupling impedance $(k_r/i\omega)$; the coupling is between the master oscillator and the satellite oscillator. This complex is sketched in Fig.1a [1-11]. In this complex, the satellite oscillators remain uncoupled to each other. The purpose in the present paper is to introduce a significant extension in scope. In this extension the isolated master oscillator remains the same. An isolated satellite oscillator, the (r) th, is specified by the impedance $Z_r(\omega)$ that may consist of both a mass and a stiffness control term. The coupling of this satellite oscillator to the master oscillator is specified by the coupling impedance $Z_{cr}(\omega)$ and a gyroscopic coupling coefficient (G_r) [12,13]. The coupling impedance $Z_{cr}(\omega)$ consists of a mass and a stiffness control term. A complex of this type is sketched in Fig. 1b. The mass and the stiffness control terms in this complex are related in the forms

$$K = K_o(1+i\eta_o); \quad (K_o/M) = \omega_o^2, \quad (1a)$$

$$k_r = k_{or}(1+i\eta_r); \quad (k_{or}/m_r) = \omega_r^2, \quad (1b)$$

$$k_{cr} = k_{ocr}(1+i\eta_{cr}); \quad (k_{ocr}/m_r) = \omega_{cr}^2, \quad (1c)$$

where the pairs $\{M, K\}$, $\{m_r, k_r\}$, and $\{m_r, k_{cr}\}$ are, respectively, in reference to the master oscillator, to the $(r)th$ satellite oscillator and to the coupling between them. The parameters (η_o) , (η_r) , and (η_{cr}) are the corresponding stiffness control loss factors, respectively. To complete the definition of the coupling, the mass (m_{cr}) and the gyroscopic coefficient (G_r) need to be specified [12, 13]. These are specified through the coupling parameters which are defined in the normalized forms

$$\bar{m}_{cr} = (m_{cr}/m_r); \quad \bar{g}_r = [G_r/(\omega_o m_r)], \quad (1d)$$

respectively. With the assistance of Fig. 1b, the linear equations of motion of the master oscillator in situ and of a typical satellite oscillator in situ are derived

$$Z_o^o(\omega)V_o(\omega) + \sum_1^R Z_{cr}(\omega)V_o(\omega) + [Z_{cr}^-(\omega) - G_r]V_r(\omega) = P_e(\omega), \quad (2a)$$

$$[Z_r(\omega) + Z_{cr}(\omega)]V_r(\omega) + [Z_{cr}^-(\omega) + G_r]V_o(\omega) = 0, \quad (2b)$$

respectively, where $V_o(\omega)$ and $V_r(\omega)$ are the responses of the mass (M) of the master oscillator and the mass (m_r) of the $(r)th$ satellite oscillator, respectively,

(R) is the number of satellite oscillators that are coupled to the master oscillator, $P_e(\omega)$ is the drive that is applied externally to the master oscillator; the satellite oscillators are not driven externally, $Z_o^o(\omega)$ is the impedance of the master oscillator in isolation

$$Z_o^o(\omega) = (i\omega M)[1 - (y)^{-2}(1 + i\eta_o)]; \quad y = (\omega / \omega_o), \quad (3a)$$

$Z_r(\omega)$ is the impedance of the $(r)th$ satellite oscillator in isolation

$$Z_r(\omega) = (i\omega m_r)[1 - (z_r)^2(1 + i\eta_r)]; \quad x_r = (\omega_r / \omega_o); \quad z_r = (x_r / y), \quad (3b)$$

$Z_{cr}(\omega)$ is the impedance of the coupling between the master oscillator and the $(r)th$ satellite oscillator

$$Z_{cr}(\omega) = (i\omega m_r)[\bar{m}_{cr} - (z_{cr})^2(1 + i\eta_{cr})];$$

$$\bar{m}_{cr} = (m_{cr} / m_r); \quad x_{cr} = (\omega_{cr} / \omega_o); \quad z_{cr} = (x_{cr} / y), \quad (3c)$$

$Z_{cr}^-(\omega)$ is an impedance that is related to the coupling impedance $Z_{cr}(\omega)$; namely

$$Z_{cr}^-(\omega) = (i\omega m_r)[\bar{m}_{cr} + (z_{cr})^2(1 + i\eta_{cr})], \quad (3d)$$

and (\bar{m}_{cr}) , (x_{cr}) , (η_{cr}) , and (G_r) are defined in Eqs. (1) and (2) [12]. The superscript (o) is reserved to designate quantities that pertain either to the master oscillator in isolation or to satellite oscillators under certain and definitive impositions. Thus, for example, from Eqs. (2a) and (3a), one may state

$$Z_o^o(\omega)V_o^o(\omega) = P_e(\omega), \quad (4)$$

where $V_o^o(\omega)$ is the response of the master oscillator in isolation. By a straightforward algebraic manipulation of Eq. (2) one derives

$$Z_o(\omega)V_o(\omega) = P_e(\omega); \quad V_r(\omega) = B_r(\omega)V_o(\omega), \quad (5)$$

where

$$Z_o(\omega) = Z_o^o(\omega) + \sum_1^R [\{Z_r(\omega)Z_{cr}(\omega)\} + (Q_{cr})^2] [Z_r(\omega) + Z_{cr}(\omega)]^{-1}, \quad (6a)$$

$$B_r(\omega) = [Z_{cr}^-(\omega) + G_r] [Z_r(\omega) + Z_{cr}(\omega)]^{-1}, \quad (6b)$$

$$(Q_{cr})^2 = 4m_{cr}k_{cr} + (G_r)^2, \quad (6c)$$

and the quantities $Z_o^o(\omega)$, $Z_r(\omega)$, $Z_{cr}(\omega)$ and $Z_{cr}^-(\omega)$ are stated explicitly in Eq.

(3). Indeed, from Eqs. (1), (3) and (6) one obtains

$$Z_o(\omega) = Z_o(y) = (i\omega M)[1 - (y)^{-2} \{[1 - S(y)] + i[\eta_o + \eta_s(y)]\}], \quad (7a)$$

$$B_r(\omega) = -[\bar{m}_{cr} + (z_{cr})^2(1 + i\eta_{cr}) - i(\bar{g}_r/y)] \cdot$$

$$[(1 + \bar{m}_{cr}) - (z_{rr})^2(1 + i\eta_{rr})]^{-1}, \quad (7b)$$

where

$$(x_{rr})^2(1 + i\eta_{rr}) = (x_r)^2(1 + i\eta_{cr}) + (x_{cr})^2(1 + i\eta_{cr}), \quad (8a)$$

$$[S(y) - i\eta_s(y)] = (y)^2 \sum_1^R \{ \bar{m}_r \{ [1 - (z_r)^2(1 + i\eta_r)] \cdot$$

$$[\bar{m}_{cr} - (z_{cr})^2(1 + i\eta_{cr})] - (\bar{q}_{cr}/y)^2 \} \cdot$$

$$[(1 + \bar{m}_{cr}) - (z_{rr})^2(1 + i\eta_{rr})]^{-1} \}, \quad (8b)$$

and, again

$$z_{rr} = (x_{rr}/y); \quad z_r = (x_r/y); \quad z_{cr} = (x_{cr}/y);$$

$$(\bar{q}_{cr}/y)^2 = 4\bar{m}_{cr}(z_{cr})^2(1 + i\eta_{cr}) + (\bar{g}_r/y)^2; \quad \bar{q}_{cr} = [Q_{cr}/(\omega_o m_r)]. \quad (8c)$$

One notes that the compound coupling parameter (\bar{q}_{cr}) is a functional of the mass and gyroscopic coupling parameters (\bar{m}_{cr}) and (\bar{g}_r) , respectively. These coupling parameters are defined in Eq. (1d). One also notes, with satisfaction, that the dependence of the terms in the sum on the gyroscopic coupling parameter (\bar{g}_r) is quadratic so that the sign assigned to the gyroscopic coefficient (G_r) plays no role in the influence of the individual satellite oscillators on the impedance of the master oscillator. The gyroscopic coupling is in quadrature to both, the mass and the stiffness control couplings.

Examination of Eqs. (7) and (8) shows that the normalized impedance that the satellite oscillators collectively induce on the master oscillator may be cast in term of the two-vector $\{S(y), \eta_s(y)\}(R)$, which is a function of (R) , as indicated. The evaluation of this two-vector, however, is predicated on explicitly specifying the two-vector $\{x_{rr}, \eta_{rr}\}(R)$, its two supplemental components $\{x_r, \eta_r\}(R)$ and $\{x_{cr}, \eta_{cr}\}(R)$ and finally assigning the compound coupling (\bar{q}_{cr}) . The two-vector $\{x_{rr}, \eta_{rr}\}(R)$ is designed, for the sake of convenience, to

stay fixed with respect to variations in the index (r). In this design, the springs, that are placed on either side of the mass of a satellite oscillator, are set to be similar. With this design, Eq. (8b) is evaluated. In this paper the induced reactive factor $S(y)$ and the induced loss factor $\eta_s(y)$ are considered. These two quantities are examined for a variety of coupling forms and coupling strengths as well as for a number of values of the modal overlap parameters (b_r) and (b_{cr}) associated with the loss factors η_r and η_{cr} , respectively [1]. By and large, (b_r) is set equal to (b_{cr}) and they are equated to (b); $b = b_r = b_{cr}$. The simplifying equalities are imposed without considerable loss in generality. Using Eq. (8b), the exact evaluations of $S(y)$ and of $\eta_s(y)$ are executed for three values of (b); $b = (0.1), (2.0)$ and (10) . In these evaluations one finds that $S(y)$ and $\eta_s(y)$ are functions of (b). On the other hand, the first order approximation of $S(y)$ and of $\eta_s(y)$, designated by $S_I(y)$ and by $\eta_I(y)$, respectively, that are derived from the replacement of the summation in Eq. (8b) by an integration, are found to be independent of (b). The evaluations are graphically displayed; three exact evaluations for the three values of (b) and the corresponding first order approximation of $S(y)$ and $\eta_s(y)$ are superimposed in each of the displays. The curves representing the first order approximations of $S(y)$ and of $\eta_s(y)$, in these

displays, are dubbed (FOA). The comparison between these four evaluations in each display can thus be made at a glance, assisting greatly in the interpretation of the data that is computed and displayed. In the frequency range of concern, when (b) is small compared with unity the values of $S(y)$ and the levels of $\eta_s(y)$ in the exact computations, undulate, as functions of (y) . (The frequency range of concern spans the resonance frequencies of the satellite oscillators.)

The excursions in the undulations increase with decrease in (b) . It transpires that the mean-value averaging of the undulated values of $S(y)$ and levels of $\eta_s(y)$ when (b) is small compared with unity; $b \ll 1$, are, respectively, coincident with curves that are independent of (b) [15-17]. (Values are arithmetically averaged, levels are geometrically averaged.) These curves for $S(y)$ are designated $S_a(y)$ and for $\eta_s(y)$ are designated $\eta_a(y)$. In the frequency range spanned by the resonance frequency distribution of the satellite oscillators - - the frequency range of concern - - $S_a(y)$ is positive; i.e., mass control, for $y < 1$ and is negative; i.e., stiffness control, for $y > 1$. Moreover, in that frequency range of concern, $S_a(y)$ is largely a "straight-line" intersecting the neutral line either at or in the vicinity of $y=1$. On the other hand, in that same frequency range $\eta_a(y)$ is also a "straight-line"; that line, except when a gyroscopic coupling is present, lies

largely horizontal at a given level. As (b) approaches and increases above unity the undulations in the exact values of $S(y)$ and in the exact levels of $\eta_s(y)$ are suppressed and, in the frequency range just defined, the phenomenon of erosion commences and increases with increasing (b) . In the case of the induced reactive factor, erosion is manifested by values that progressively converge from $S_a(y)$ onto the first order approximation to $S(y)$, as (b) increases. The first order approximation to $S(y)$; namely $S_I(y)$, is equal to zero; $S_I(y)=0$ and in general, $S_a(y) \neq S_I(y)$. On the other hand, in the case of the induced loss factor, erosion is manifested by levels that progressively decrease, from the first order approximation of $\eta_s(y)$, as (b) increases [6, 7]. The first order approximation of $\eta_s(y)$; namely $\eta_I(y)$, is coincident with $\eta_a(y)$; $\eta_a(y) = \eta_I(y)$.

III. Resonance Frequency Distribution of and Assignment of Individual

Loss Factors to the Satellite Oscillators

It has been argued that the coupling between two oscillators may cause a shift in the resonance frequency that each has in isolation. Indeed, it was suggested that this shift may be used to determine the “coupling strength” [18, 19]. One may then question as to what exactly are these shifts and are they significant. The shifts, as such, and the implications that they may harbor are not addressed in the present paper; here these shifts are overridden by design. The design intends to derive a suitable resonance frequency distribution and a proper assignment of individual loss factors to the satellite oscillators. The design is expressed, then, in terms of the two-vector $\{x_{rr}, \eta_{rr}\}(R)$, where (x_{rr}) is the normalized resonance frequency and (η_{rr}) is the loss factor associated with the $(r)th$ satellite oscillator. Examination of Eqs. (7) and (8) shows that the normalized resonance frequencies of the satellite oscillators, in situ, are ascertained by satisfying the equality

$$(1 + \bar{m}_{cr})(y)^2 = (x_{rr})^2; \quad (1 + \bar{m}_{cr}) = (z_{rr})^2; \quad (x_{rr})^2 = (x_r)^2 + (x_{cr})^2. \quad (9a)$$

As in Reference 1, here too (x_{rr}) is assigned a priori with equal numbers of

resonance frequencies on either side of the resonance frequency (ω_o) of the master oscillator and the distribution is aligned in ascending order; namely

$$x_{rr} \leq x_{qq} ; \quad q = (r + 1) ; \quad 1 \leq r \leq (R - 1). \quad (9b)$$

A scheme that simultaneously satisfies Eqs. (9a) and (9b) and the mid-point just imposed, demands a supplemental condition of design between the two spring stiffnesses that support the mass of a satellite oscillator. [cf. Fig 1b.] This condition of design requires that

$$(x_{rr})^2 = (1 + \bar{m}_{cr}) \quad \text{for} \quad \bar{r} = (1/2), \quad (9c)$$

where, in Eq. (9c), (\bar{r}) may be allowed a continuous connotation [15, 16]. Consulting Reference 1 and using Eq. (9a), one may express the loss factors that are associated with the (r)th satellite oscillator in the forms

$$\begin{aligned} \eta_r &= [b_r / 2(x_r)^2] \partial(x_r)^2 / \partial r ; & \eta_{cr} &= [b_{cr} / 2(x_{cr})^2] [\partial(x_{cr})^2 / \partial r] ; \\ \eta_{rr} &= [(x_{rr})^2]^{-1} \{ (x_r)^2 \eta_r + (x_{cr})^2 \eta_{cr} \}, \end{aligned} \quad (10)$$

where (b_r) and (b_{cr}) are the modal overlap parameters assigned to the back spring and the fore spring. These two springs support the mass (m_r).

[cf. Fig. 1b.] For the sake of simplicity and computational advantage, the stiffness on either side of the mass of a satellite oscillator are assumed to be "similar" in the sense

$$(x_r) = (\alpha_r)^{1/2} (x_r^o); \quad (x_{cr}) = (\alpha_{cr})^{1/2} (x_r^o); \quad (x_{rr}) = (\alpha_r + \alpha_{cr})^{1/2} (x_r^o), \quad (11)$$

where (α_r) and (α_{cr}) are dubbed the spring factors. In keeping with the definitions of (\bar{m}_{cr}) and (\bar{g}_r) , as the mass coupling parameter and the gyroscopic coupling parameter, the spring factor (α_{cr}) may be designated the stiffness coupling parameter. It is conducive to specify (x_r^o) in a form that is compatible with one of the forms introduced in Reference 1; namely

$$x_r^o = [1 + \{1 - 2\bar{r}\} \gamma(\bar{R})]^{-1/2}, \quad (12)$$

where

$$\bar{r} = r(R+1)^{-1}; \quad \bar{R} = R(R+1)^{-1}; \quad \gamma(\bar{R}) = [\gamma/(2\bar{R})]; \quad \gamma < 1, \quad (13)$$

and (r) may be discrete; $1 \leq r \leq R$, or continuous $(\varepsilon) < r < (R + \varepsilon)$ with $\varepsilon < 1$.

It should be appreciated, however, that although in this report Eq. (12) is cast in stone, other forms for (x_r^o) may be readily introduced and similarly manipulated.

Also and similarly, as introduced in Reference 1, the normalized mass (\bar{m}_r) of the $(r)th$ satellite oscillator is assumed to be independent of (r) and to be of the form

$$\bar{m}_r = (m_r / M) = (M_s / M)(R)^{-1}; \quad M_s = \sum_{1}^R (m_r). \quad (14)$$

With the intended exceptions of the last section in this report it is convenient, without a great loss in generality, to assume that the spring factors (α_r) and

(α_{cr}) , the coupling parameters (\bar{g}_r) and (\bar{m}_{cr}) and the modal overlap parameters (b_r) and (b_{cr}) are to be independent of (r) ; namely

$$\alpha_r = \alpha; \quad \alpha_{cr} = \alpha_c; \quad \bar{g}_r = \bar{g}; \quad \bar{m}_{cr} = \bar{m}_c; \quad b_r = b_{cr} = b, \quad (15)$$

and it is observed, as already intimated, that the modal overlap parameters (b_r) and (b_{cr}) are set equal to (b) . [cf. Appendix A.] From Eqs. (9c), (10), (11) and (12), one then finds

$$(\alpha + \alpha_c) = (1 + \bar{m}_c), \quad (9d)$$

$$\eta_r = \eta_{cr} = \eta_{rr} = \eta(\bar{r}); \quad \eta(\bar{r}) = (\bar{b} / \pi) [\gamma(\bar{R})(x_r^o)^2], \quad (16)$$

where

$$\bar{b} = [(\pi b) (R+1)^{-1}]. \quad (17)$$

Under this imposition, the two-vector $\{(x_{rr}), (\eta_{rr})\} (R)$ assumes the simple form

$$\{(x_{rr}), (\eta_{rr})\} (R) = \{(1 + \bar{m}_c)^{1/2} (x_r^o), \eta(\bar{r})\}, \quad (18a)$$

and, if further, the mass coupling parameter (\bar{m}_c) is negligible; $(\bar{m}_c) \ll 1$, then

$$\{(x_{rr}^o), (\eta_{rr}^o)\} (R) = \{(x_r^o), \eta(\bar{r})\}, \quad (18b)$$

where the superscript (o) in (x_{rr}) and (η_{rr}) recognizes that (x_{rr}^o) and (η_{rr}^o) are restricted to specific impositions. [cf. Eq. (4).] With $R = 27$ and $\bar{m}_c = 0$, Eq.

(18) is evaluated and depicted in Fig. 2a, as a function of (\bar{r}) ; Fig. 2a.1 depicts

(x_{rr}) and Fig. 2a.2 depicts (η_{rr}) . In Fig. 2a the modal overlap parameter (b) is

increased from (0.1) to (2.0) and then onto (10). To these changes (η_{rr}) increases by a factor of (20) and then by a factor of (10^2), whereas, to these changes in (b), (x_{rr}) remains intact. With $R = 7$ and $\bar{m}_c = 0$, Eq. (18) is evaluated and depicted, in the format of Fig. 2a, in Fig. 2b. On the other hand, with $R = 27$, but with $\bar{m}_c = 0.75$, where, for example, in addition $\alpha = 1.75$, $\alpha_c = \bar{g}_c = 0$, Eq. (18) is evaluated and depicted, in the format of Fig. 2a, in Fig. 2c. It is noted that for a continuous r , except for obvious end conditions, Figs. 2a.1 and 2b.1 are identical. However, Figs. 2a.2 and 2b.2 are not identical. On the other hand, it is noted that Figs. 2a.2 and 2c.2 are identical, however, Figs. 2a.1 and 2c.1 are not identical. The commonalties and disparities among Figs. 2a, 2b and 2c, are as expected. [It is also noted, in passing, that (x_{rr}) and (η_{rr}), stated in Eq. (18) are independent of the gyroscopic coupling parameter (\bar{g}_r).]

It remains then to use the two-vector stated in Eq. (18) to evaluate the induced reactive factor $S(y)$ and the induced loss factor $\eta_s(y)$. Indeed, using Eq. (18) in Eq. (8b), one derives the more explicit expression for $S(y)$ and for $\eta_s(y)$ in the form

$$\begin{aligned}
[S(y) - i\eta_s(y)] &= (y)^2 \sum_1^R \bar{m}_r \{ [1 - \alpha(z_r^o)^2 \{1 + i\eta(\bar{r})\}] [\bar{m}_c - \alpha_c(z_r^o)^2 \{1 + i\eta(\bar{r})\}] \\
&\quad - 4\bar{m}_c \alpha_c (z_r^o)^2 \{1 + i\eta(\bar{r})\} - (\bar{g}/y)^2 \} \cdot [(1 + \bar{m}_c) - (\alpha + \alpha_c)(z_r^o)^2 \{1 + i\eta(\bar{r})\}]^{-1}; \\
z_r^o &= (x_r^o / y), \tag{8d}
\end{aligned}$$

where (\bar{m}_c) , (\bar{g}) , (y) , (α) , (α_c) , (x_r^o) , (\bar{m}_r) and $\eta(\bar{r})$ are stated in Eqs. (1d), (3a), (11), (12), (14) and (16), respectively. The computations of $S(y)$ and of $\eta_s(y)$ are largely carried out assigning the standard values

$$(M_s / M) = 10^{-1}, \quad b = (0.1) \quad \text{and} \quad R = 27, \tag{19}$$

where (M_s) is stated in Eq. (14), (b) is the modal overlap parameter and (R) is the number of satellite oscillators in the set. When these standard assignments are deviated from, specific mentions are to be rendered, notwithstanding that, at times, the employment of these standard values may be reiterated.

IV. Revisiting the Results Presented in Reference 1

It may be useful, at this stage, to reproduce results that are depicted in Reference 1. To this end, the following impositions are rendered

$$\alpha \Rightarrow 0 ; \alpha_c = 1; \bar{m}_{cr} = 0; \bar{g}_r = 0. \quad (20)$$

These impositions render the complex commensurate with that defined in Reference 1 and sketched in Fig. 1a. [cf. Fig. 1b.] For these impositions, Eqs. (16) and (18b) and Fig. 2a are validated. One finds that Figs. 2a.1 and 2a.2 are akin to Figs. 3a and 7a of Reference 1, respectively. In addition to evaluating the two-vector specified in Eqs. (16) and (18b), the corresponding induced reactive factor $S^o(y)$ and induced loss factor $\eta_s^o(y)$ are evaluated using Eq. (8d) and the assignment stated in Eqs. (19) and (20). Again, the superscript (o) in $S(y)$ and in $\eta_s(y)$ indicates that the evaluations are restricted to specific impositions. These evaluations of $S^o(y)$ and of $\eta_s^o(y)$ are depicted in Fig. 3a. The modal overlap parameter (b) is increased from the value of (0.1) to (2.0) and then onto (10) and $S^o(y)$ and $\eta_s^o(y)$ are evaluated and depicted in Figs. 3b and 3c, respectively. There are no counterparts to Figs. 3a.1, 3b.1 and 3c.1 in Reference 1. However, the identity of Figs. 3a.2 and 3b.2 with Figs. 5a and 6a of Reference

1, respectively, is clear. In particular, the undulations that exist in Fig. 3a.2 and the suppression of these undulations in Fig. 3b.2 correspond to a phenomenon that is discussed in detail in Reference 1. Figure 3c does not have a counterpart in Reference 1. This figure is included in order to bring in another phenomenon; the phenomenon of erosion previously observed with respect to the induced loss factor $\eta_s(y)$ [6, 7]. Again, the phenomenon of erosion besets both, the induced reactive factor $S(y)$ and the induced loss factor $\eta_s(y)$. It transpires that mean-value averaging (arithmetic mean) of the values of $S(y)$ and the mean-value averaging (geometrical mean) of the levels of $\eta_s(y)$, respectively, for modal overlap parameters (b) that are small compared with unity, coincide and are thus independent of (b) [1, 17]. This coincidence is illustrated in Fig. 3d. In this figure $S(y)$ and $\eta_s(y)$ are separately depicted for three small values of the modal overlap parameter (b); $b = (0.01), (0.1)$ and (0.3) . The coincident curves representing the mean-values of $S(y)$ and the mean-levels of $\eta_s(y)$ for all small values of (b); $b \ll (1.0)$, clearly emerge in Fig. 3d. These coincident curves are designated $S_a(y)$ and $\eta_a(y)$, respectively. An erosion is here a phrase to describe deviations of the values of $S(y)$ and of the levels of $\eta_s(y)$ from these mean-values and mean-levels, respectively, when (b) approaches and

increases beyond the value of unity. An erosion is then a dependence of the values of $S(y)$ and of the levels of $\eta_s(y)$ on (b) as this parameter approaches and exceeds unity. To define erosion more precisely, a subsequently derived first order approximations to $S(y)$ and to $\eta_s(y)$ are brought to bear. Again, the validations of the first order approximation to the values and levels, designated $S_I(y)$ and $\eta_I(y)$, respectively, is predicated on small values for the modal overlap parameters (b) ; $b \ll 1$. The curves that depict $S_I(y)$ and $\eta_I(y)$ are dubbed (FOA). It transpires that $S_I(y) = 0$ and $\eta_I(y) = \eta_a(y)$. Again, as the values of (b) increase more and more above unity, erosion in $S(y)$ is manifested by a progressive convergence of $S(y)$ from $S_a(y)$ onto $S_I(y) = 0$. On the other hand, as the values of (b) increase more and more above unity, erosion in $\eta_s(y)$ is manifested by a departure of $\eta_s(y)$ from $\eta_a(y) \equiv \eta_I(y)$ toward lower and lower levels. Erosions are most pronounced at the edges of the frequency range of concern; the higher the values of the modal overlap parameters (b) above unity, the more the inroad from the edges into the center of the frequency range. (Again, the frequency range of reference is that spanning the resonance frequency distribution of the satellite oscillators.) To bring into focus the existence and nature of erosion for $S(y)$ and for $\eta_s(y)$, as just discussed, Figs.

3a, 3b and 3c are overlaid in Fig. 3e. Also, superimposed on Fig. 3e are the curves just dubbed (FOA). The presence of erosion, as just described, is thus revealed in Fig. 3e. This figure shows, however, that neither is erosion in $S(y)$ completed nor is erosion in $\eta_s(y)$ significant in the vicinity of $y = 1$. To largely complete the erosion in $S(y)$ and to cause an erosion in $\eta_s(y)$ at and in the vicinity of $y=1$, the normalized overlap parameter (\bar{b}) ; $\bar{b} = [(\pi b)(R+1)^{-1}]$, needs approach and exceeds unity [1, 6, 7]. This extreme case of erosion is illustrated in Fig. 3f. In this figure the only change, in parameters that specify the complex assigned to Fig. 3e, is the number(R) of satellite oscillators. The number (R) is (7) instead of (27), so that for $b = 10$, (\bar{b}) comfortably exceeds unity in Fig. 3f. After this brief digression, it is time to return to consideration of Reference 1 and beyond.

The limited scope of Reference 1 curtails the modeling and the analysis of the complex there considered, notwithstanding that complexes employed to date are largely subjected to similar limitations [2-11]. A poignant question arises: what is fresh about the complex defined herein as compared with the complex defined in Reference 1? Whereas in Reference 1 a satellite oscillator in isolation is characterized by a mere mass control term, here it is characterized by the

oscillator impedance $Z_r(\omega)$, as stated in Eq. (3b). This oscillator, in addition to the mass control term, may also possess a stiffness control term. Moreover, the coupling impedance $Z_{cr}(\omega)$, as stated in Eq. (3c), may, in addition to the stiffness control term, possess also a mass control term. Finally, the coupling between a satellite oscillator and a master oscillator may be allowed to include a gyroscopic control term [12, 13]. Obviously, the complex sketched in Fig. 1b and formulated in Eqs. (5) – (8) is more versatile than that in Reference 1, as sketched in Fig. 1a. It may be useful, therefore, to investigate a few of the attributes of this versatility even under the similarity conditions imposed in Eq. (11) and the simplifying assumptions proposed in Eqs. (14) and (15).

V. Various Coupling Forms and Coupling Strengths

It is of interest to compute and display the induced reactive factor $S(y)$ and the induced loss factor $\eta_s(y)$, as functions of (y) , for a variety of selected coupling forms and coupling strengths. The coupling forms are defined according to whether the coupling is dominated by either a stiffness coupling, a gyroscopic coupling, a mass coupling or combinations of these coupling types. The coupling strengths of these forms are determined by the values of the coupling parameters; the stiffness coupling parameter (α_c), the gyroscopic coupling parameter (\bar{g}); $\bar{g}_r = \bar{g}$, and the mass coupling parameter (\bar{m}_c). The values of these coupling parameters may be categorized from weaker-coupling, to moderate-coupling onto stronger-coupling in the range of values of 0.03, 0.15 and 0.75, respectively. In this categorization, the coupling of the satellite oscillators to the master oscillator, defined in Reference 1, is of stiffness control coupling form; i.e., $\alpha_c \neq 0$, $\bar{g} = \bar{m}_c = 0$, and of (very) strong coupling strength; namely, $\alpha_c = 1.0$ [$\alpha=0.0$]. Such a coupling form and a coupling strength define satellite oscillators commonly designated sprung-masses [1-11]. The new evaluations in this paper are exhibited in Figs. 4-7. Of significance are not only

the variations in the coupling forms and in the coupling strengths, but, also, the influence that changes in the modal overlap parameters have on the nature of the induced reactive factor $S(y)$ and induced loss factor $\eta_s(y)$. A first set of figures is evaluated with $b = (0.1)$, a second with $b=(2.0)$ and a third with $b=(10)$. A major feature, common to all evaluations, is that the undulations in the first set, for which $b=(0.1)$, is suppressed in the second and in the third, for which $b=(2.0)$ and $b=(10)$, respectively [1]. Figures 4-7 are cast in the format of Fig. 3e; corresponding figures in the three sets are overlaid so that the undulations in the first set and their suppression in the second and third are observed at a glance. Another major feature, common to all evaluations, is that the erosions, discussed briefly in the preceding Section with respect to $S(y)$ and $\eta_s(y)$ and depicted in Figs. 3e and 3f, thread all figures. It is noted that when $(\bar{b}) [=(\pi b)(R+1)^{-1}]$ approaches and exceeds unity, erosions in $S(y)$ are nearly completed and in $\eta_s(y)$ erosions occur even at and in the vicinity of $y=1$. These extreme erosions, however, in addition to the dependence on (\bar{b}) , seem to carry a slight dependence on the coupling forms and strengths. These dependencies, which are more clearly apparent when the coupling is weak; e.g., in Figs. 6b and 7d, are, at this stage, merely noted, notwithstanding that the linear scale, reserved for the

induced reactive factor $S(y)$, hardly exhibits values that belong to moderate and weak coupling strengths. Supplementally, some of the emerging details in Figs. 4-7 may be summarized as follows:

1. The format of Fig. 3e is reproduced in Fig. 4a, except that the stiffness coupling parameter is reduced from $\alpha_c = 1.0$ to $\alpha_c = 0.75$; i.e., from *very strong* to strong stiffness control coupling. This change decreases the values of $S(y)$ and the levels of $\eta_s(y)$ in Fig. 4a as compared with those in Fig. 3e. The decrease is, however, slight. A more drastic decrease in the values of $S(y)$ and in the levels of $\eta_s(y)$ occurs in Fig. 4b as compared with Fig. 3e. In Fig. 4b the stiffness coupling parameter is $\alpha_c = 0.15$, whereas in Fig. 3e $\alpha_c = 1.0$. This decrease in the values of $S(y)$ and in the levels of $\eta_s(y)$ is largely related to the difference in the coupling strengths. In Fig. 4b the coupling strength is moderate. Again, it is noted that on the linear scale, on which the induced reactive factor $S(y)$ is a priori depicted, the values, even for moderate coupling strengths, are well nigh negligible. (There is little logic to expanding the linear scale to gain insight into the behavior of negligible values. The negligibility itself is information enough.)

2. The format of Figs. 4a and 4b is reproduced in Figs. 5a and 5b, respectively, except that the stiffness coupling form is changed to a gyroscopic coupling form; namely, $\alpha_c = \bar{m}_c = 0, \bar{g} \neq 0$. In Fig. 5a the coupling is strong; $\bar{g} = 0.75$, and in Fig. 5b the coupling is moderate; $\bar{g} = 0.15$. The similarity between Figs. 4 and 5 is obvious. Also obvious is the slope in the curves in Fig. 5. This slope is characteristic of the gyroscopic coupling. The gyroscopic coupling enters in the form of (\bar{g}/γ) and not merely in the form of (\bar{g}) . [cf. Eq. (8).]

3. The format of Figs. 4a and 4b is reproduced in Figs. 6a and 6b, respectively, except that the stiffness coupling form is changed to a mass coupling form; namely, $\alpha_c = \bar{g} = 0, \bar{m}_c \neq 0$. In Fig. 6a the coupling is moderate; $\bar{m}_c = 0.15$, and in Fig. 6b the coupling is weak; $\bar{m}_c = 0.03$. The similarity between Figs. 4 and 6 is obvious although the values of $S(\gamma)$ and the levels of $\eta_s(\gamma)$ in the former are higher than in the latter, largely in consequence of the disparities in the coupling strengths.

4. Finally, the format of Fig. 4a is reproduced in Fig. 7, except that the stiffness coupling form is modified to accommodate, in addition, another form of coupling. In Fig. 7a, the additional coupling form is mass control; namely: $\alpha_c = \bar{m}_c = 0.75[\alpha = 0.1], \bar{g} = 0$, which is a very strong coupling strength. In

Figs. 7b, 7c and 7d, the additional coupling is gyroscopic control; namely, in Fig. 7b: $\alpha_c = 0.53$ [$\alpha=0.43.$], $\bar{g}=0.54$, $\bar{m}_c = 0$, which is a strong coupling strength, in Fig. 7c: $\alpha_c = 0.10$ [$\alpha=0.9.$], $\bar{g} = 0.11$, $\bar{m}_c = 0$, which is a moderate coupling strength and finally, in Fig. 7d: $\alpha_c = 0.02$ [$\alpha=0.98.$], $\bar{g} = 0.022$, $\bar{m}_c=0$, which is commensurate with a weak coupling strength. The values of $S(y)$ and the levels of $\eta_s(y)$ in these figures are set largely by the coupling strengths; e.g., the higher the coupling strength the higher are the levels of $\eta_s(y)$.

In the normalized frequency range of concern, the values of $S(y)$ and the levels of $\eta_s(y)$ in Figs. 3-7 that pertain to modal overlap parameters (b) that are small compared with unity; e.g., $b = (0.1)$, undulate. On the other hand, again in the normalized frequency range of concern, the curves in Figs. 3-7 that pertain to modal overlap parameters that exceed unity; e.g., $b=(2.0)$ and (10) , are reasonably smooth. A few questions arise: Can these features be estimated by replacing the summation in Eq. (8d) by an integration and if so, can this integral be performed with ease? Can the result of this performance interpret the response behavior of the master oscillator in terms of the various parameters that define the complex? And last, but by no means least, what about the undulations, do they feature in the result of this integration?

VI. Replacing a Summation by an Integration

The index (r) is given a continuous connotation and the summation in Eq. (8b) is replaced by integration. Under a condition that allows this replacement, Eq. (8b) assumes the form [1]

$$\begin{aligned}
 [S(y) - i\eta_s(y)] &= (y)^3 \int_{z_r(\bar{\varepsilon})}^{z_r(\bar{R}+\bar{\varepsilon})} dz_r(\bar{r}) [f(r)\mu(\bar{r})] \cdot \\
 &\quad \{[1 - \{z(\bar{r})\}^2 (1+i\eta(\bar{r}))][\bar{m}_c(r) - \{z_c(\bar{r})\}^2 (1+i\eta_c(\bar{r}))] - [\bar{q}_c(\bar{r})/y]^2\} \cdot \\
 &\quad \{[1 + \bar{m}_c(\bar{r})] - [\{z_r(\bar{r})\}^2 (1+i\eta_r(\bar{r}))]\}^{-1}, \tag{21}
 \end{aligned}$$

where

$$\begin{aligned}
 [\bar{q}_c(\bar{r})/y]^2 &= 4\bar{m}_c(\bar{r})\{z_c(\bar{r})\}^2 (1+i\eta_c(\bar{r})) + [(\bar{g}(\bar{r})/y)]^2; \\
 \bar{m}(\bar{r}) &= \mu(\bar{r})(R+1)^{-1}; \quad f(\bar{r})dz_r(\bar{r}) = d\bar{r}; \quad \{z_r(\bar{r})\}^2 = \{z(\bar{r})\}^2 + \{z_c(\bar{r})\}^2; \\
 \bar{\varepsilon} &= \varepsilon(R+1)^{-1}; \quad (\bar{R}+\bar{\varepsilon}) = (R+\varepsilon)(R+1)^{-1}. \tag{22}
 \end{aligned}$$

If $\eta_r(\bar{r})$ is small enough so that the vanishing of the real part of the denominator in the integral in Eq. (20) predominates the values of the integral, the integral yields

$$\begin{aligned}
 \{S(y) - i\eta(y)\} &= (\pi/2)y^3 [f(\bar{r}_o)\mu(\bar{r}_o)][1 + \bar{m}_c(\bar{r}_o)]^{-1/2} [\{\bar{m}_c(\bar{r}_o) - \{z_c(\bar{r}_o)\}^2\} \cdot \\
 &\quad [\{z(\bar{r}_o)\}^2 \eta(\bar{r}_o) - \{z_c(\bar{r}_o)\}^2 \eta_c(\bar{r}_o)] + 4\bar{m}_c(\bar{r})\{z_c(\bar{r}_o)\}^2 \eta_c(\bar{r}_o)\} \\
 &\quad - i[\bar{m}_c(\bar{r}_o) - \{z_c(\bar{r}_o)\}^2]^2 + [\{z(\bar{r}_o)z_c(\bar{r}_o)\}^2 \eta(\bar{r}_o)\eta_c(\bar{r}_o)] + [\bar{q}_c(\bar{r}_o)/y]^2\}, \tag{23}
 \end{aligned}$$

where

$$\begin{aligned}
 (\bar{\varepsilon}) &< \bar{r}_o < (\bar{R} + \bar{\varepsilon}); \\
 \{z_{r_o}(\bar{r}_o)\}^2 &= (1 + \bar{m}_{cr}) = \{z(\bar{r}_o)\}^2 + \{z_c(\bar{r}_o)\}^2; \\
 \{z_{r_o}(\bar{r}_o)\}^2 \eta_{r_o}(\bar{r}_o) &= \{z(\bar{r}_o)\}^2 \eta(\bar{r}_o) + \{z_c(\bar{r}_o)\}^2 \eta_c(\bar{r}_o).
 \end{aligned} \tag{24}$$

Equation (24) defines the specific value of (\bar{r}_o) and it is recognized that (\bar{r}_o) is a function of (y) and vice versa. Adopting the impositions and the simplifications that are conducted in Eqs. (16) and (18), one may derive from Eqs. (23) and (24) the results

$$S(y) = D A \{\eta(y)\}; \quad S(y) \Rightarrow S_I(y) = 0, \tag{25a}$$

$$\eta_s(y) = D [C + O \{\eta(y)\}^2]; \quad \eta_s(y) \Rightarrow \eta_I(y) = DC, \tag{25b}$$

with

$$D = [\pi / 2 \gamma(\bar{R})] [M_s / (M \bar{R})] [(1 + \bar{m}_c)]^{-1}, \tag{26a}$$

$$A = [(\bar{m}_c + \alpha_c)^2 + (\bar{m}_c - \alpha_c)], \tag{26b}$$

$$C = [(\bar{m}_c + \alpha_c)^2 + (\bar{g} / y)^2], \tag{26c}$$

$$O = [(1 + \bar{m}_c - \alpha_c) \alpha_c], \tag{26d}$$

and where

$$f(\bar{r}_o) = [(\alpha + \alpha_c)^{(1/2)} \gamma(\bar{R})(y)^3]^{-1}; \quad \mu(\bar{r}_o) = (M_s / M \bar{R}), \tag{26e}$$

$$\eta(y) = \eta(\bar{r}_o) = (\bar{b} / \pi) [\gamma(\bar{R})(y)^2]; \quad \eta(\bar{r}_o) = \eta_c(\bar{r}_o) = \eta_{r_o}(\bar{r}_o), \tag{26f}$$

$$(1 + \bar{m}_c) = (\alpha + \alpha_c); \quad [1 + (\gamma/2)]^{(1/2)} \leq y \leq [1 - (\gamma/2)]^{(1/2)}. \quad (26g)$$

The underlying condition of the validity on Eq. (25) is detailed in Reference 1. This condition holds even though the coupling forms are elaborated to include not only a weaker stiffness coupling, but also mass and gyroscopic coupling forms. Moreover, the coupling parameters may define various degrees of coupling strengths. Strictly, the validity of Eq. (25) demands the equality of $S(y)$ to the *primary term* $S_I(y)$ and $\eta_s(y)$ to the *primary term* $\eta_I(y)$. These equalities designate, $S_I(y)$ and $\eta_I(y)$ the first order approximations to $S(y)$ and to $\eta_s(y)$, respectively. The terms $A\{\eta(y)\}$ and $O\{\eta(y)\}^2$ are of the order of the higher approximations to the integral, notwithstanding that situations exist in which (A) and (O) are identically equal to zero; e.g., when the satellite oscillators are sprung-masses for which $\alpha_c = 1$, $\bar{g} = \bar{m}_c = 0$. [cf. Eq. (20).] In these situations the equality of the integral evaluations of $S(y)$ to $S_I(y)$ and of $\eta_s(y)$ to $\eta_I(y)$ need not be specifically invoked. (More on this subject when in a subsequent paper higher order approximations, than the first, are to be evaluated.) Clearly and significantly, the primary terms $S_I(y)$ and $\eta_I(y)$ and, therefore, the first order approximations of $S(y)$ and of $\eta_s(y)$ are independent of the modal overlap parameter (b). Without much-a-do, in this paper only the

first order approximations are implemented and considered. In this approximation the *first order approximation* to $S(y)$ is the primary term $S_I(y)$ and to $\eta_s(y)$ is the primary term $\eta_I(y)$.

Equation (25) reveals the parametric composition of the first order approximation to the induced reactive factor $S(y) \Rightarrow S_I(y)$ and to the induced loss factor $\eta_s(y) \Rightarrow \eta_I(y)$. Again, one is reminded that the induced reactive factor $S(y)$ and the induced loss factor $\eta_s(y)$ describe the influence of the coupled satellite oscillators on the impedance of the master oscillator. In the absence of coupling and in units of $[i(\omega_o M)y^2]$ the reactive factor is $[y^2 - 1]$; in the presence of coupling it is $[y^2 + S(y) - 1]$. On the other hand, in the absence of couplings the loss factor is (η_o) ; in the presence of couplings it is $[\eta_o + \eta_s(y)]$. When $S(y)$ is positive the satellite oscillators contribute, through the couplings, a mass-like term, when negative, a stiffness-like term. On the other hand, since the satellite oscillators add merely passive elements to the complex, $\eta_s(y)$ is invariably positive. Equation (25) confirms this statement and exposes the proportionality of $S_I(y)$ and of $\eta_I(y)$ to (D). Therefore, $S_I(y)$ and $\eta_I(y)$ are directly proportional to the mass ratio (M_s/M) ; it is estimated that for a reasonable complex with (M_s/M) equal to about a tenth, (D) is of the order of

unity. [cf. Eq. (19).] The equality of $S_I(y)$ to zero and the quadratic dependence of the primary term $\eta_I(y)$ of $\eta_s(y)$, in terms of (C) , which entertain the term-components $(\bar{m}_c + \alpha_c)^2$ and $(\bar{g}/y)^2$, is of significance. Again, it is emphasized that the primary terms $S_I(y)$ and $\eta_I(y)$ are the *true* first order approximation to $S(y)$ and to $\eta_s(y)$, respectively; in this context the terms $DA\{\eta(y)\}$ and $DO\{\eta(y)\}^2$ are superfluous. In any case, Eq. (26) indicates that $DO\{\eta(y)\}^2$ in $\eta_s(y)$ is rarely dominant even when the loss factor $\eta(y)$ of a typical satellite oscillator exceeds any of the coupling parameters; $\bar{m}_c, \alpha_c, (\bar{g}/y) \leq \eta(y)$, notwithstanding that in the absence of any couplings $S(y)$ and $\eta_s(y)$, as stated in Eq. (25), are negligible on account of $A=0$ and of $C=0$ and $O=0$, respectively. When couplings do exist, there are values of $S(y)$ that are non-zero whereas those of $S_I(y)$ are equal to zero. Yet when the coupling strengths are weak, and even moderate, the values of $|S(y)|$ are small compared with unity even if (y) is at the edges of the frequency range of concern. On the other hand, when couplings do exist, the levels in both, the first order approximation and the exact evaluations of $\eta_s(y)$, are certainly not negligible, even if the couplings are weak. (Note that (η_o) of the order of (10^{-4}) is not unreasonable [12].)

As already discussed and demonstrated in Figs. 3-7 the curves for a modal overlap parameter (b) that is small compared with unity; $b \ll 1$, possess values and levels that are undulated. The excursions in the undulations are the more pronounced the smaller is the value of (b) [11]. Nonetheless, the mean-value averaging of the undulating values of $S(y)$ and of the undulating levels of $\eta_s(y)$ converge unto two single curves, which are designated $S_a(y)$ and $\eta_a(y)$, respectively. [cf. Fig. 3d.] As (b) increases, approaching and exceeding unity, the undulations, again true to form, are suppressed. As already intimated in Section III, increasing (b) beyond unity brings in the phenomenon of erosion which increases as the modal overlap parameter (b) reaches higher and higher above unity.

To accentuate the nature of erosion in $S(y)$ and in $\eta_s(y)$, the first order approximation (FOA) of $S(y)$ [$=S_I(y)$] and of $\eta_s(y)$ [$=\eta_I(y)$] are appropriately superimposed on Figs. 4-7. [cf. Figs. 3d, 3e and 3f.] It is now observed, in these figures, that the mean-value averaging of the undulations of the exact values of $S(y)$ and of the exact levels of $\eta_s(y)$, when (b) is small compared with unity; $b \ll 1$, relate to the first order approximation (FOA) of $S(y)$ and of $\eta_s(y)$ in the form: $S_a(y) \neq S_I(y)$ except at $y=1$ and $\eta_a(y) = \eta_I(y)$, respectively. Since

$S_a(y)$ and $S_I(y)$ and $\eta_a(y)$ and $\eta_I(y)$ are independent of (b) , these relationships are also independent of (b) . [cf. Figs. 3d and 3e.] (The independence of $\eta_I(y)$ of (b) has been stretched by some to conclude that (b) may be rendered, a priori, equal to zero. Neglecting to mention in this rendering that mean-value averaged levels are substituted for highly undulated levels, is not a viable scientific procedure, unless ignorance is bliss [11].) On the other hand, when (b) approaches and exceeds unity, the exact values of $S(y)$ and the exact levels of $\eta_s(y)$ become free of undulations, but these values and levels erode with further increases of (b) [1, 6, 7, 15]. The erosion in the exact values of $S(y)$ is a departure from the curve designated $S_a(y)$, progressively converging on the first order approximation at $S_I(y) = 0$, as (b) increases higher and higher above unity. In contrast, the erosion in the exact levels of $\eta_s(y)$ commences and progresses from the levels of the first order approximation, at $\eta_I(y)$, toward lower and lower levels, as (b) increases higher and higher above unity. To account for these progressive dependencies on (b) , higher order approximations are clearly required [20]. What is doubtful is whether higher and higher order approximations can account for the undulations when (b) needs to remain small compared with unity. To account for the undulations, an entirely different approximation procedure is thus called for. In this paper devising such an approximation procedure is not attempted.

VII. A Typical Member of an Ensemble of Complexes Supporting

Various Parametric Combinations

In the preceding evaluations, the distribution of resonance frequencies (x_{rr}) and the assigned loss factors (η_{rr}) for the satellite oscillators are sequential functions of the normalized index (\bar{r}). These two quantities, exemplified in Figs. 2a.1, 2b.1 and 2c.1 and in Figs. 2a.2, 2b.2 and 2c.2, respectively, may be smoothed out by extrapolation and interpolation into monotonic and continuous functions of (\bar{r}); (\bar{r}) = $[r(R+1)^{-1}]$. This kind of smoothness is rarely found in practice and a question arises as to what are the expected consequences of more practical assignments for these parameters and others? In this section a few layers are removed in the quest to discover the phenomena that may be encountered, in the induced reactive factor $S(y)$ and in the induced loss factor $\eta_s(y)$, by the insertion of these more realistic parametric values. Since the assignment for the parameters that define the satellite oscillators and their couplings to the master oscillator can hardly be drawn, a more generalized approach is undertaken to investigate the influence of introducing variations in these parametric values. In particular, in this section two parameters are selected

to carry these variations; either individually or in unison. In the first, the index (r) of a satellite oscillator is assigned a distribution of pseudo-statistical values. [Pseudo-statistical is in reference to a sample selected out of an ensemble of random samples.] The index (r) is distributed sequentially and fractionally, in the range $1 \leq r \leq 27$. A pseudo-statistical index is designated $\Lambda(r)$, where $\Lambda(r) \leq \Lambda(q)$; $q = (r+1)$; $1 \leq r \leq (R-1)$. [cf. Eq. (9b).] In the second, the modal overlap parameter (b_r) is assigned a distribution of pseudo-statistical values that span the ranges $(2) \geq b_r \geq (0.1)$ and $(3.5) \geq b_r \geq (1)$, respectively. The distribution of $\Lambda(r)$ and of (b_r), with $R = 27$, that are employed in this section are depicted graphically in Figs. 8a, 8b, and 8c. The two-vector $\{(x_{rr}), (\eta_{rr})\}(R)$, as stated in Eqs. (16) and (18), is typically depicted, for the pseudo-statistical values shown in Figs. 8a, 8b, and 8c, in Figs. 9a, 9b, and 9c, respectively. Figure 9a depicts (x_{rr}) as a function of $\bar{\Lambda}(r)$ and Figs. 9b and 9c depict (η_{rr}), as a function of (\bar{r}), where $\bar{\Lambda}(r) = [\Lambda(r)(R+1)^{-1}]$ and $\bar{r} = [r(R+1)^{-1}]$. [cf. Fig. 2a.] It is observed, in Fig. 9a, that the pseudo-statistical variations embody the phenomenon of mode bunching in which variations in the modal density of the satellite oscillators drastically vary as a function of $\Lambda(r)$ [21]. On the other hand, as Figs. 9b and 9c show, the loss

factor (η_{rr}) , as a function of (r) , faithfully follows the variations assigned to (b_r) . In Fig. 9b some of the values of (b_r) are less than unity, in Fig. 9c all the values of (b_r) are in excess of unity.

The influence of the variations, described in Fig. 8, on the induced reactive factor $S(y)$ and on the induced loss factor $\eta_s(y)$, as functions of (y) , are exemplified in Figs. 10.1 10.2, as a pair, and in Figs. 11.1 and 11.2., as a pair, respectively. Each pair of figures represents a set of figures. The first pair of figures in each set; e.g., Figs. 10.1a and 10.2a depict the base situation in which $\bar{\Lambda}(r) = \bar{r}$ and $b_r = 1$. The second pair of figures in each set; e.g., Figs. 10.1b and 10.2b, depict the situation in which $\bar{\Lambda}(r)$ is as shown in Fig. 8a and $b_r = 1$. The third pair of figures in each set; e.g., Fig. 10.1c and 10.2c, depicts the situation in which $\bar{\Lambda}(r) = r$ and (b_r) is as shown in Fig. 8b. The fourth pair of figures in each set; e.g., Figs 10.1d and 10.2d, depict the situation in which $\bar{\Lambda}(r) = \bar{r}$ and (b_r) is as shown in Fig. 8c. The fifth pair of figures in each set; e.g., Figs. 10.1e and 10.2e, depict the combined situation in which $\bar{\Lambda}(r)$ and (b_r) are as shown in Figs. 8a and 8b, respectively. Finally, the sixth pair of figures in each set; e.g., Fig. 10.1f and 10.2f, depict the combined situation in which $\bar{\Lambda}(r)$ and (b_r) are as shown in Figs. 8a and 8c, respectively. It is

recognized then that each pair of figures in a set presents a complete evolution in the process of applying the pseudo-statistical variations depicted in Fig. 8 to the two parameters $\bar{\Lambda}(r)$ and (b_r) . Also, each pair of figures in a set selects a specific coupling form and a specific coupling strength. Thus, Fig. 10 pertains to a *strong* stiffness coupling: $\alpha_c=1.0$ [$\alpha=0.0$.], $\bar{m}_c = \bar{g} = 0$, and Fig. 11 pertains to a mix of stiffness and of gyroscopic coupling of *moderate* strength: $\alpha_c = 0.1$ [$\alpha = 0.9$.], $\bar{g} = 0.11$, $\bar{m}_c = 0$. [cf. Figs. 3e and 7c.] [One recalls that the values of $S(y)$ relating to moderate and especially weak coupling strengths are largely negligible compared with unity, even if (b) is as small as (0.1) . Therefore, the values of $S(y)$ depicted in Fig. 11 are hardly discernible.]

The first pair of figures of each set; namely, Figs. 10.1a and 10.2a, and 11.1a and 11.2a exhibit undulations in the values of the induced reactive factor $S(y)$ and in the levels of the induced loss factor $\eta_s(y)$, as functions of (y) . However, these undulations are small and they are completely suppressed as soon as (b_r) approaches the value of (2) . [cf. Fig. 3b.] The variations depicted in Fig. 8 are clearly discernible in all the subsequent figures in the series entitled Figs. 10 and 11. True to form, there is but a tinge of edge erosion in Figs. 10.1a and 10.2a, and in Figs. 11.1a and 11.2a yet in the likes of Fig. 3b stronger sign of erosion

has already reared its head. From Figs 10.1a and 10.2a, and from Figs. 11.1a and 11.2a to Fig. 3b, (b) is changed from unity to merely two. To confirm this statement and to provide for convenient and interpretable data from which to judge the more erratic data that incorporates the pseudo-statistical variations, the first order approximation of $S(y)$ and of $\eta_s(y)$, given in Eq. (25), are superimposed on Figs. 10.1a and 10.2a, and on Figs. 11.1a and 11.2a and on all other figures in the series entitled Figs. 10 and 11.

Again, the pseudo-statistical variations are defined by two competing and nearly independent factors, i.e., by $\Lambda(r)$ and $b(r)[=(b_r)]$. In Figs. 9a, 10.1b, 10.2b, 11.1b and 11.2b; it is observed that at a mode bunching (a rich modal density) region the influence of the satellite oscillators is more pronounced than at a mode sparsity (a poor modal density) region [21]. On the other hand, when the modal overlap parameter (b_r) entertains values that are small compared with unity, the values and levels, as functions of (y) , tend to fluctuate. The fluctuations are pronounced at and in the vicinity of the resonance frequencies of those satellite oscillators to which these small values of (b_r) are assigned. At and in the vicinity of the resonance frequencies of those satellite oscillators to which (b_r) are assigned values that approach and exceed unity, no such fluctuations are

present; e.g., see Figs. 10.1c, 10.2c, 11.1c and 11.2c, and Figs. 10.1d, 10.2c, 11.1d and 11.2d and contrast them, respectively [22]. When variations in both parameters are combined, both characteristics can be identified in the values of the induced reactive factor $S(y)$ and in the levels of the induced loss factor $\eta_s(y)$; e.g., see Figs. 10 and 11 and contrast, in particular, Figs. 10.1e, 10.2e, 11.1e and 11.2e with Figs. 10.1f, 10.2f, 11.1f and 11.2f, respectively.

Appendix A

The sweeping assumptions rendered in Eq. (15), which leads to Eqs. (9d) and (16), culminating in Eq. (18), may be introduced more gradually. The purpose for this Appendix is to effect such a gradual introduction. In this manner when some of these assumptions are relieved, reevaluation of the induced reactive factor $S(y)$ and of the induced loss factor $\eta_s(y)$ may be readily instituted.

From Eqs. (9c) and (12), the design demands that

$$(\alpha_r + \alpha_{cr}) (x_r^o)^2 = (1 + \bar{m}_{cr}) \text{ for } \bar{r} = (1/2), \quad (\text{A1})$$

and if (x_r^o) becomes, by design, unity at $\bar{r} = (1/2)$, the expression reduces to

$$(\alpha_r + \alpha_{cr}) = (1 + \bar{m}_{cr}) \text{ for } \bar{r} = (1/2). \quad (\text{A2a})$$

From Eq. (12) it is observed with satisfaction that (x_r^o) is, indeed, unity at $\bar{r} = (1/2)$. On the other hand, from Eqs. (10) and (11) one obtains

$$\begin{aligned} (x_r)^2 \eta_r &= (b_r / 2) [\partial \{x_r (x_r^o)^2\} / \partial r]; \quad (x_{cr})^2 \eta_{cr} = (b_{cr} / 2) [\partial \{\alpha_{cr} (x_r^o)^2\} / \partial r]; \\ \eta_{rr} &= [2(\alpha_r + \alpha_{cr})(x_r^o)^2]^{-1} \{b_r [\partial \{\alpha_r (x_r^o)^2\} / \partial r] + b_{cr} [\partial \{\alpha_{cr} (x_r^o)^2\} / \partial r]\}, \end{aligned} \quad (\text{A3})$$

where again, (r) is allowed to have a continuous connotation as explained in Reference 1. In particular, if the spring factors (α_r) and (α_{cr}) are independent of (r) , Eq. (A3) simplifies to read

$$\eta_r = (\bar{b}_r / \pi) [\gamma(\bar{R})(x_r^o)^2]; \quad \eta_{cr} = (\bar{b}_{cr} / \pi) [\gamma(\bar{R})(x_r^o)^2];$$

$$\eta_{rr} = \beta_r \eta_{cr}; \quad \alpha_r = \alpha; \quad \alpha_{cr} = \alpha_c, \quad (\text{A4})$$

where (x_r^o) is extrapolated and interpolated to become a continuous function of (r)

$$[(\partial \ln(x_r^o / \partial r)] = (R+1)^{-1} [\gamma(\bar{R})(x_r^o)^2], \quad (\text{A5})$$

$$(\beta_r b_{cr}) = (\alpha + \alpha_c)^{-1} [(b_r \alpha) + (b_{cr} \alpha_c)], \quad (\text{A6})$$

$$\bar{b}_r = [(\pi b_r)(R+1)^{-1}]; \quad \bar{b}_{cr} = [(\pi b_{cr})(R+1)^{-1}], \quad (\text{A7})$$

and from Eq. (A2a), by design

$$(\alpha + \alpha_c) = (1 + \bar{m}_c). \quad (\text{A2b})$$

From Eqs. (10)–(12) and (A2)–(A7) one may cast the designed two-vector in the form

$$\{(x_{rr}), (\eta_{rr})\}(R) = \{(1 + \bar{m}_c)^{1/2}, (\beta_r)\} \cdot \{(x_{rr}^o), (\eta_{rr}^o)\}(R), \quad (\text{A8})$$

$$\{(x_{rr}^o), (\eta_{rr}^o)\}(R) = \{(x_r^o), (\bar{b}_{cr} / \pi) [\gamma(\bar{R})(x_r^o)^2]\}, \quad (\text{A9})$$

where

$$\beta_r = \begin{cases} (1 + \bar{m}_c)^{-1} [\alpha(b_r/b_{cr}) + \alpha_c] & ; \quad b_r \neq b_{cr}, \\ \beta = \begin{cases} (1 + \bar{m}_c)^{-1} [\alpha(b/b_c) + \alpha_c]; & b_r = b, \quad b_{cr} = b_c \\ 1 & ; \quad b = b_r = b_{cr}, \end{cases} \end{cases} \quad \begin{matrix} \text{(A10a)} \\ \text{(A10b)} \\ \text{(A10c)} \end{matrix}$$

the quantities (\bar{m}_c) , (x_r^o) , $\gamma(\bar{R})$ and (\bar{b}_{cr}) are stated in Eqs. (1d), (12), (13) and (A7), respectively, and the superscript (o) in (x_{rr}) and (η_{rr}) recognizes that (x_{rr}^o) and (η_{rr}^o) are restricted to specific impositions. [cf. Eq. (4).] For the sake of computational and interpretive advantage the validity of Eqs. (A4) and (A10c) is universally adopted in this paper. [cf. Eq. (15).] Under this imposition, Eqs. (A8) and (A4) simplify

$$\{(x_{rr}), (\eta_{rr})\}(R) = \{(1 + \bar{m}_c)^{1/2} (x_r^o), \eta(\bar{r})\}; \quad \bar{b} = [(\pi b)(R + 1)^{-1}], \quad \text{(A11)}$$

$$\eta(\bar{r}) = \eta_r = \eta_{cr} = \eta_{rr}; \quad \eta(\bar{r}) = (\bar{b}/\pi)[\gamma(\bar{R})(x_r^o)^2], \quad \text{(A12)}$$

where (x_r^o) is stated in Eq. (12), and (β_r) becomes equal to unity. [cf. Eqs. (18a) and (16).]

References

1. G. Maidanik, "Induced damping by a nearly continuous distribution of nearly undamped oscillators: Linear Analysis" 2001, Journal of Sound and Vibration, **240**, 717-731.
2. G. Maidanik, "Power dissipation in a sprung mass attached to a master structure," 1995, Journal of the Acoustical Society of America, **98**, 3527-3533.
3. A. Pierce, V. W. Sparrow and D. A. Russell, "Fundamental structural-acoustic idealizations for structures with fuzzy internals," 1995, Journal of Acoustics and Vibration, **117**, 339-348.
4. M. Strasberg and D. Feit, "Vibration damping of large structures by attached small resonant structures," 1996, Journal of the Acoustical Society of America, **99**, 335-344.
5. R. L. Weaver, "Mean and mean-square responses of a prototypical master/fuzzy structure," 1996, Journal of the Acoustical Society of America, **99**, 2528-2529.

6. M. J. Brennan, "Wideband vibration neutralizer," 1997, Noise Control Engineering Journal, **45**, 201-207.
7. G. Maidanik and K. J. Becker, "Noise control of a master harmonic oscillator coupled to a set of satellite harmonic oscillators," 1998, Journal of the Acoustical Society of America, **104**, 2628-2637; "Characterization of multiple-sprung mass for wideband noise control," 1999, Journal of the Acoustical Society of America, **106**, 3119-3127.
8. R. J. Nagem, I. Veljkovic and G. Sandri, "Vibration damping by a continuous distribution of undamped oscillators," 1997, Journal of Sound and Vibration, **207**, 429-434.
9. T. L. Smith, K. Rao and I. Dyer, "Attenuation of plate flexural waves by a layer of dynamic absorbers," 1986, Noise Control Engineering Journal, **26**, 56-60.
10. G. Maidanik and J. Dickey, "Singly and regularly ribbed panels," 1988, Journal of Sound and Vibration, **123**, 309-314.
11. Yu. A. Kobelev, "Absorption of sound waves in a thin layer," 1987, Soviet Physics Acoustics, **33**, 295-296.

12. R. H. Lyon, Statistical Energy Analysis of Dynamical Systems: Theory and Applications, 1975, MIT, Cambridge; and R. H. Lyon and R. G. Dejung, Theory and Application of Statistical Energy Analysis, 1995, Butterworth-Heinemann, Boston.
13. R. H. Lyon and G. Maidanik, "Power flow between linearly coupled oscillators," 1962, *Journal of the Acoustical Society of America*, **34**, 623-639.
14. M. Strassberg, "Insuring causality of frequency-response function with hysteretic damping," 2001, *Journal of the Acoustical Society of America*, **109**, 2471A.
15. G. Maidanik and K. J. Becker, "Dependence of the Induced loss factor on the coupling forms and coupling strengths: Linear Analysis," 2001, NSWCCD-70-TR-2001/055.
16. G. Maidanik, "Dependence of the Induced loss factor on the coupling forms and coupling strengths: Energy Analysis", 2001, NSWCCD-70-TR-2001/060.

17. E. Skudrzyk, "The mean-value method of predicting the dynamic response of complex vibrators," 1980, Journal of the Acoustical Society of America, **67**, 1105-1135.
18. S. H. Crandall and R. Lotz, "On the coupling loss factor in statistical energy analysis," 1971, Journal of the Acoustical Society of America, **49**, 352-356.
19. G. Maidanik, "Response of coupled dynamic systems," 1976, Journal of Sound and Vibration, **46**, 561-583.
20. M. R. Spiegel, Complex Variables with an Introduction to Conformal Mapping and its Applications, 1964, Schaum's Outline Series, McGraw-Hill Book Company, New York.
21. G. Maidanik and K. J. Becker, "Modal densities of simple dynamic systems," 1997, Journal of the Acoustical Society of America, **102**, 3130A.
22. M. Strasberg, "When is a "fuzzy" not a fuzzy (Continued)?" 2000, Journal of the Acoustical Society of America, **107**, 2885A.

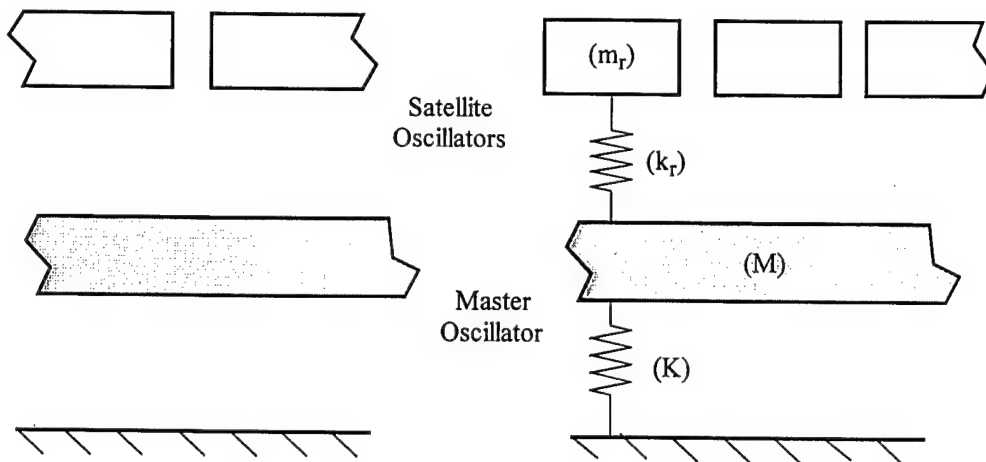


Fig. 1a. A master oscillator attached to a set of sprung-masses.

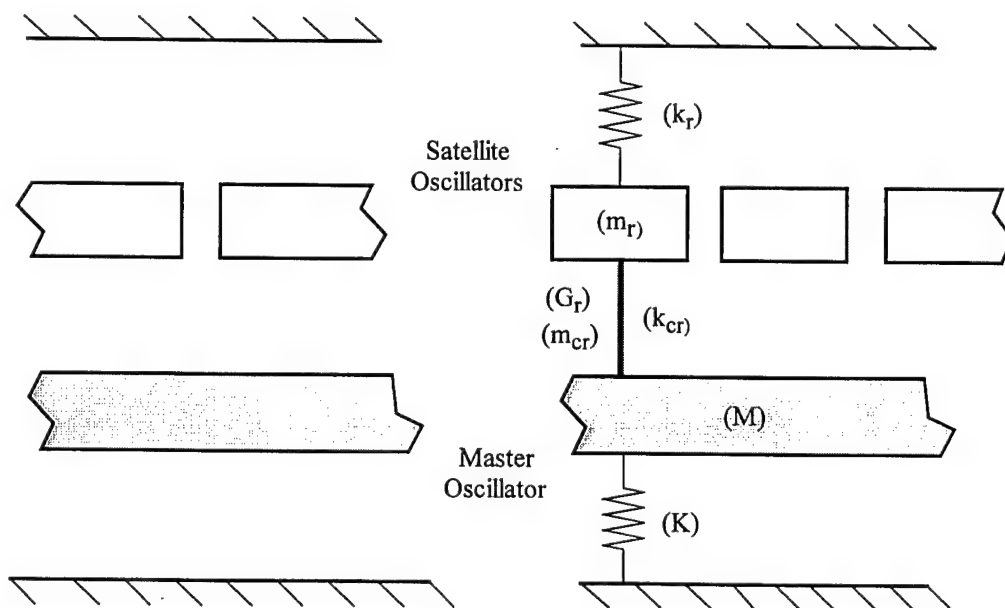
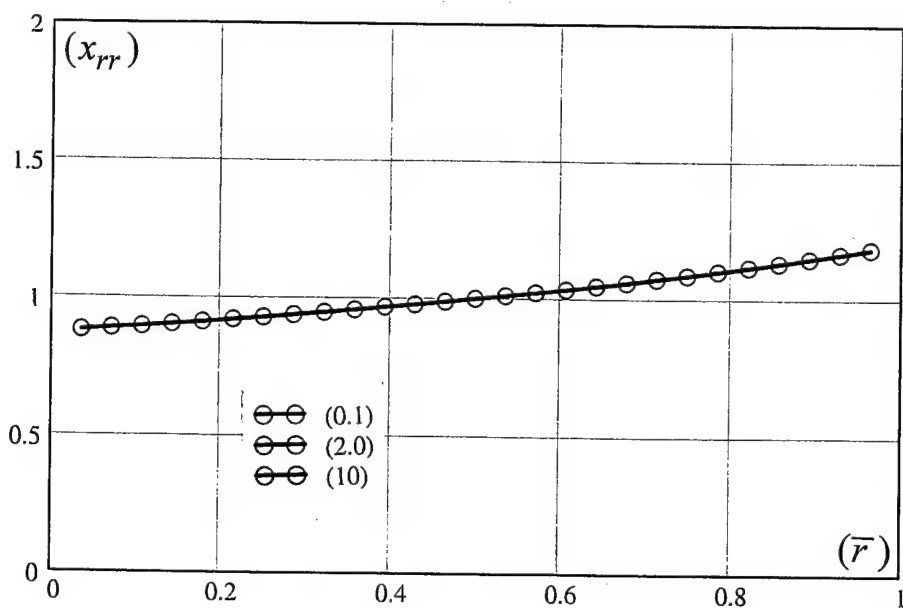


Fig. 1b. A set of satellite oscillators coupled to a master oscillator.

a.1.



a.2.

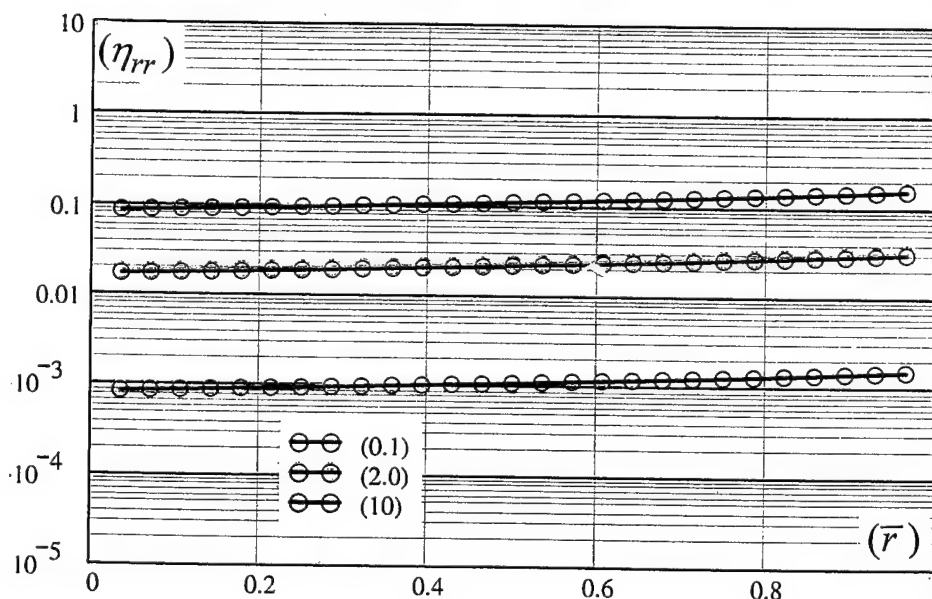
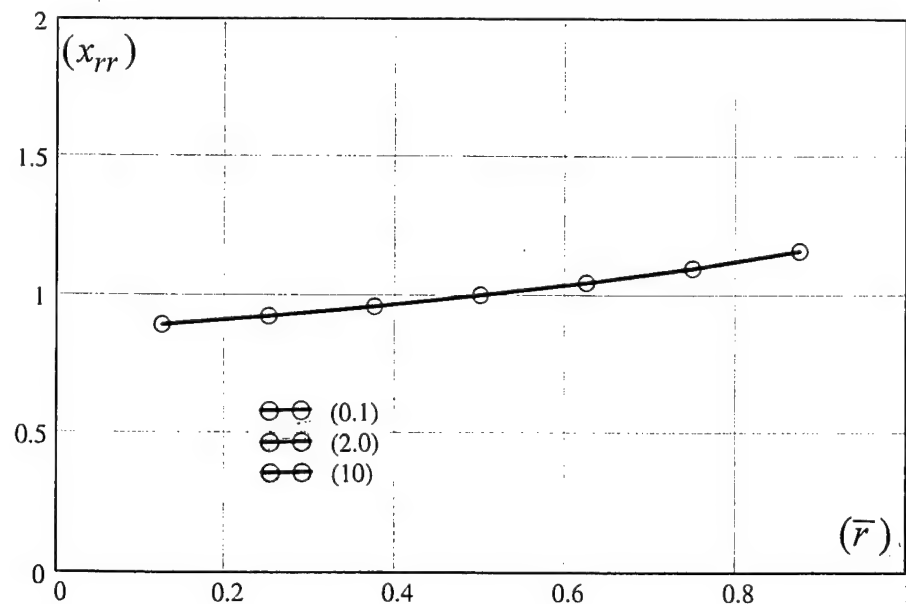


Fig. 2. (1.) Resonance frequency distribution (x_{rr}) and (2.) Corresponding assigned loss factor (η_{rr}) for the satellite oscillators as a function of the normalized index (\bar{r}) , respectively. (*)

a.1 and a.2. With $R = 27$ and $\bar{m}_c = 0$. $[x_{rr} = x_{rr}^o, \eta_{rr} = \eta_{rr}^o.]$

(*) When regions of curves clearly overlap, the color of the one with the higher modal overlap parameter (b) wins.

b.1.



b.2.

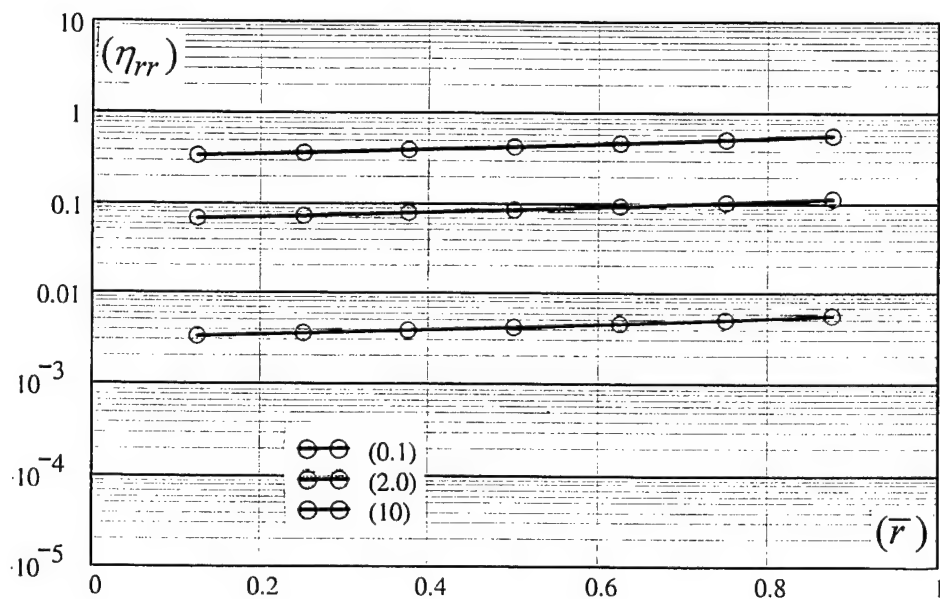
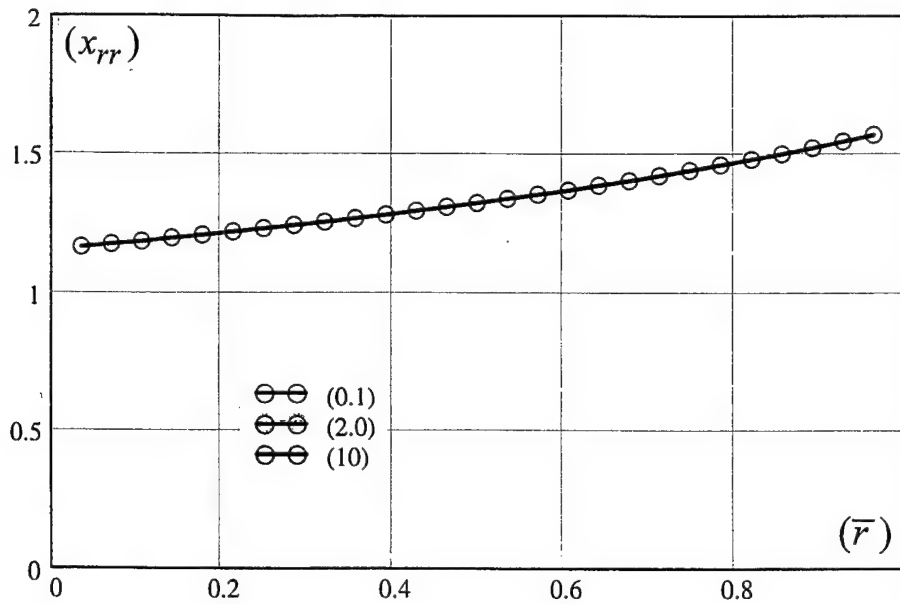


Fig. 2. (1.) Resonance frequency distribution (x_{rr}) and (2.) Corresponding assigned loss factor (η_{rr}) for the satellite oscillators as a function of the normalized index (\bar{r}), respectively. (*)

b.1 and b.2. As in a.1 and a.2, except that (R) is changed from (27) to (7).

$$[x_{rr} = x_{rr}^o, \eta_{rr} = \eta_{rr}^o.]$$

c.1.



c.2.

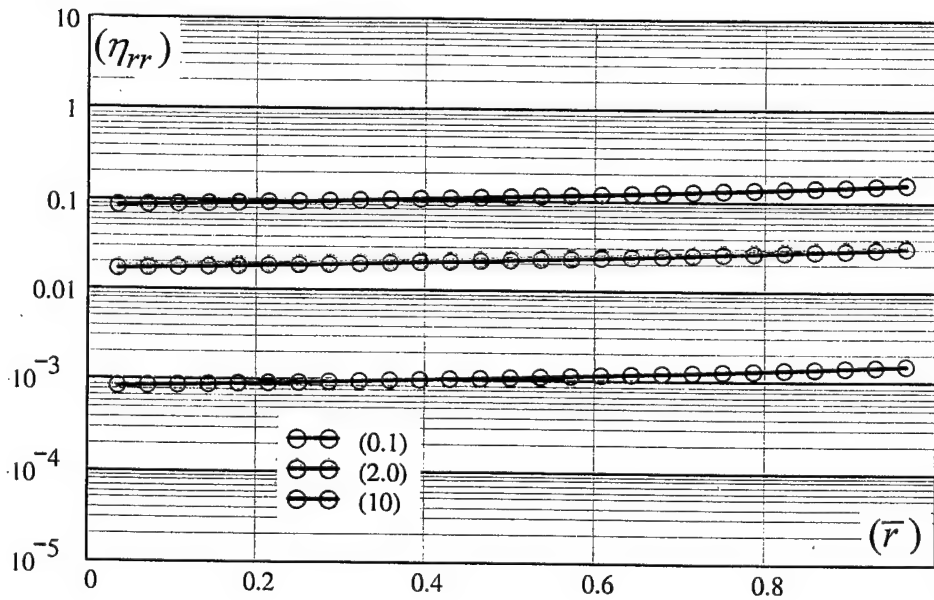


Fig. 2. (1.) Resonance frequency distribution (x_{rr}) and (2.) Corresponding assigned loss factor (η_{rr}) for the satellite oscillators as a function of the normalized index (\bar{r}) , respectively. (*)

c.1 and c.2. As in Fig. 2a, except that (\bar{m}_c) is changed from (0) to (0.75).

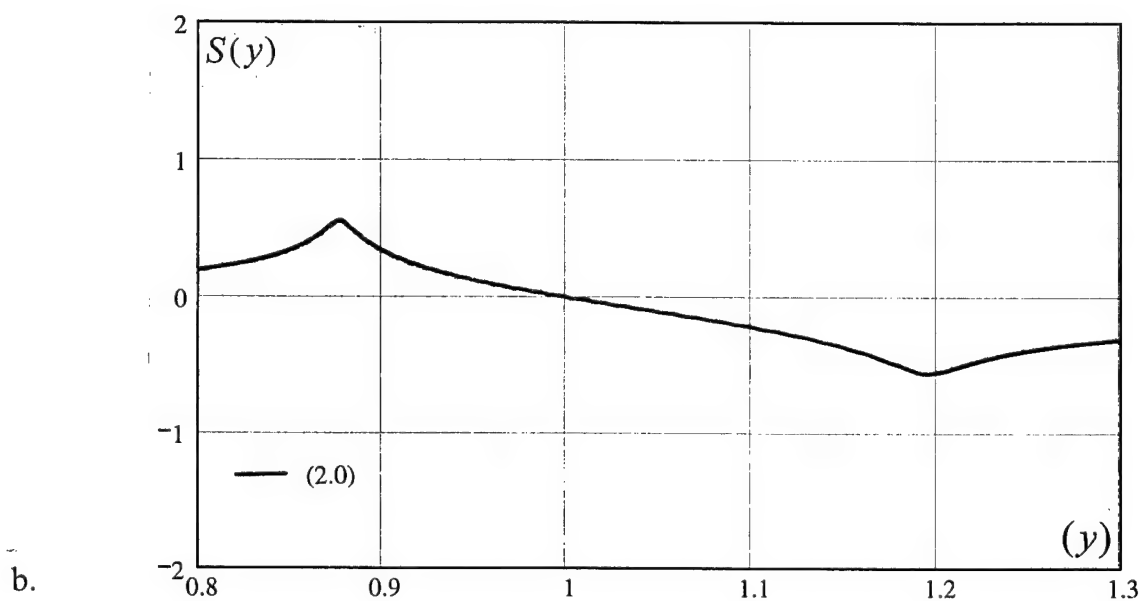
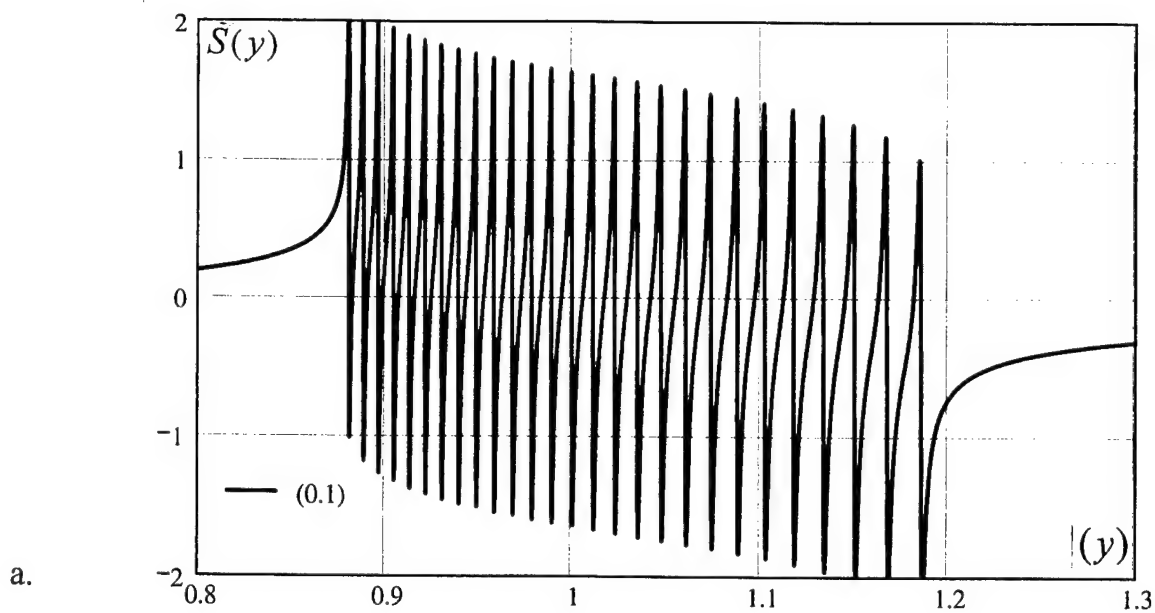


Fig. 3.1. Induced reactive factor $S(y)[=S^o(y)]$, as a function of (y) , for a stiffness control coupling form with $\alpha_c=1.0$ [$\alpha=0.0.$], $\bar{g} = \bar{m}_c = 0$. [Sprung-masses.]

a. With $b = (0.1)$

b. With $b = (2.0)$

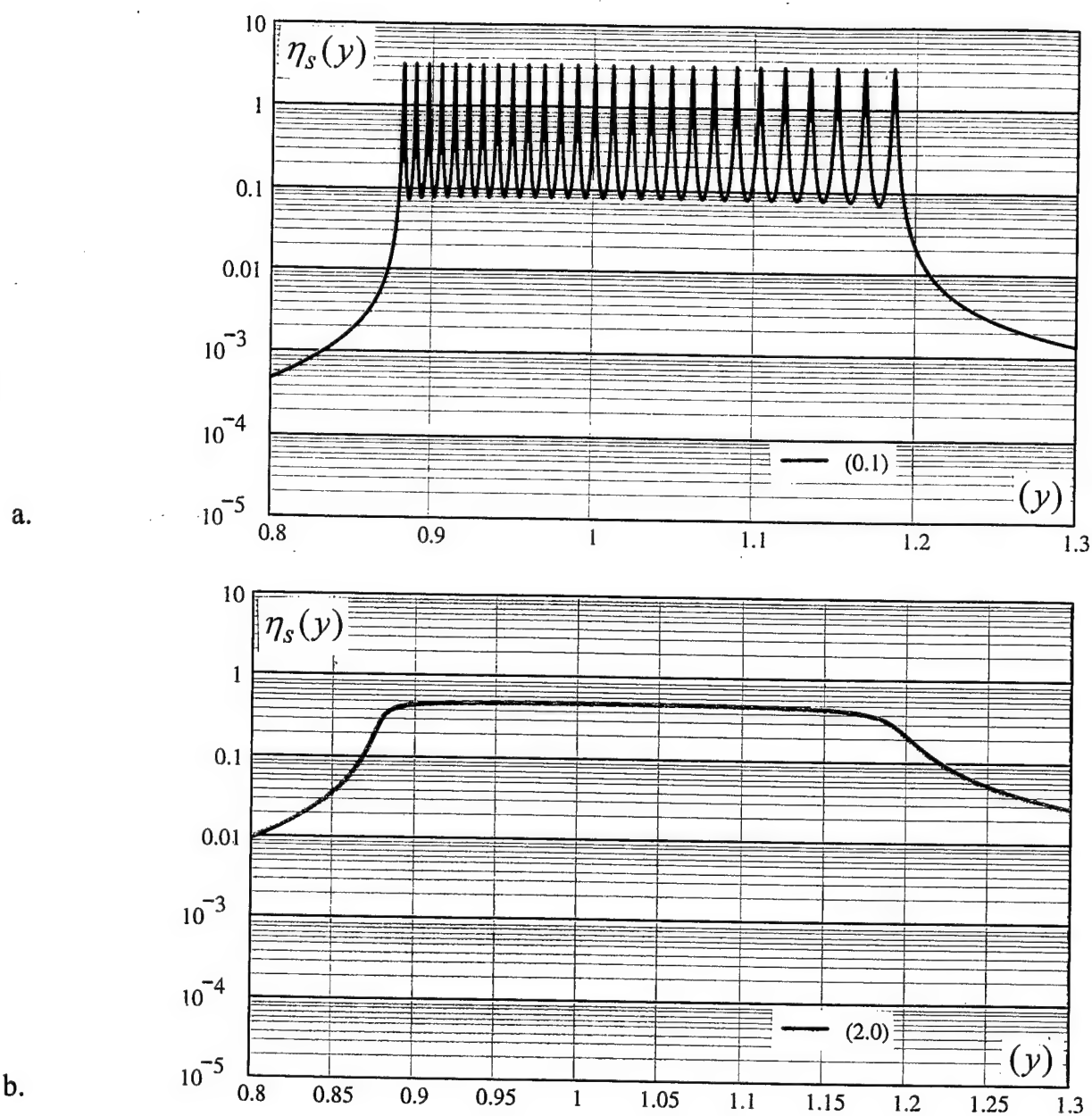


Fig. 3.2. Induced loss factor $\eta_s(y) [= \eta_s^o(y)]$, as a function of (y) , for a stiffness control coupling form with $\alpha_c = 1.0$ [$\alpha = 0.0.$], $\bar{g} = \bar{m}_c = 0$. [Sprung-masses.]

a. With $b = (0.1)$

b. With $b = (2.0)$

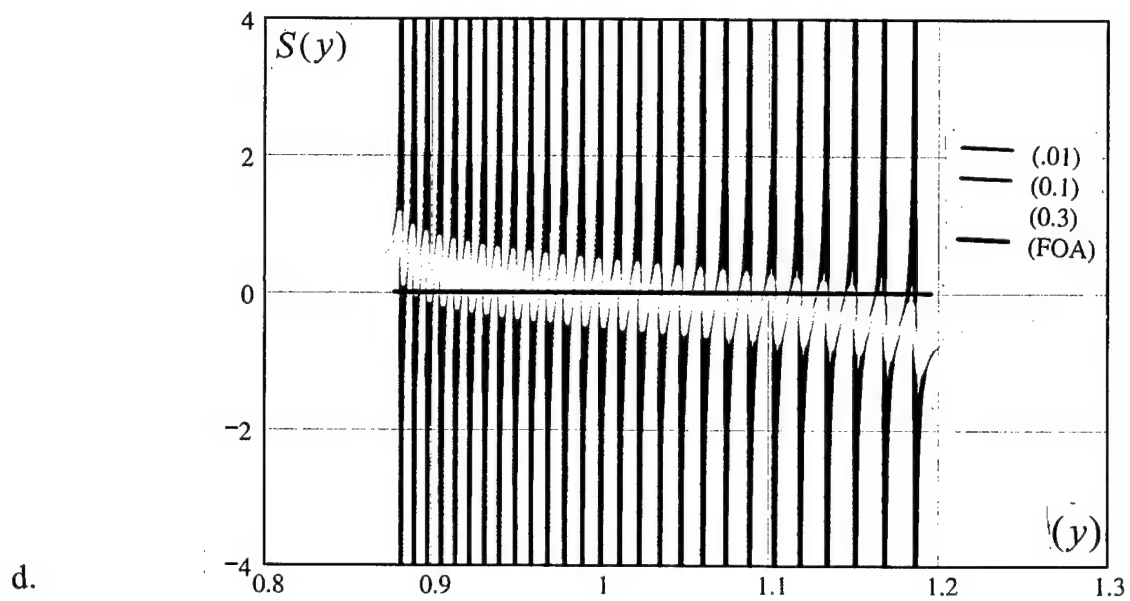
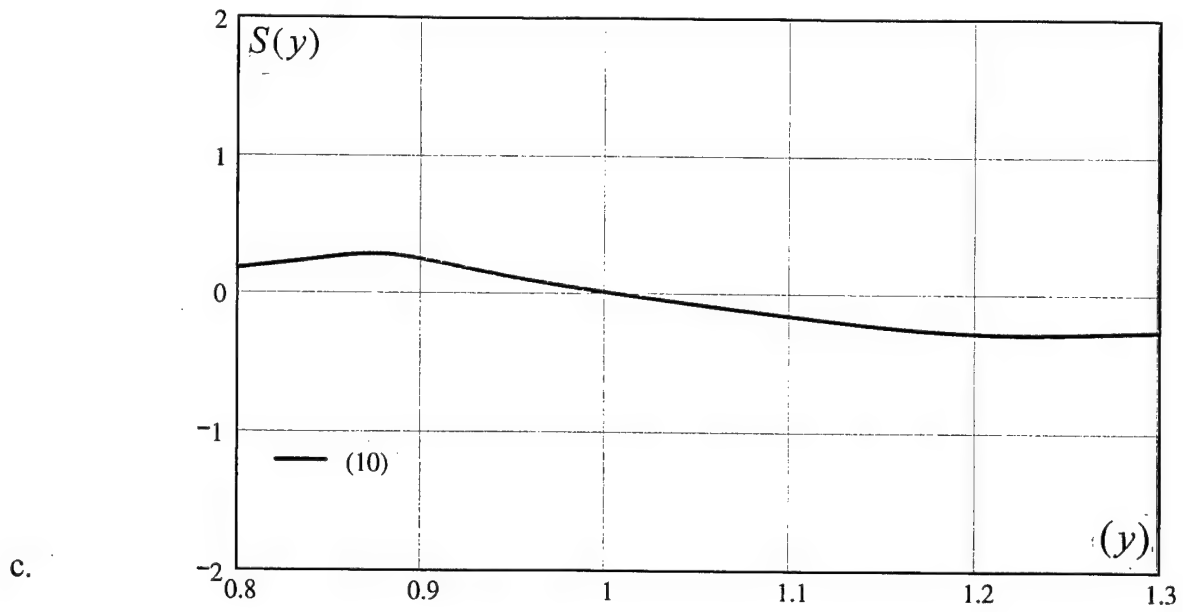
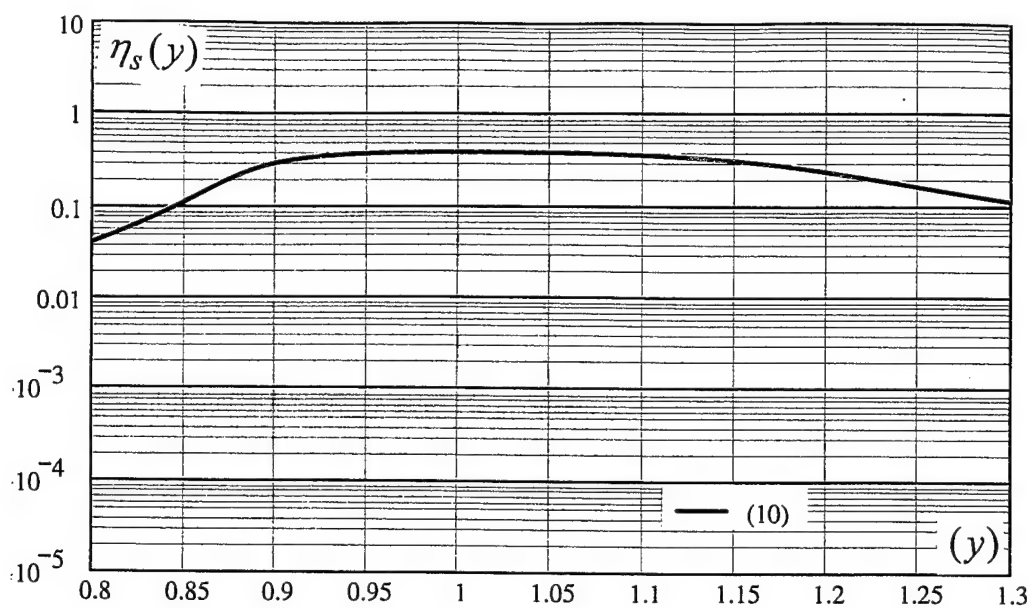


Fig. 3.1. Induced reactive factor $S(y)[=S^o(y)]$, as a function of (y) , for a stiffness control coupling form with $\alpha_c = 1.0$ [$\alpha = 0.0$.], $\bar{g} = \bar{m}_c = 0$. [Sprung-masses.]

c. With $b = (10)$

d. A superimposition of $b = (0.01)$, (0.1) and (0.3) , and (FOA) . (*)

c.



d.

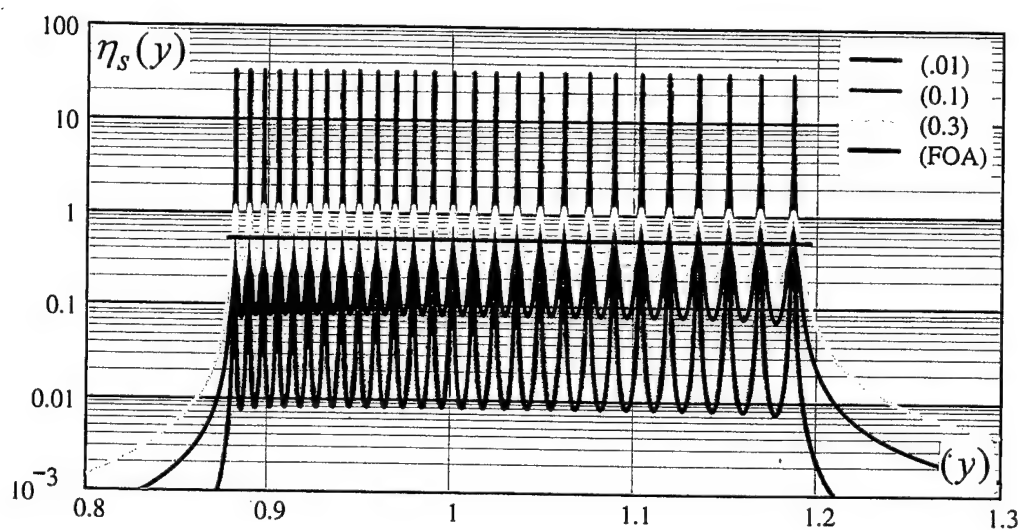


Fig. 3.2. Induced loss factor $\eta_s(\gamma) [= \eta_s^o(\gamma)]$, as a function of (γ) , for a stiffness control coupling form with $\alpha_c = 1.0$ [$\alpha = 0.0$.], $\bar{g} = \bar{m}_c = 0$. [Sprung-masses.]

c. With $b = (10)$

d. A superimposition of $b = (0.01)$, (0.1) and (0.3) , and (FOA). (*)

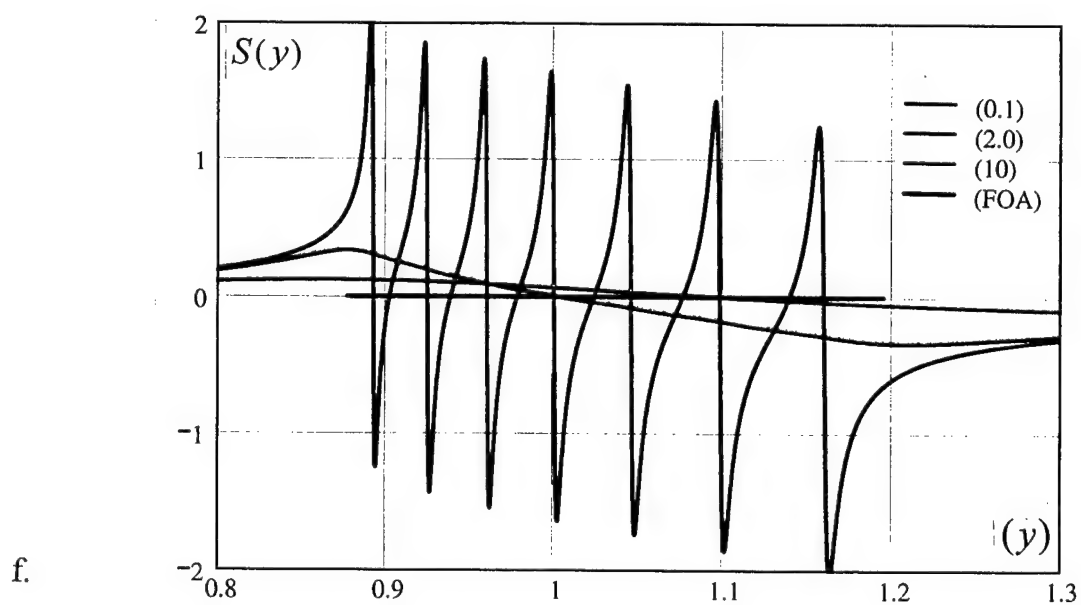
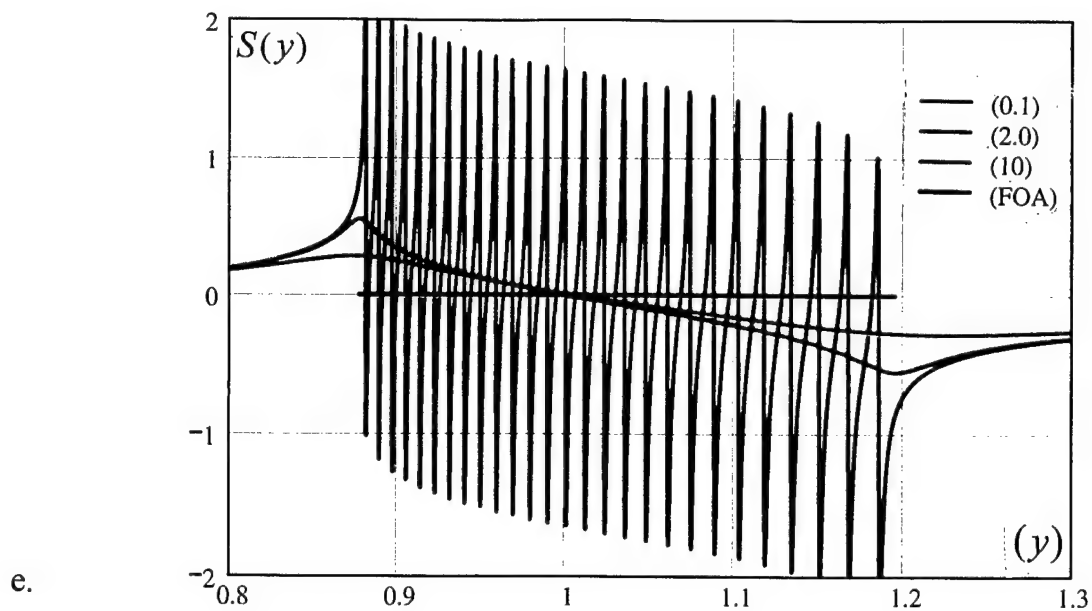
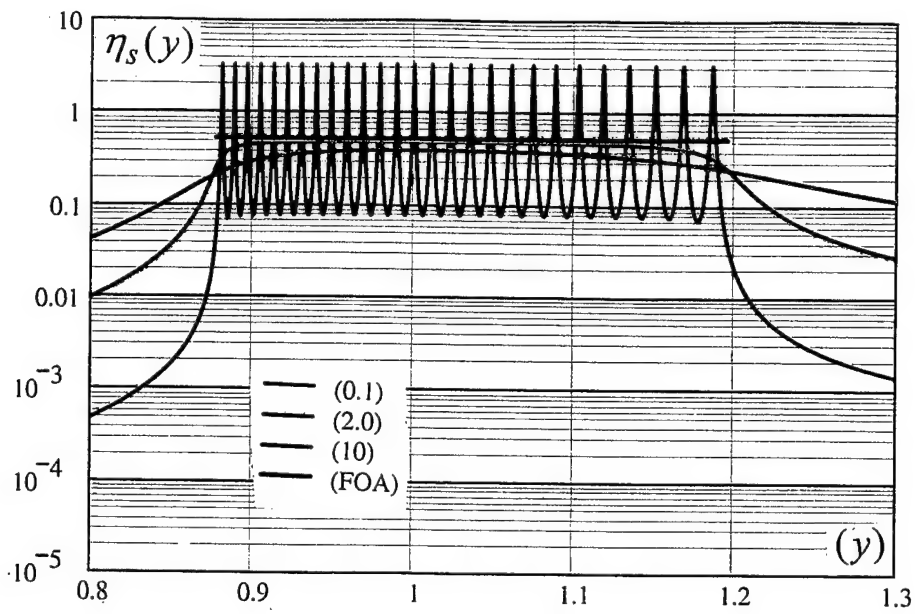


Fig. 3.1. Induced reactive factor $S(y)[=S^o(y)]$, as a function of (y) , for a stiffness control coupling form with $\alpha_c=1.0$ [$\alpha=0.0.$], $\bar{g} = \bar{m}_c = 0$. [Sprung-masses.]

e. A superimposition of a, b, and c, and (FOA).

f. As in 3.e above except that $R = (7)$ and not (27) .

e.



f.

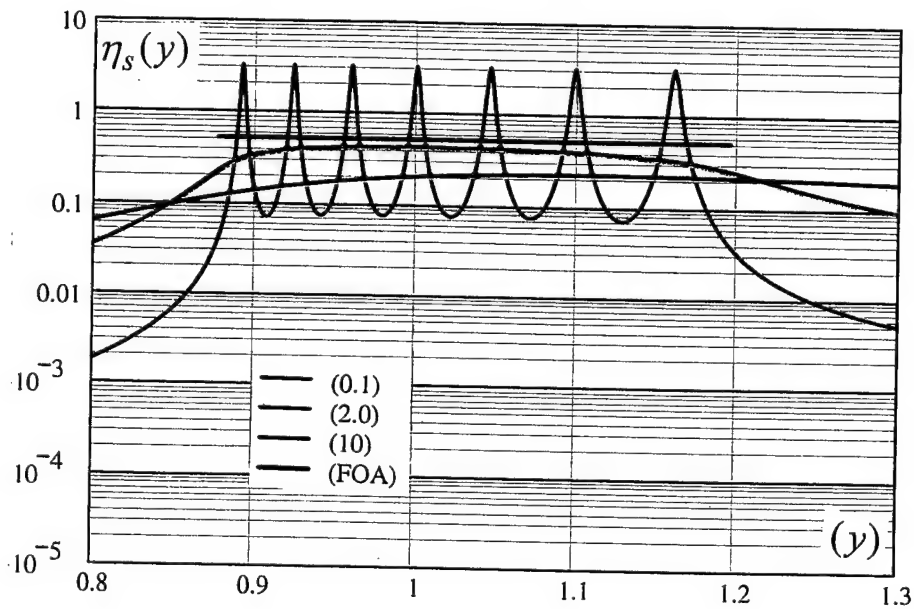


Fig. 3.2. Induced loss factor $\eta_s(y) [= \eta_s^o(y)]$, as a function of (y) , for a stiffness control coupling form with $\alpha_c = 1.0$ [$\alpha = 0.0$.], $\bar{g} = \bar{m}_c = 0$. [Sprung-masses.]

e. A superimposition of a, b, and c, and (FOA).

f. As in 3.e above except that $R = (7)$ and not (27) .

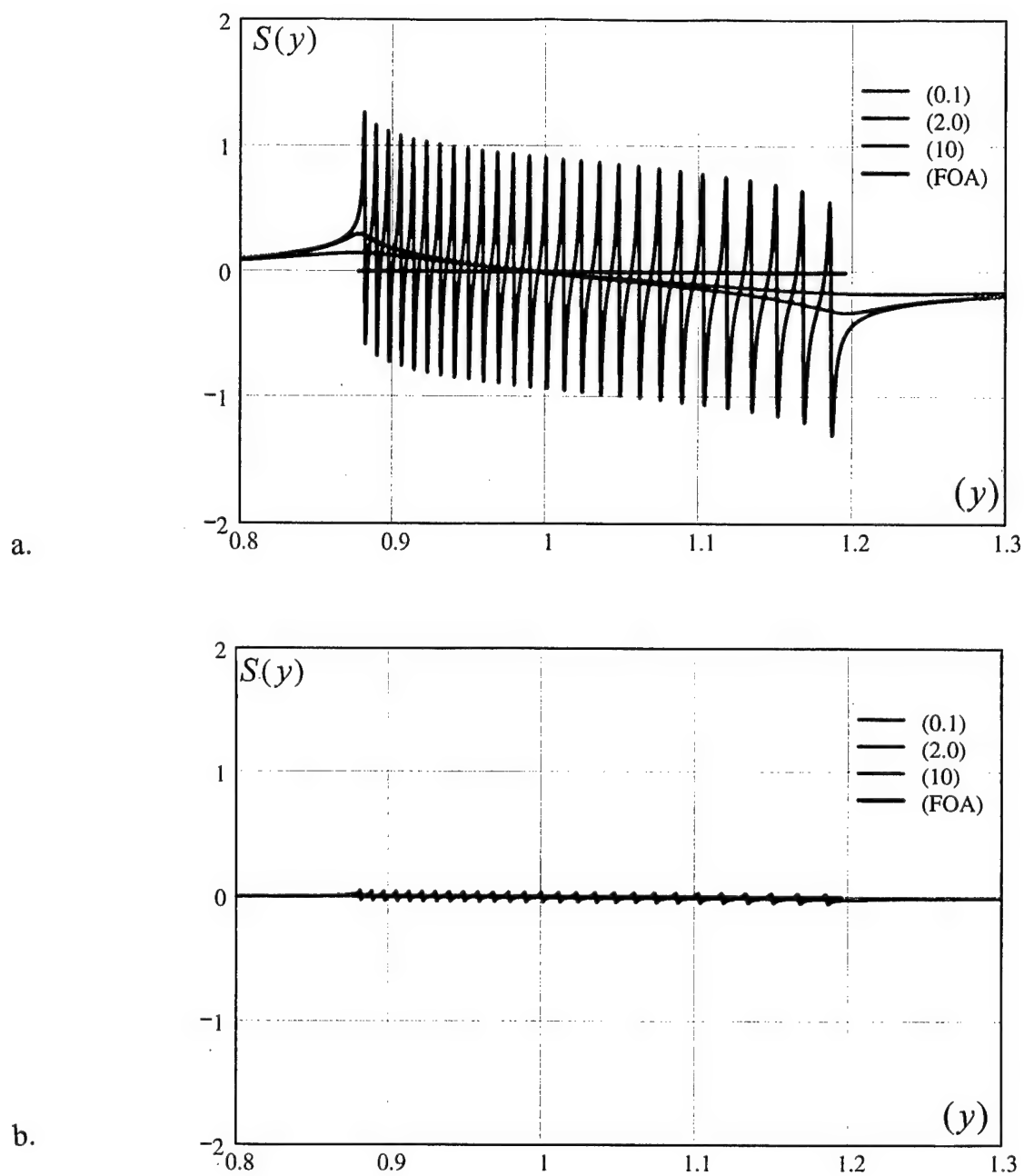


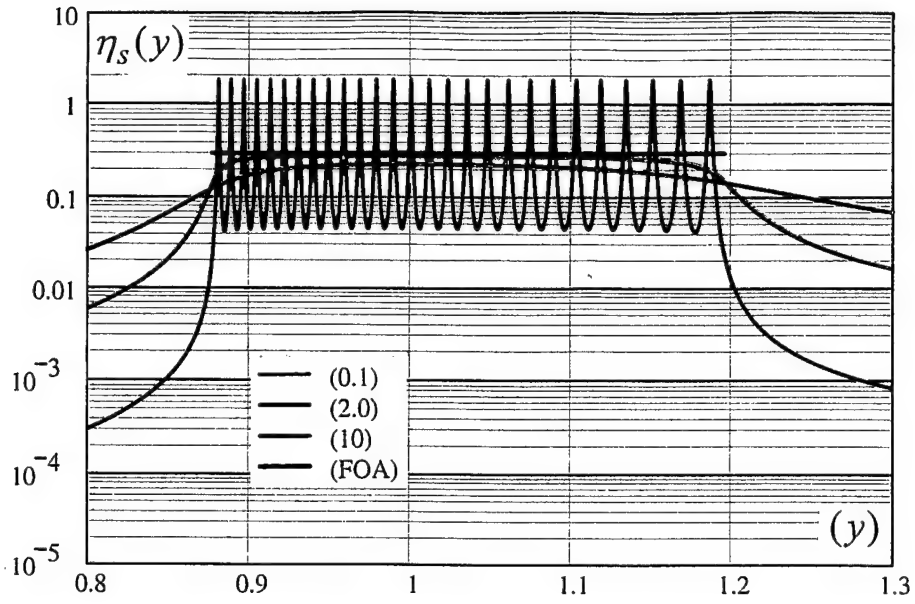
Fig. 4.1. Induced reactive factor $S(y)$, as a function of (y) , for a stiffness control coupling

form. $[R = 27 \text{ and } (M_s / M) = 0.1.]$

a. $\alpha_c = 0.75$ $[\alpha = 0.25.]$, $\bar{g} = \bar{m}_c = 0$. [Strong coupling.]

b. $\alpha_c = 0.15$ $[\alpha = 0.85.]$, $\bar{g} = \bar{m}_c = 0$. [Moderate coupling.]

a.



b.

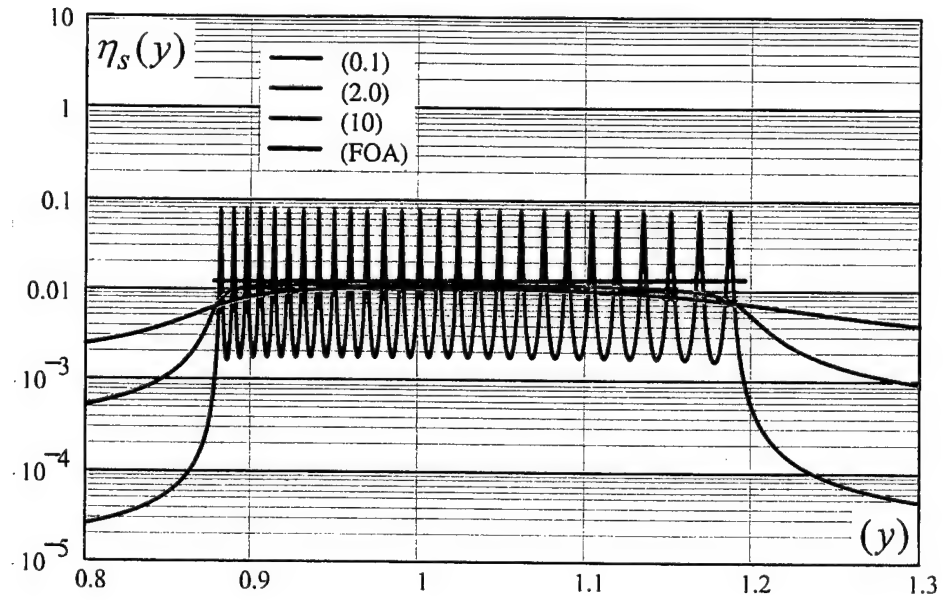


Fig. 4.2. Induced loss factor $\eta_s(y)$, as a function of (y) , for a stiffness control

coupling form. [$R = 27$ and $(M_s/M) = 0.1$.]

a. $\alpha_c = 0.75$ [$\alpha = 0.25$.], $\bar{g} = \bar{m}_c = 0$. [Strong coupling.]

b. $\alpha_c = 0.15$ [$\alpha = 0.85$.], $\bar{g} = \bar{m}_c = 0$. [Moderate coupling.]

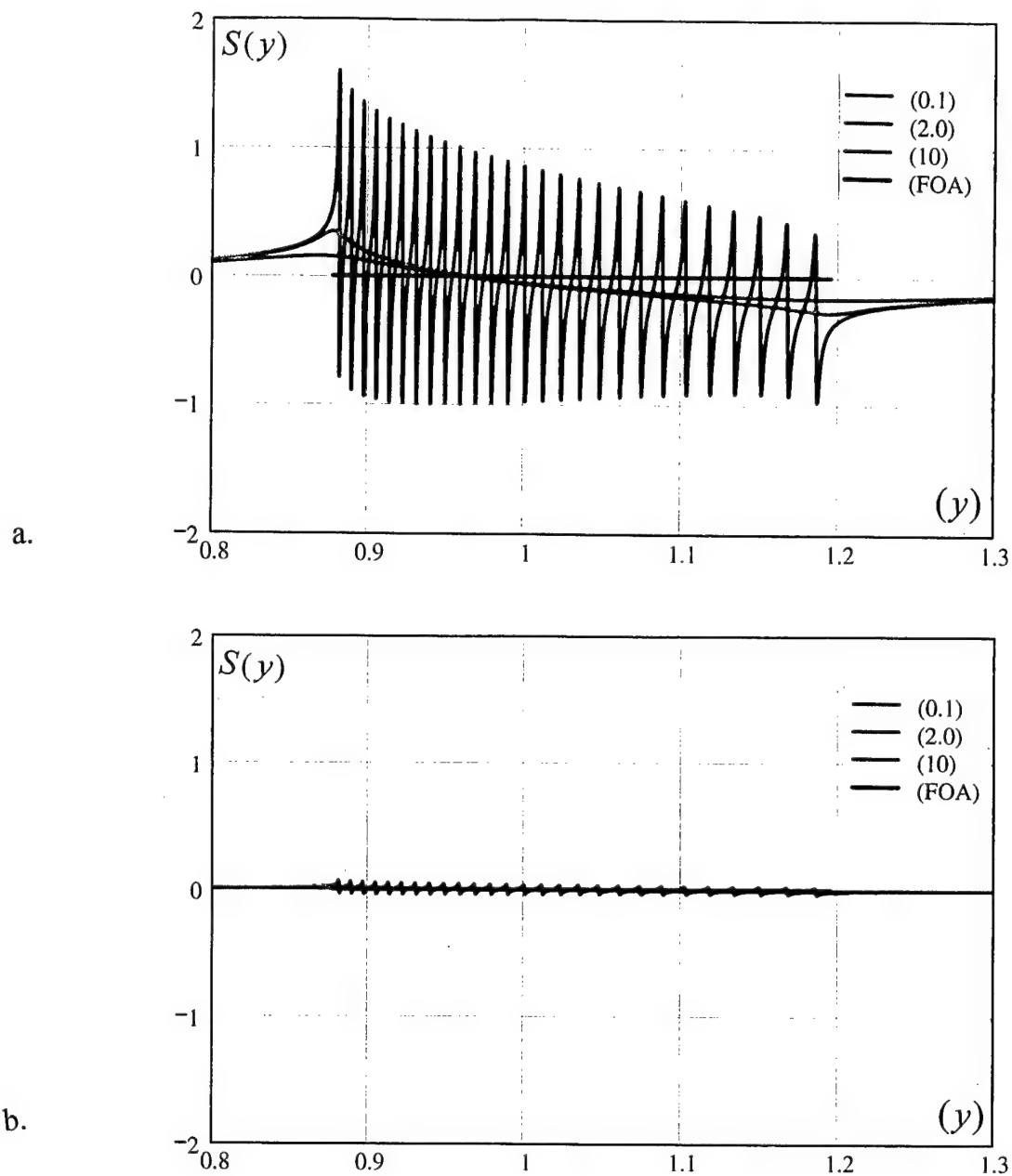


Fig. 5.1. Induced reactive factor $S(y)$, as a function of (y) , for a gyroscopically controlled coupling form. [$R = 27$ and $(M_s / M) = 0.1$.]

a. $\alpha_c = \bar{m}_c = 0$ [$\alpha = 1.0$.], $\bar{g} = 0.75$. [Strong coupling.]

b. $\alpha_c = \bar{m}_c = 0$ [$\alpha = 1.0$.], $\bar{g} = 0.15$. [Moderate coupling.]

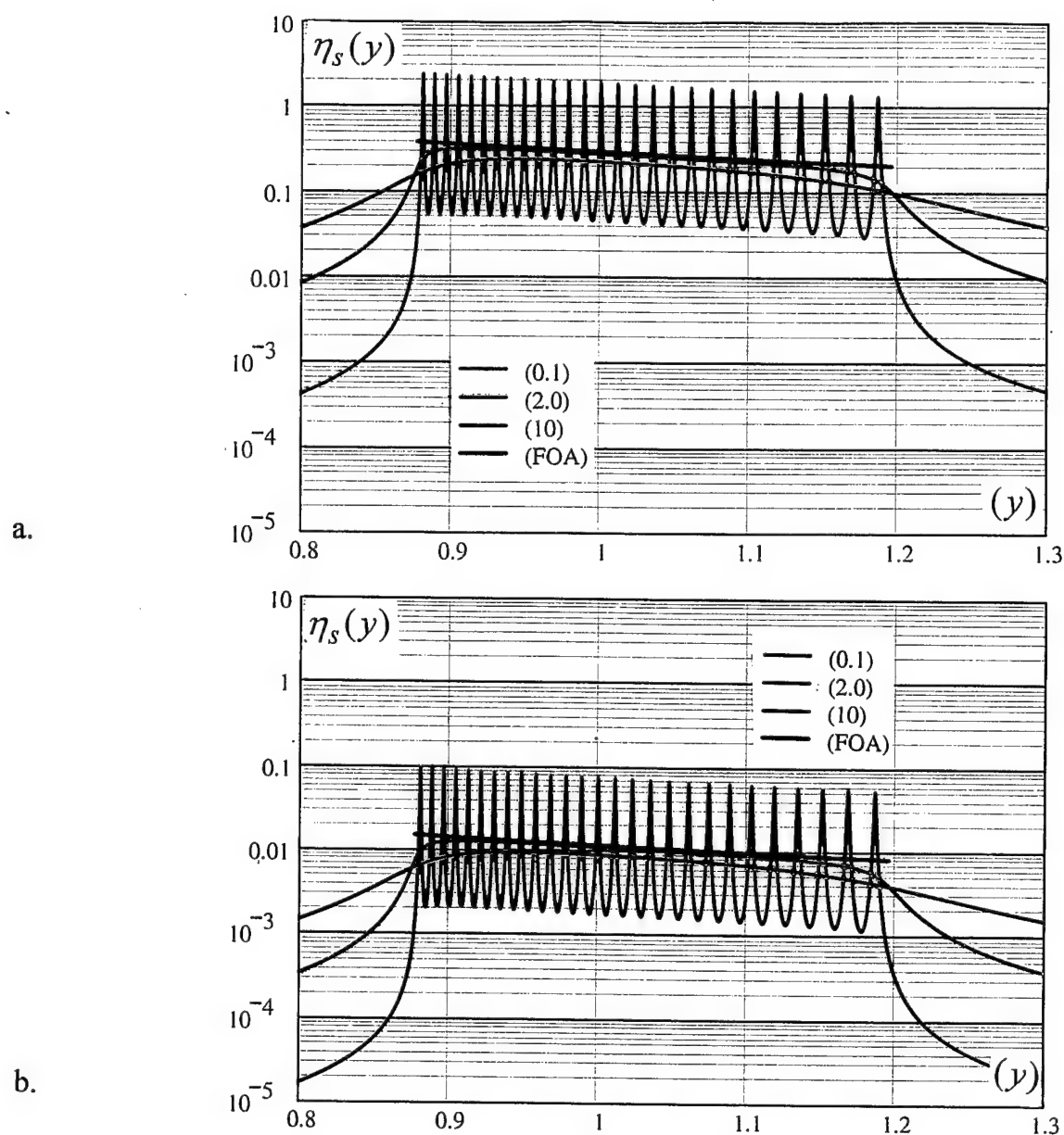


Fig. 5.2. Induced loss factor $\eta_s(y)$, as a function of (y) , for a gyroscopically

controlled coupling form. [$R = 27$ and $(M_s/M) = 0.1$.]

a. $\alpha_c = \bar{m}_c = 0$ [$\alpha = 1.0$.], $\bar{g} = 0.75$. [Strong coupling.]

b. $\alpha_c = \bar{m}_c = 0$ [$\alpha = 1.0$.], $\bar{g} = 0.15$. [Moderate coupling.]

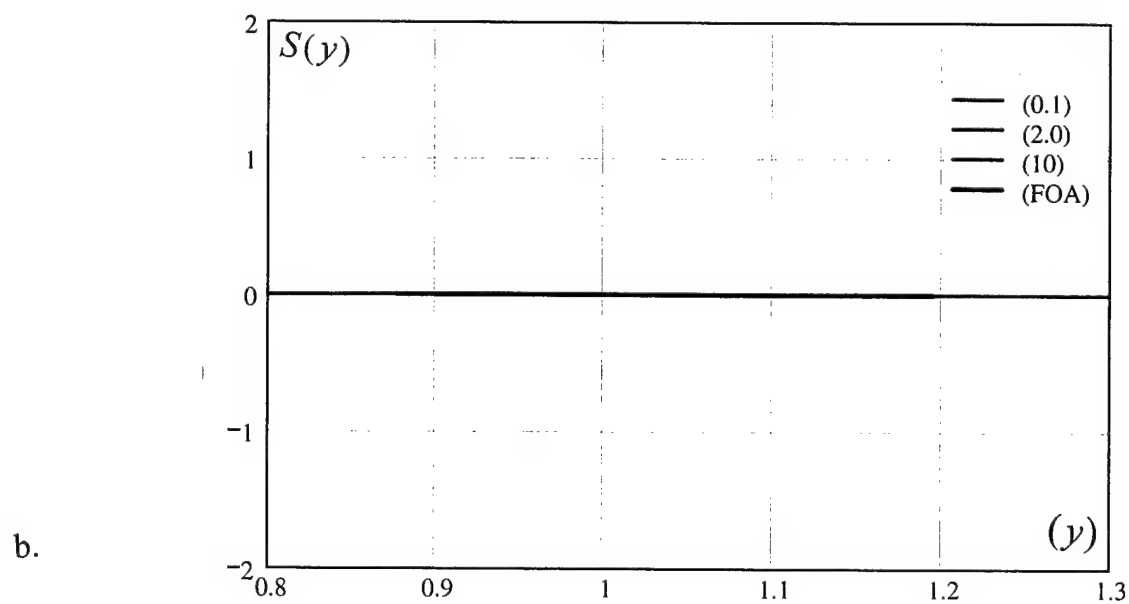
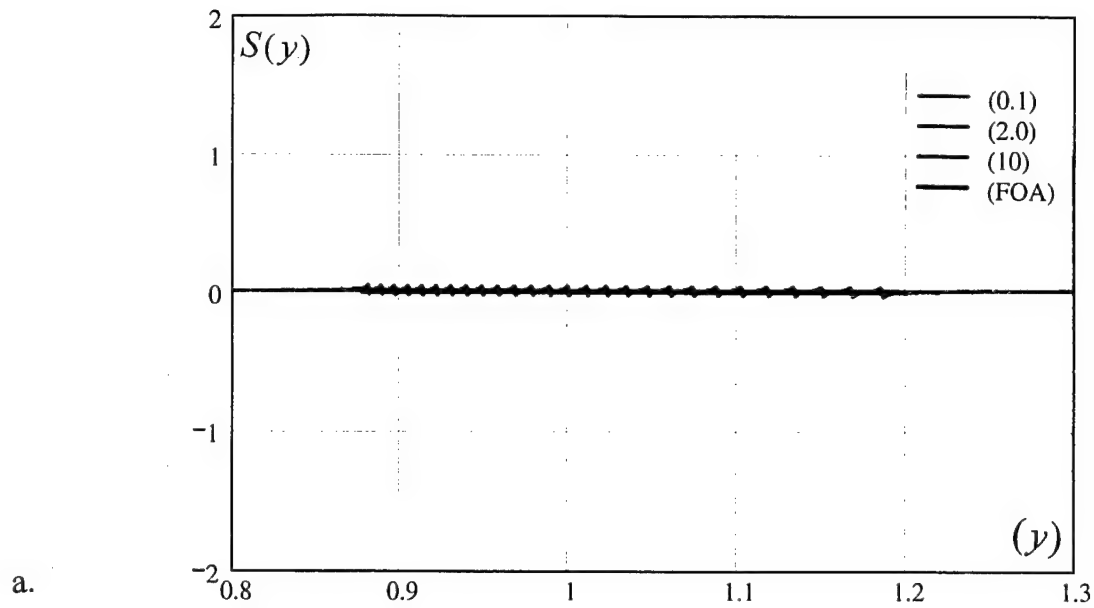


Fig. 6.1. Induced reactive factor $S(y)$, as a function of (y) , for a mass control coupling form. [$R = 27$ and $(M_s/M) = 0.1$.]

a. $\alpha_c = \bar{g} = 0$ [$\alpha = 1.15$.], $\bar{m}_c = 0.15$. [Moderate coupling.]

b. $\alpha_c = \bar{g} = 0$ [$\alpha = 1.03$.], $\bar{m}_c = 0.03$. [Weak coupling.]

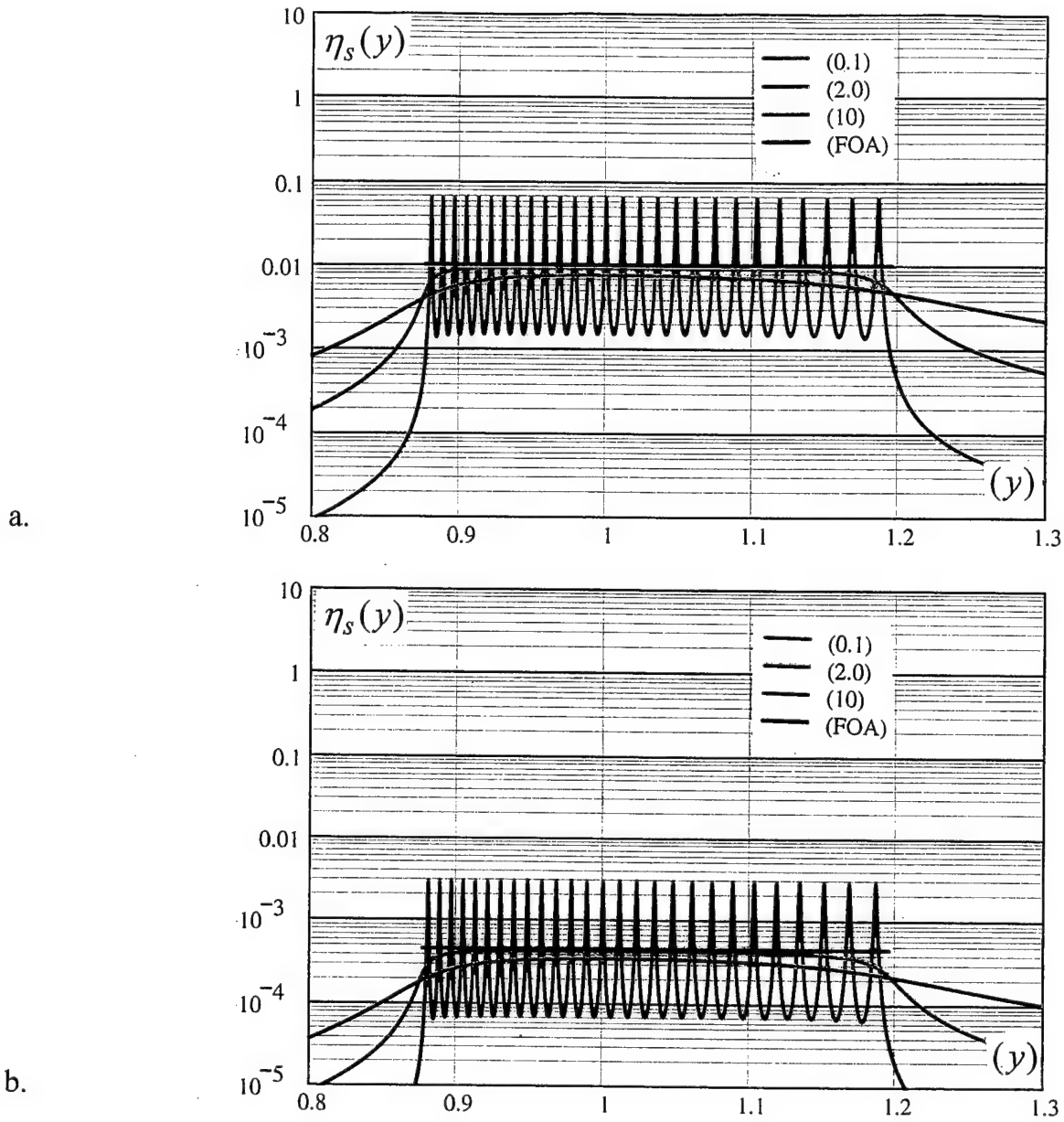


Fig. 6.2. Induced loss factor $\eta_s(y)$, as a function of (y) , for a mass control coupling form. [$R = 27$ and $(M_s/M) = 0.1$.]

a. $\alpha_c = \bar{g} = 0$ [$\alpha = 1.15$.], $\bar{m}_c = 0.15$. [Moderate coupling.]

b. $\alpha_c = \bar{g} = 0$ [$\alpha = 1.03$.], $\bar{m}_c = 0.03$. [Weak coupling.]

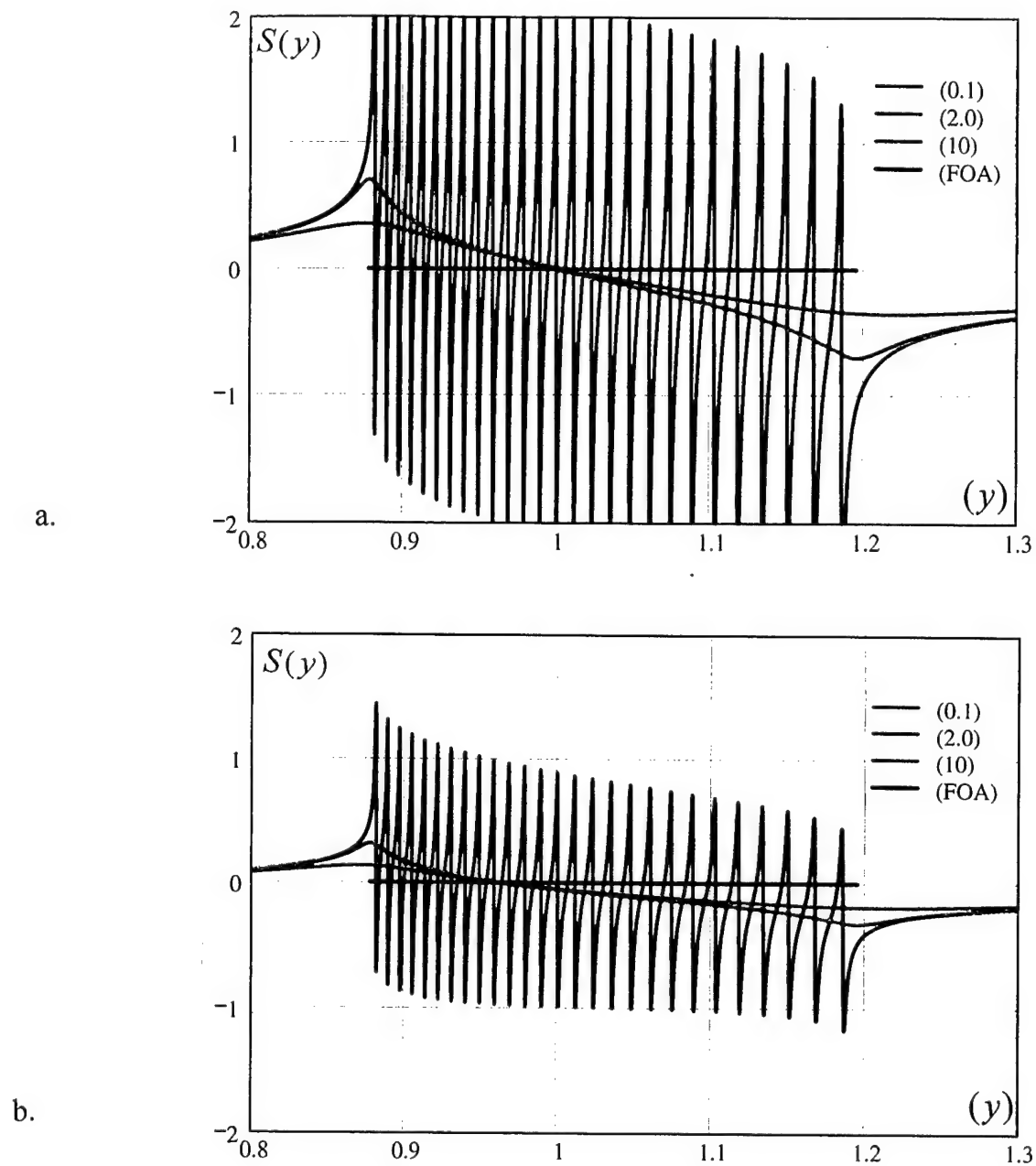
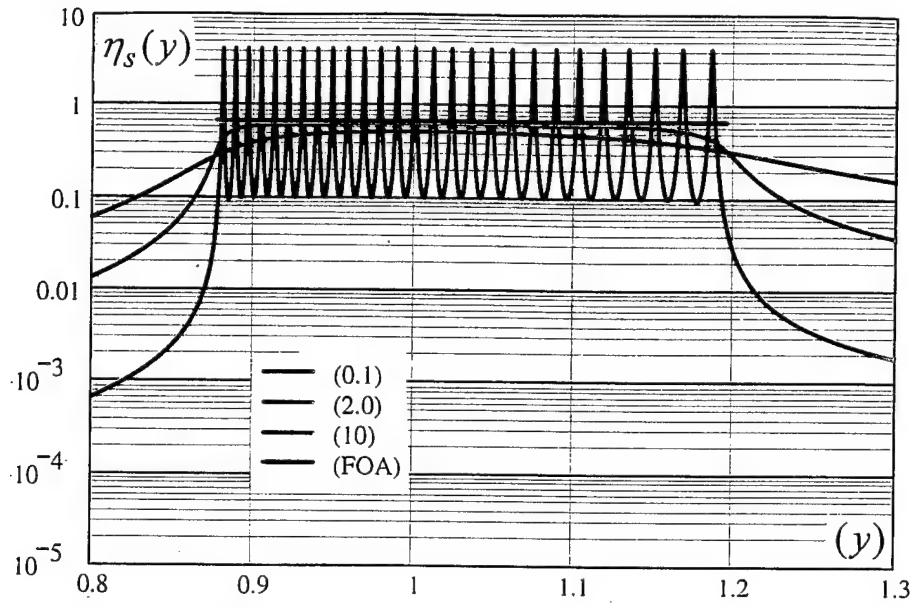


Fig. 7.1. Induced reactive factor $S(y)$, as a function of (y) , for mixed control coupling forms. [$R = 27$ and $(M_s/M) = 0.1$.]

a. $\alpha_c = \bar{m}_c = 0.75$ [$\alpha = 1.0$.], $\bar{g} = 0$. [Very strong coupling.]

c. $\alpha_c = 0.53$ [$\alpha = 0.47$.], $\bar{g} = 0.54$, $\bar{m}_c = 0$. [Strong coupling.]

a.



b.

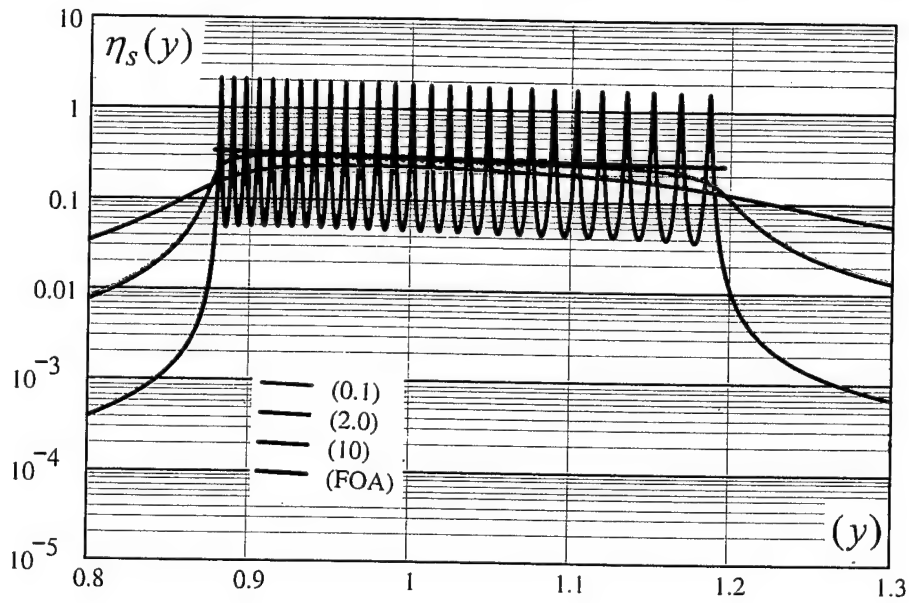


Fig. 7.2. Induced loss factor $\eta_s(y)$, as a function of (y) , for mixed control coupling forms. [$R = 27$ and $(M_s/M) = 0.1$.]

a. $\alpha_c = \bar{m}_c = 0.75$ [$\alpha = 1.0$.], $\bar{g} = 0$. [Very strong coupling.]

b. $\alpha_c = 0.53$ [$\alpha = 0.47$.], $\bar{g} = 0.54$, $\bar{m}_c = 0$. [Strong coupling.]

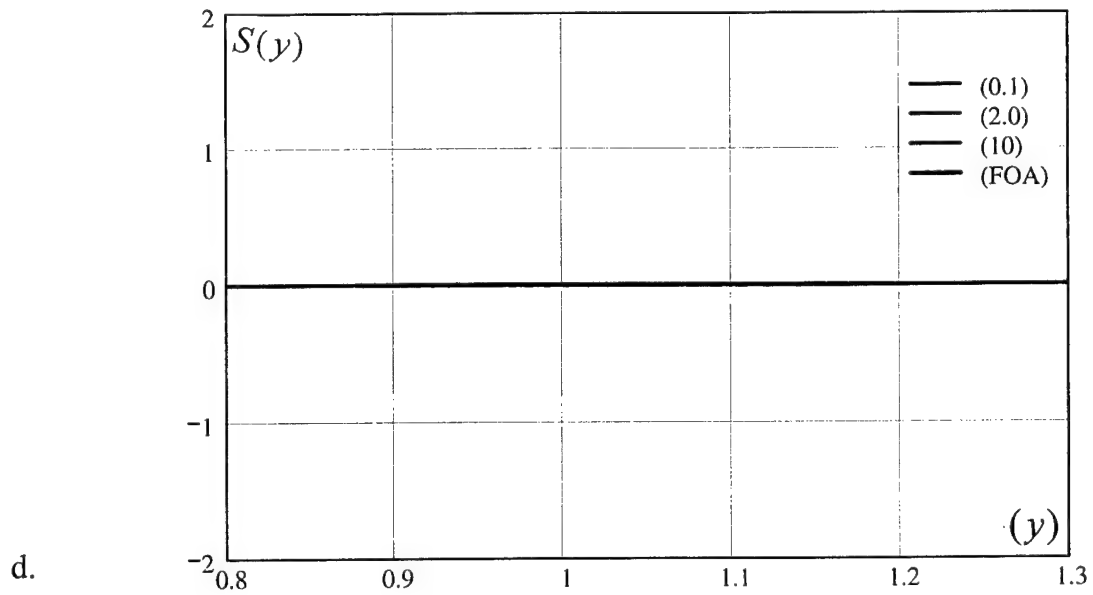
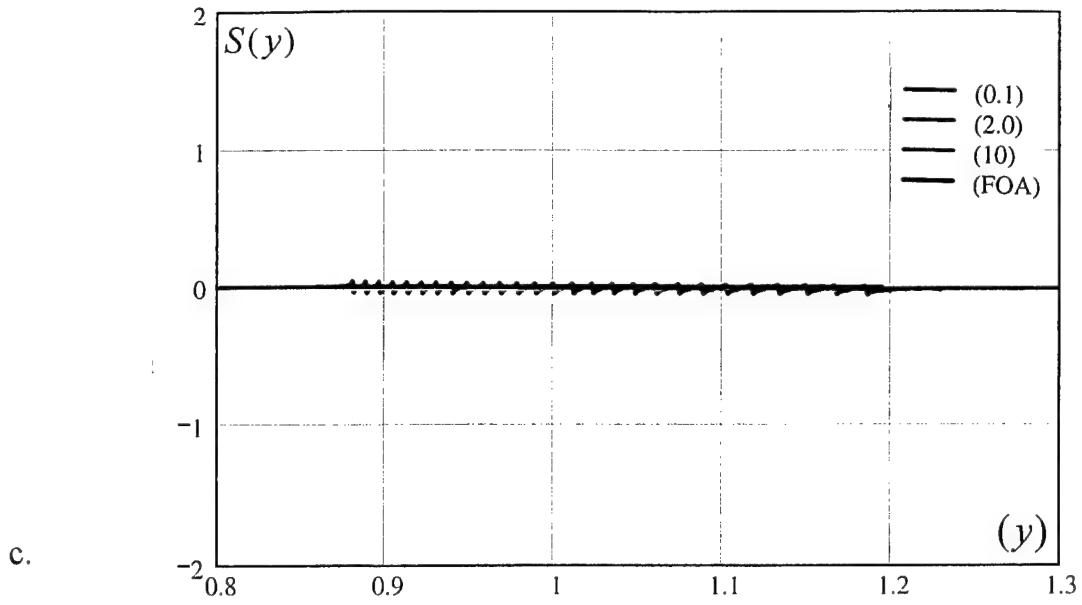
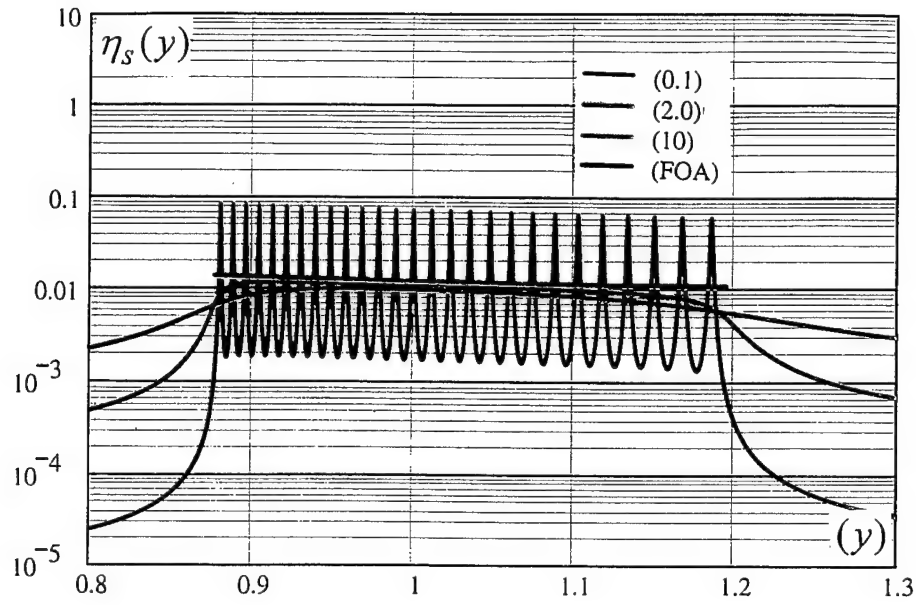


Fig. 7.1. Induced reactive factor $S(y)$, as a function of (y) , for mixed control coupling forms. [$R = 27$ and $(M_s / M) = 0.1$.]

c. $\alpha_c = 0.10$ [$\alpha = 0.90$.], $\bar{g} = 0.11$, $\bar{m}_c = 0$. [Moderate coupling.]

d. $\alpha_c = 0.02$ [$\alpha = 0.98$.], $\bar{g} = 0.022$, $\bar{m}_c = 0$. [Weak coupling.]

c.



d.

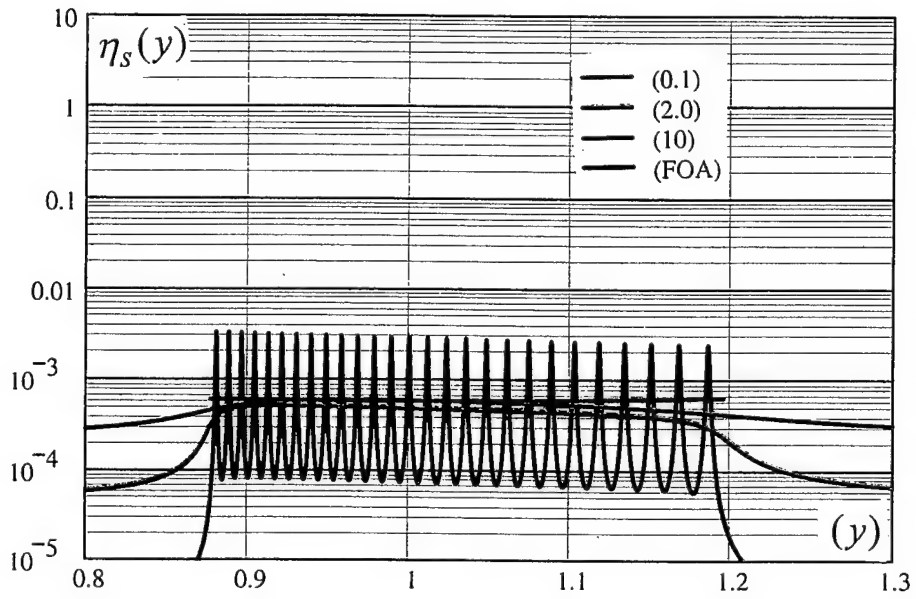


Fig. 7.2. Induced loss factor $\eta_s(y)$, as a function of (y) , for mixed control coupling forms. [$R = 27$ and $(M_s/M) = 0.1$.]

c. $\alpha_c = 0.10$ [$\alpha = 0.90$.], $\bar{g} = 0.11$, $\bar{m}_c = 0$. [Moderate coupling.]

d. $\alpha_c = 0.02$ [$\alpha = 0.98$.], $\bar{g} = 0.022$, $\bar{m}_c = 0$. [Weak coupling.]

Fig. 8 Pseudo-statistical variations:

c. In the modal overlap parameter

 $(b_r); (1.0) \leq b_r \leq (3.5).$

b. In the modal overlap parameter

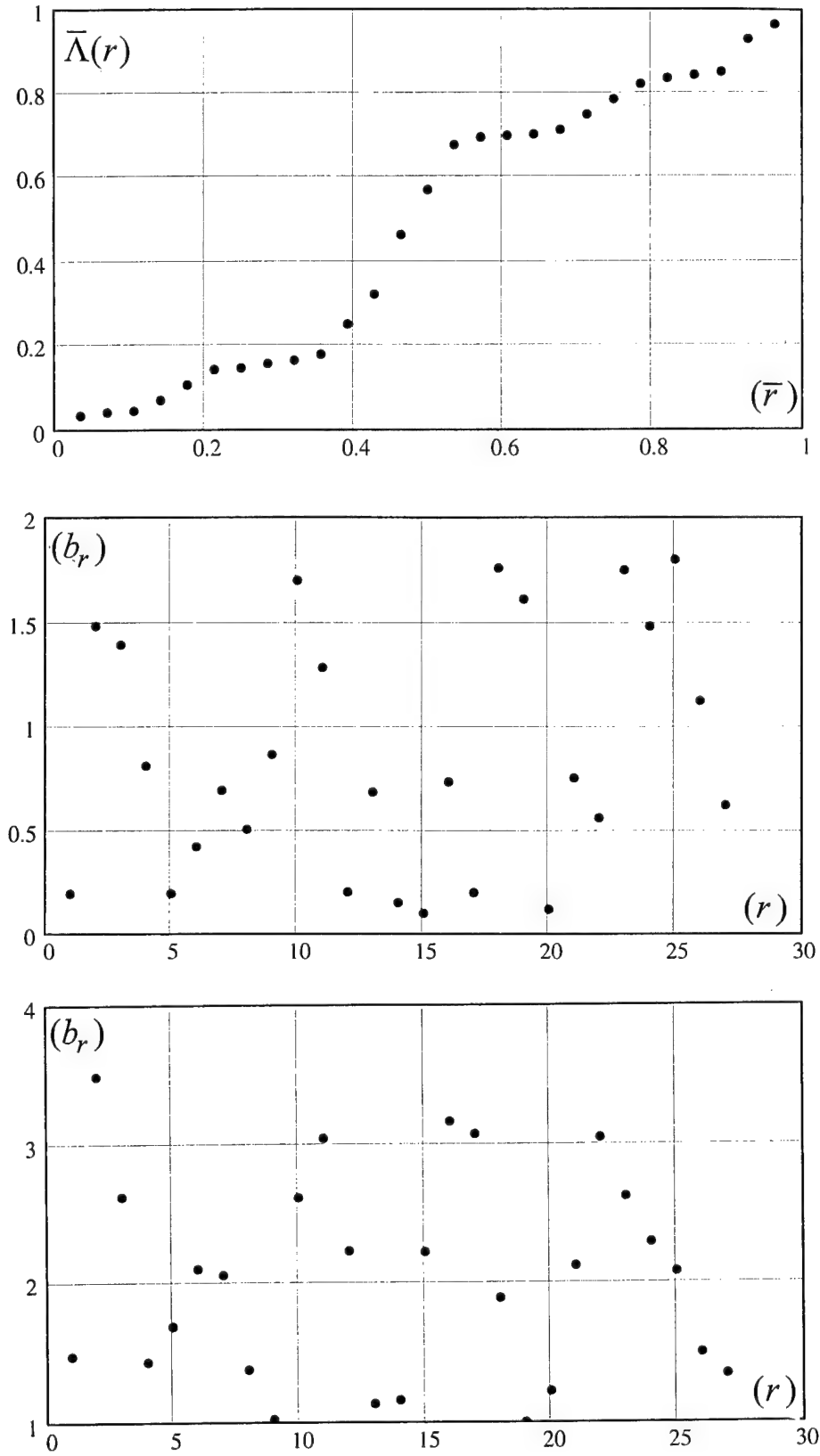
 $(b_r); (0.1) \leq b_r \leq (2.0).$ a. In the normalized index $\bar{\Lambda}(r)$,as a function of the normalized
(integer) index (\bar{r}) .

Fig. 9. Modification of pseudo-statistical variations:

- c. In the loss factors assigned to individual satellite oscillators, with (b_r) as depicted in Fig. 8c. [cf. Figs. 2a.2 and 2b.2.]
- b. In the loss factors assigned to individual satellite oscillators, with (b_r) as depicted in Fig. 8b. [cf. Figs. 2a.2 and 2b.2.]
- a. In the resonance frequency distribution of satellite oscillators, as a function $\bar{\Lambda}(r)$, with $\bar{\Lambda}(r)$ as depicted in Fig. 8a. [cf. Figs. 2a.1 and 2b.1.]

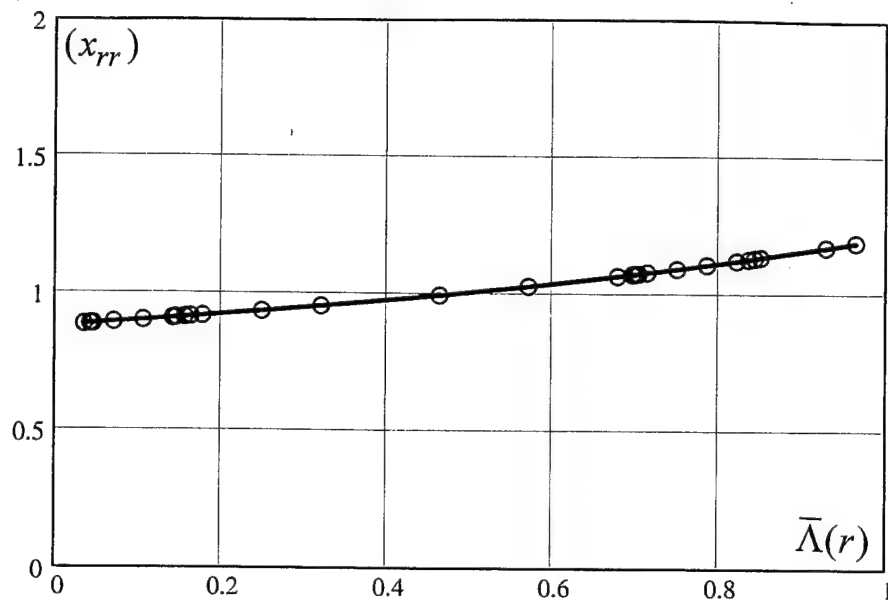
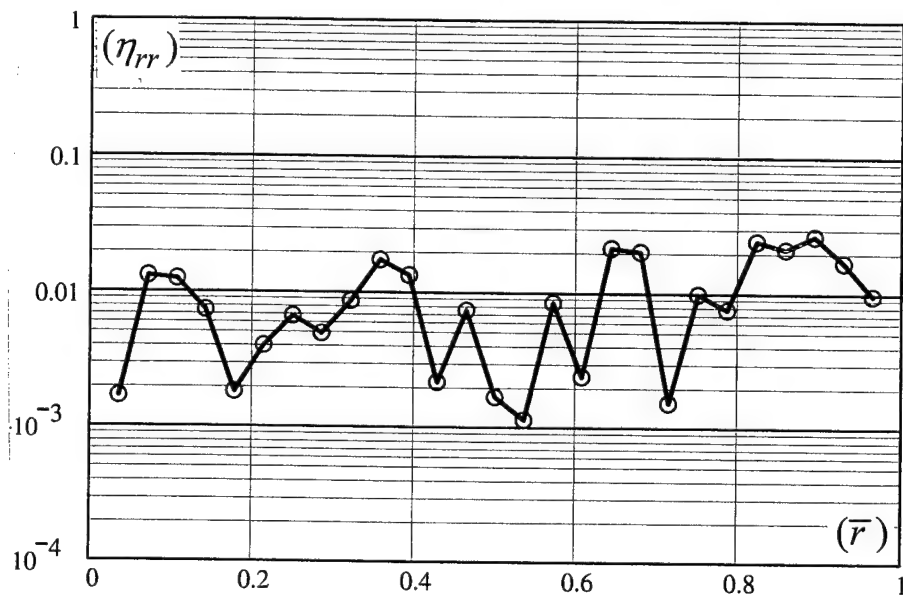
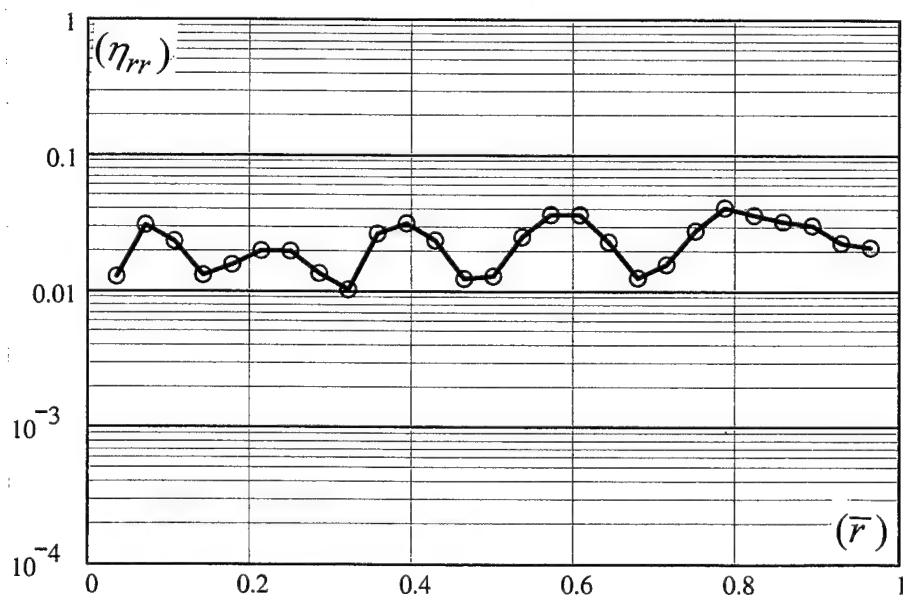


Fig. 10.1. Induced reactive factor $S(y) = [S^o(y)]$, as a function of (y) , for a strong coupling defined by $\alpha_c = 1.0[\alpha = 0.0.]$, $\bar{m}_c = \bar{g} = 0$; implementing a number of pseudo-statistical variations $[R = 27 \text{ and } (M_s / M) = 0.1.]$ First order approximation is superimposed.

a. $\bar{\Lambda}(r) = \bar{r}$ and $b_r = 1$, a base case.

b. $\bar{\Lambda}(r)$ as is given in Fig. 8a and

$b_r = 1$.

c. $\bar{\Lambda}(r) = \bar{r}$ and (b_r) as is given in

Fig. 8b.

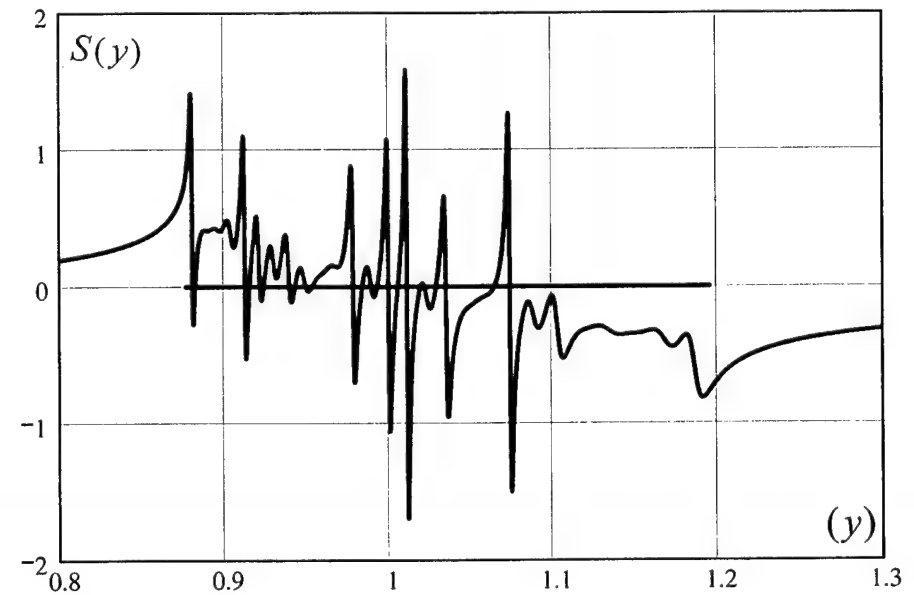
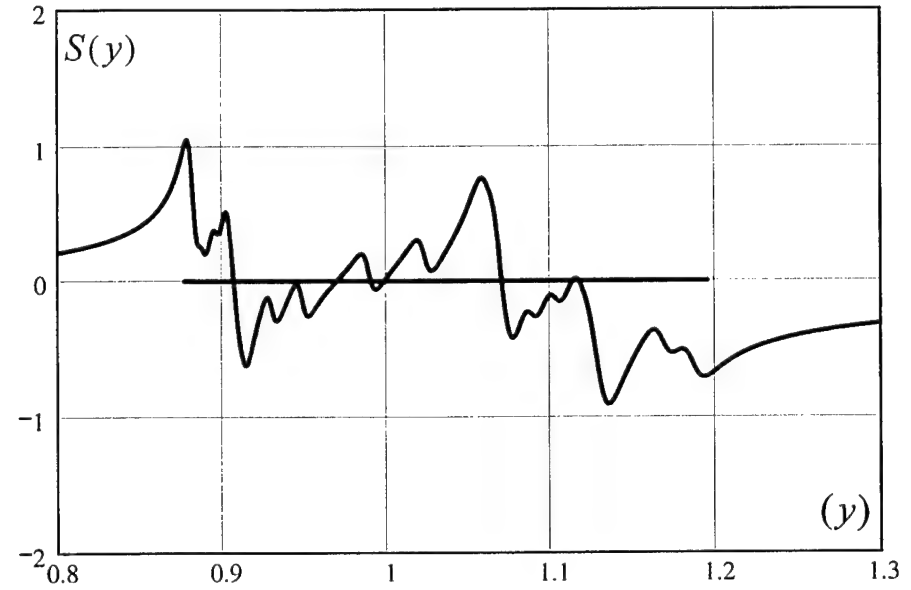
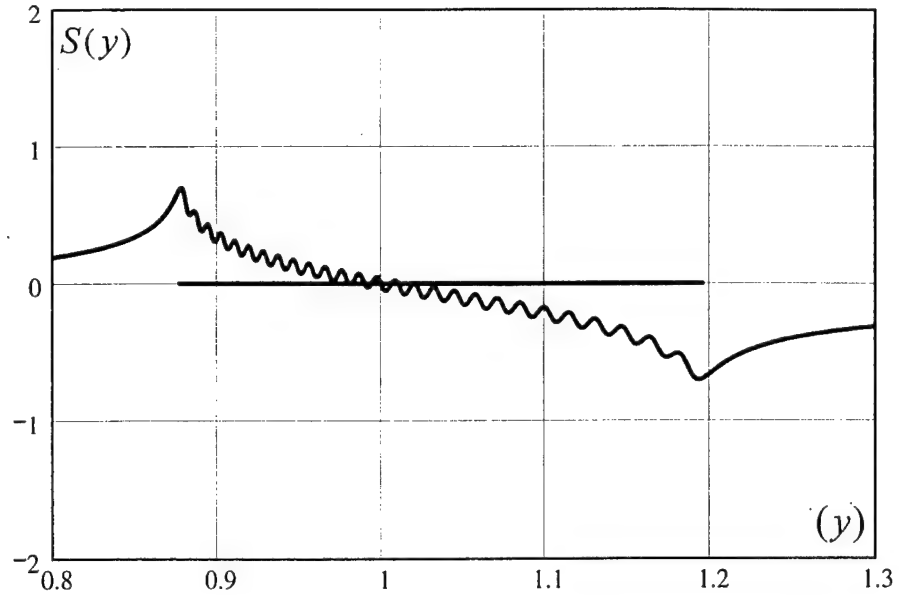


Fig. 10.2. Induced loss factor $\eta_s(y) [= \eta_s^0(y)]$, as functions of (y) , for a strong coupling defined by $\alpha_c = 1.0$ [$\alpha = 0.0$], $\bar{m}_c = \bar{g} = 0$; implementing a number of pseudo-statistical variations [$R = 27$ and $(M_s/M) = 0.1$.] First order approximation is superimposed.

c. $\bar{\Lambda}(r) = \bar{r}$ and (b_r) as is given in
 b. $\bar{\Lambda}(r)$ as is given in Fig. 8a and
 a. $\bar{\Lambda}(r) = \bar{r}$ and $b_r = 1$, a base case
 $b_r = 1$.

Fig. 8b.

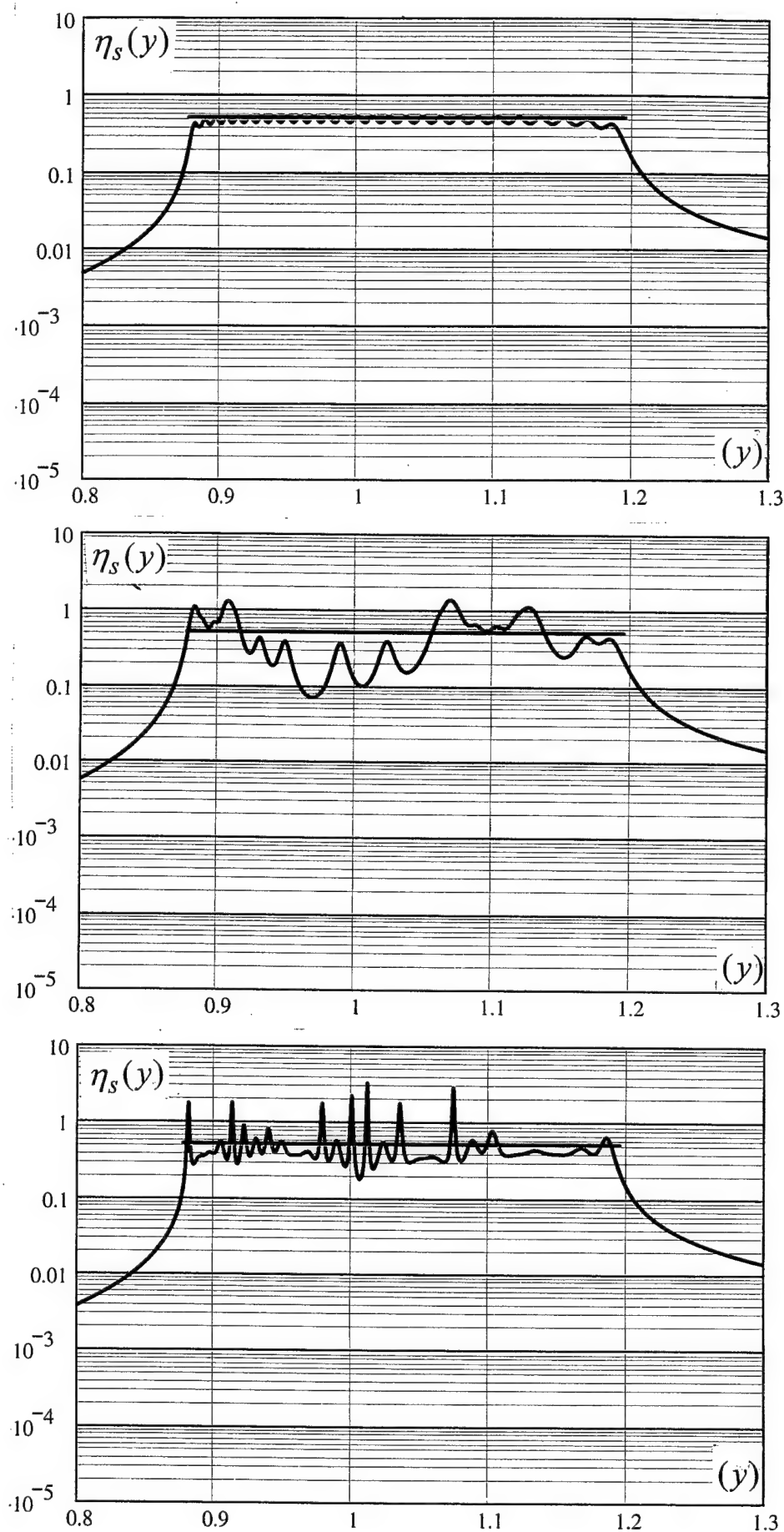


Fig. 10.1. Induced reactive factor $S(y) = [S^o(y)]$, for a strong coupling defined by $\alpha_c = 1.0[\alpha = 0.0.]$, $\bar{m}_c = \bar{g} = 0$; implementing a number of pseudo-statistical variations [$R = 27$ and $(M_s / M) = 0.1.$] First order approximation is superimposed.

f. $\bar{\Lambda}(r)$ as is given in Fig. 8a and (b_r) as is given in Fig. 8c.

e. $\bar{\Lambda}(r)$ as is given in Fig. 8a and (b_r) as is given in Fig. 8b.

d. $\bar{\Lambda}(r) = \bar{r}$ and (b_r) as is given in Fig. 8c.

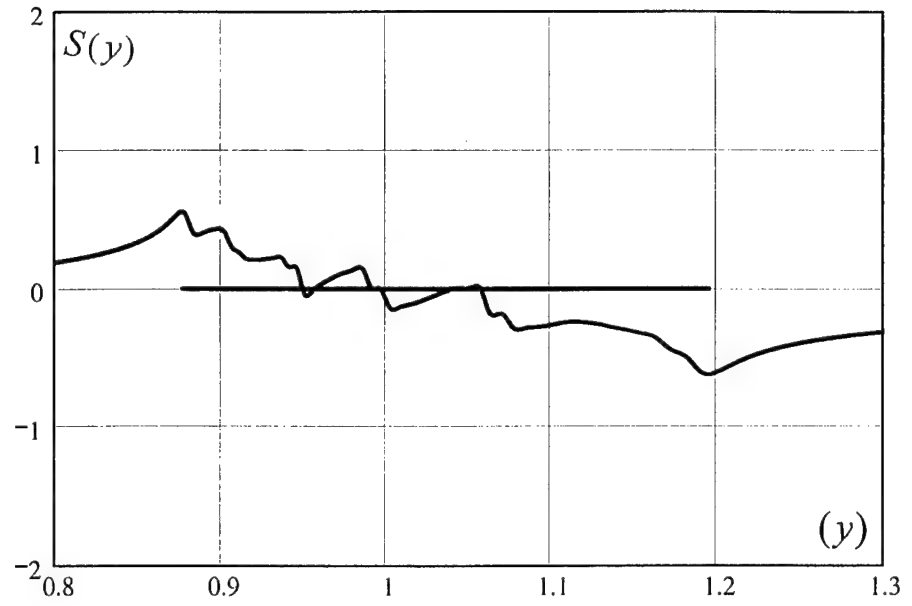
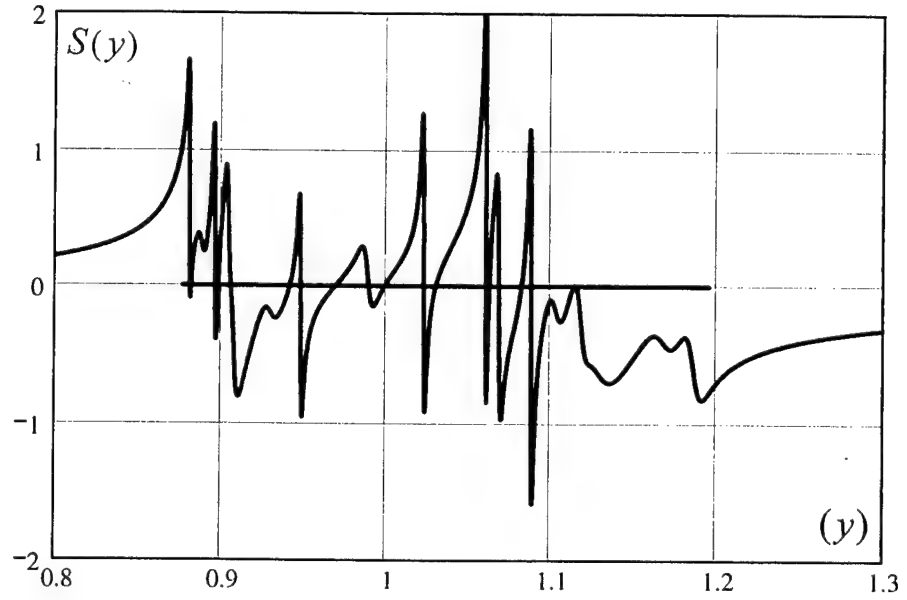
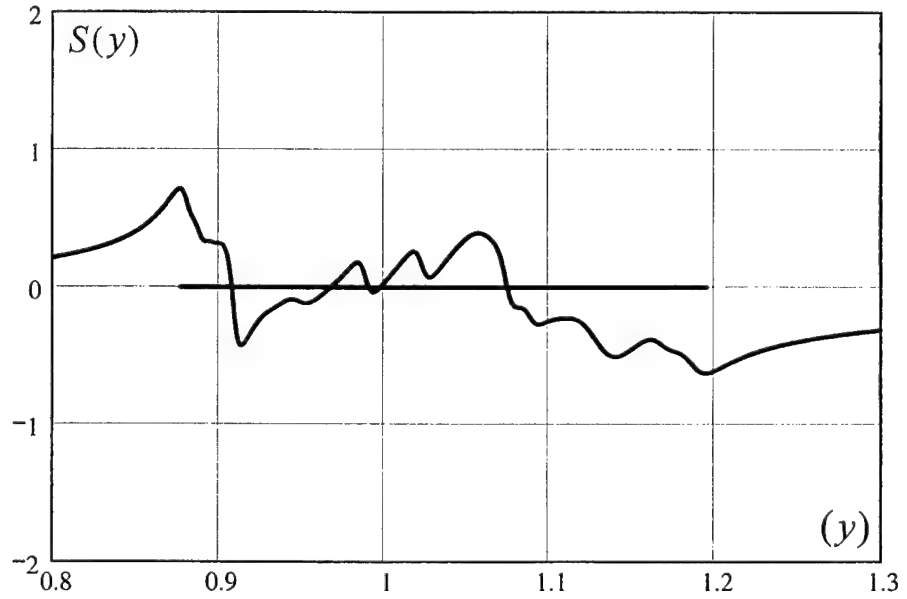


Fig. 10.2. Induced loss factor $\eta_s(y)[= \eta_s^o(y)]$, as functions of (y) , for a strong coupling defined by $\alpha_c = 1.0[\alpha = 0.0.]$, $\bar{m}_c = \bar{g} = 0$; implementing a number of pseudo-statistical variations [$R = 27$ and $(M_s/M) = 0.1.$] First order approximation is superimposed.

f. $\bar{\Lambda}(r)$ as is given in Fig. 8a and

e. $\bar{\Lambda}(r)$ as is given in Fig. 8a and

d. $\bar{\Lambda}(r) = \bar{r}$ and (b_r) as is given in

(b_r) as is given in Fig. 8c.

(b_r) as is given in Fig. 8b.

Fig. 8c.

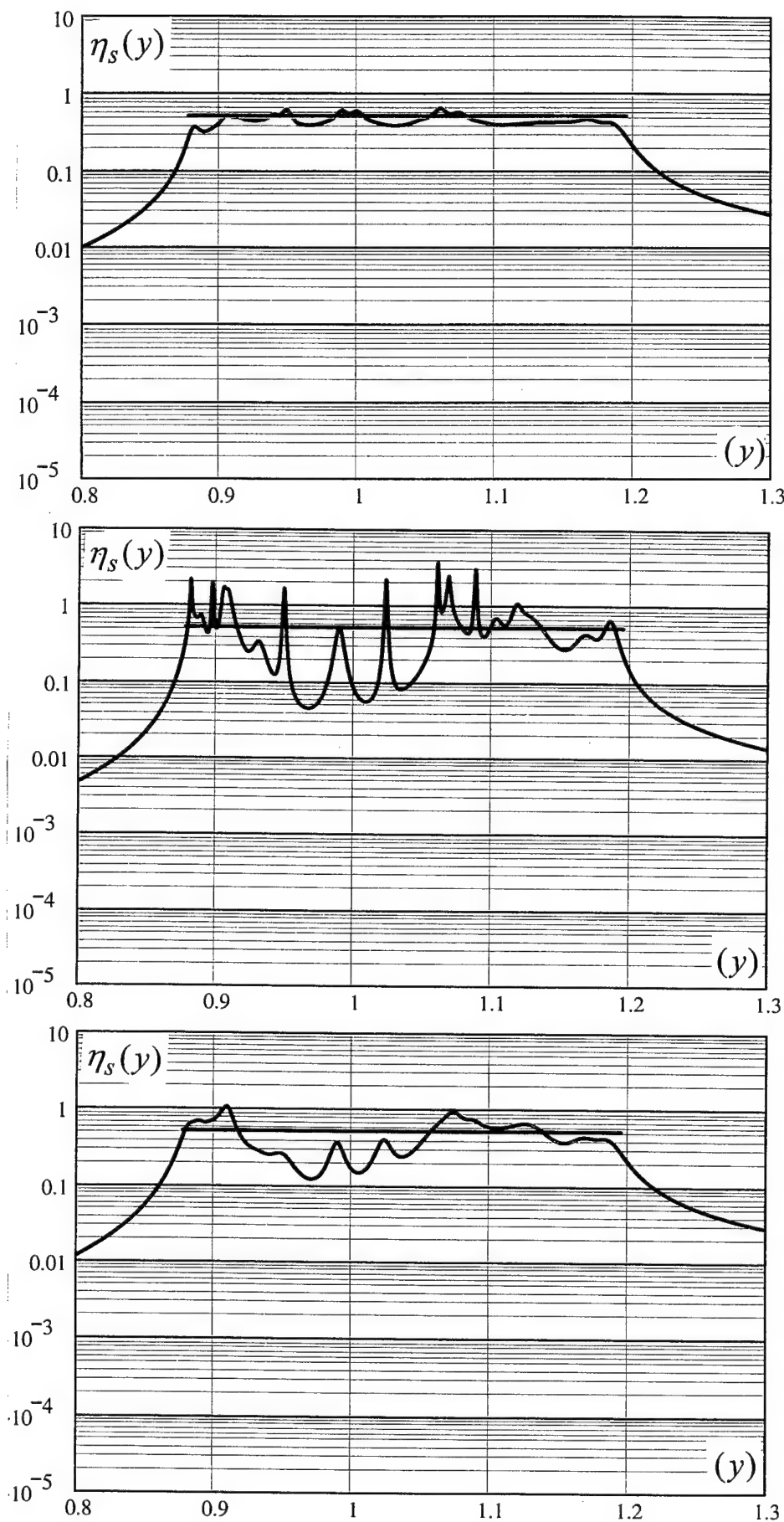
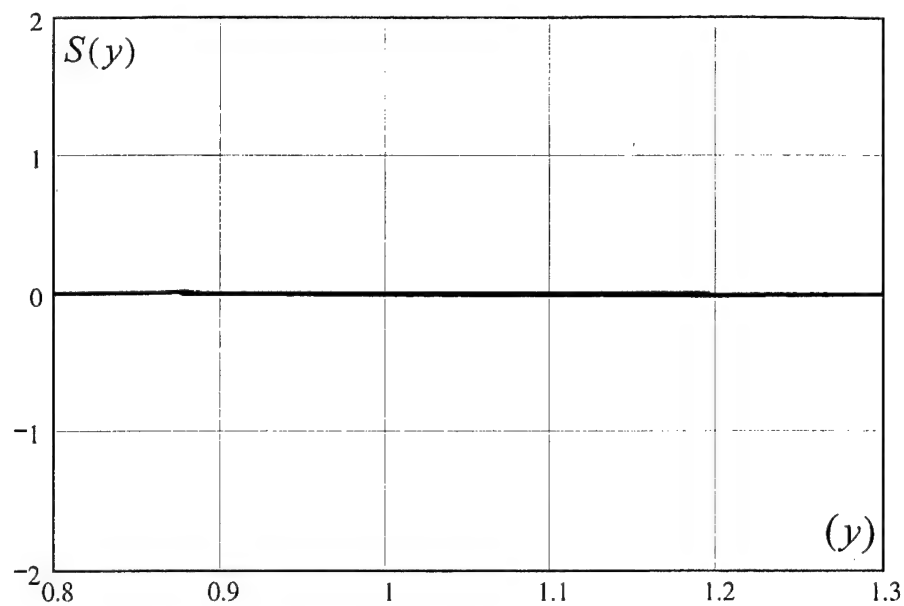


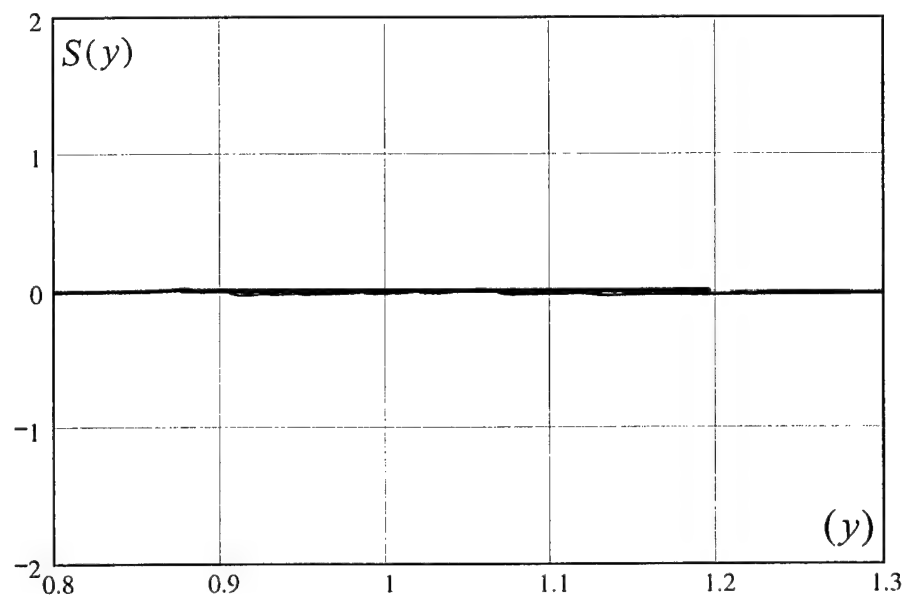
Fig. 11.1. As in Fig. 10.1, except that the coupling is a mix of stiffness and gyroscopic control: $\alpha_c = 0.1[\alpha = 0.9.]$,

$\bar{g} = 0.11, \bar{m}_c = 0$. The coupling strength here is moderate.

a. As in 10a.



b. As in 10b.



c. As in 10c.

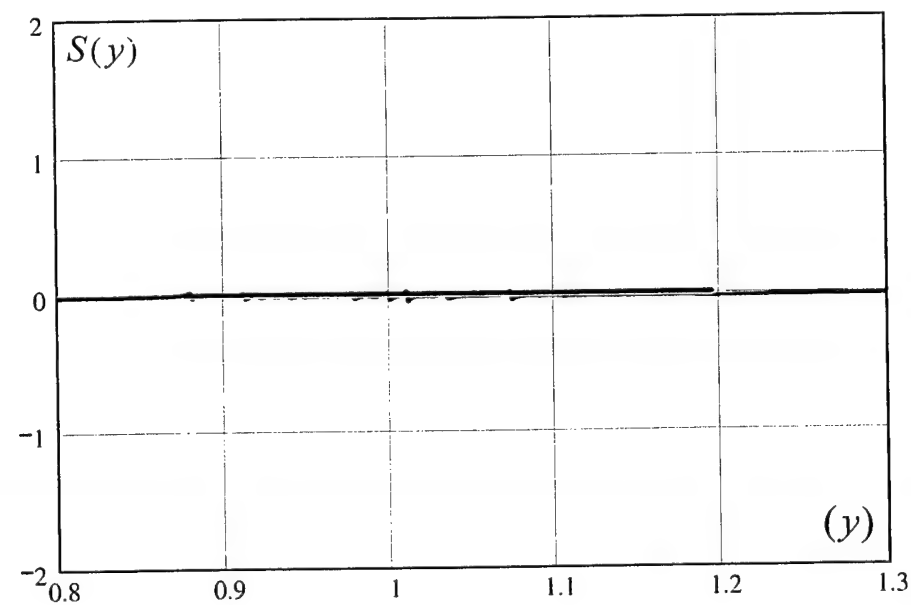
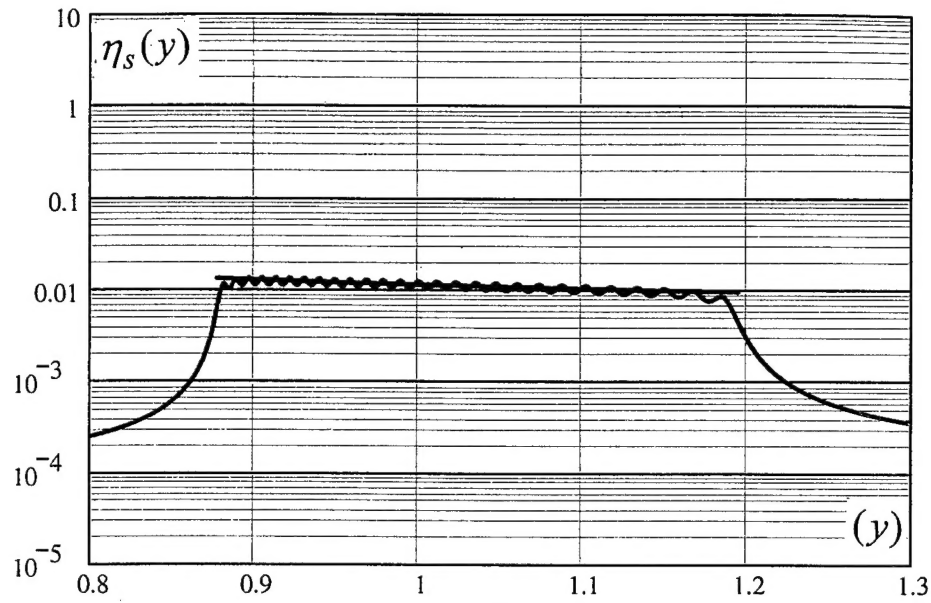
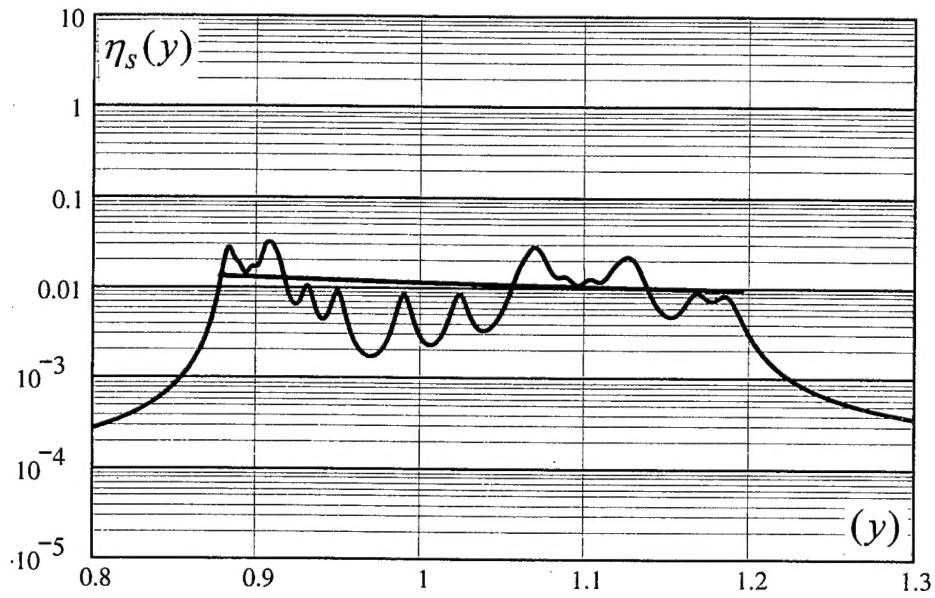


Fig. 11.2. As in Fig. 10.2, except that the coupling is a mix of stiffness and gyroscopic control: $\alpha_c = 0.1[\alpha=0.9.]$, $\bar{g} = 0.11$, $\bar{m}_c = 0$. The coupling strength here is moderate.

a. As in 10a.



b. As in 10b.



c. As in 10c.

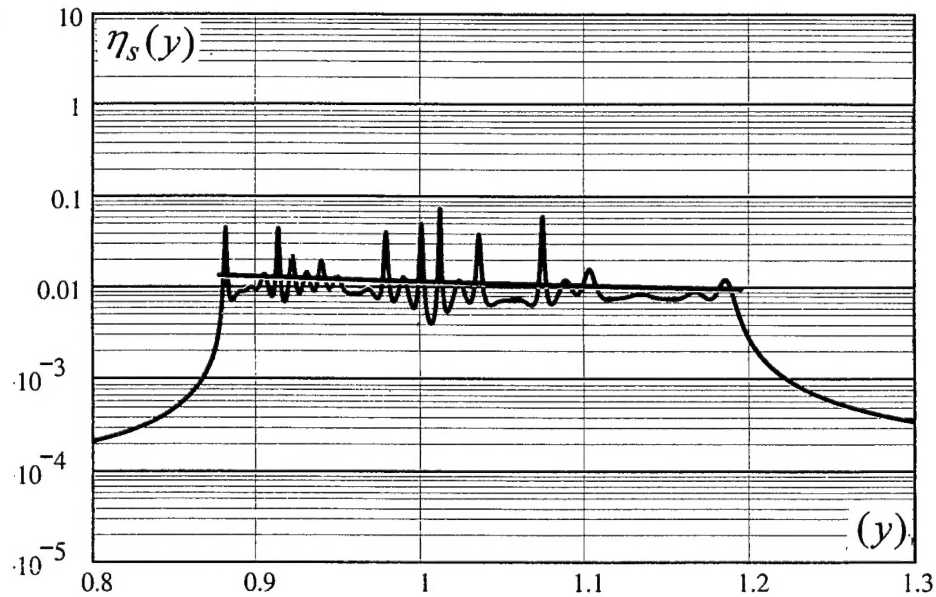


Fig. 11.1. As in Fig. 10.1, except that the coupling is a mix of stiffness and gyroscopic control: $\alpha_c = 0.1[\alpha = 0.9.]$,

$\bar{g} = 0.11$, $\bar{m}_c = 0$. The coupling strength here is moderate.

f. As in 10f.

e. As in 10e.

d. As in 10d.

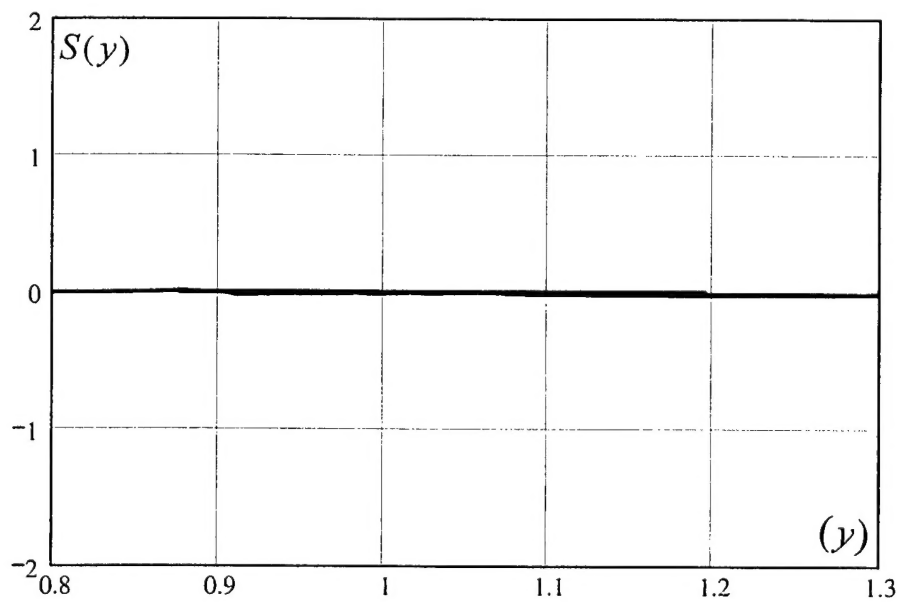
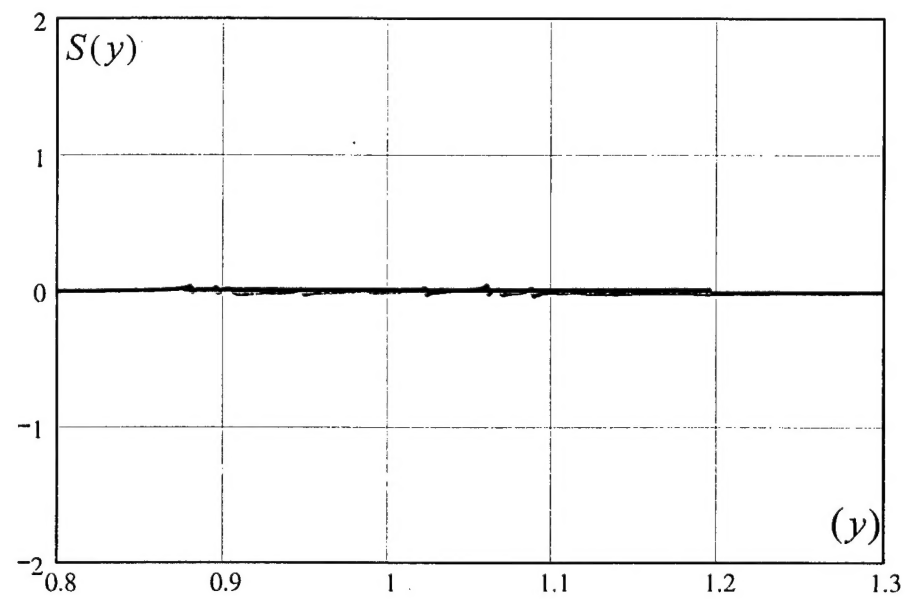
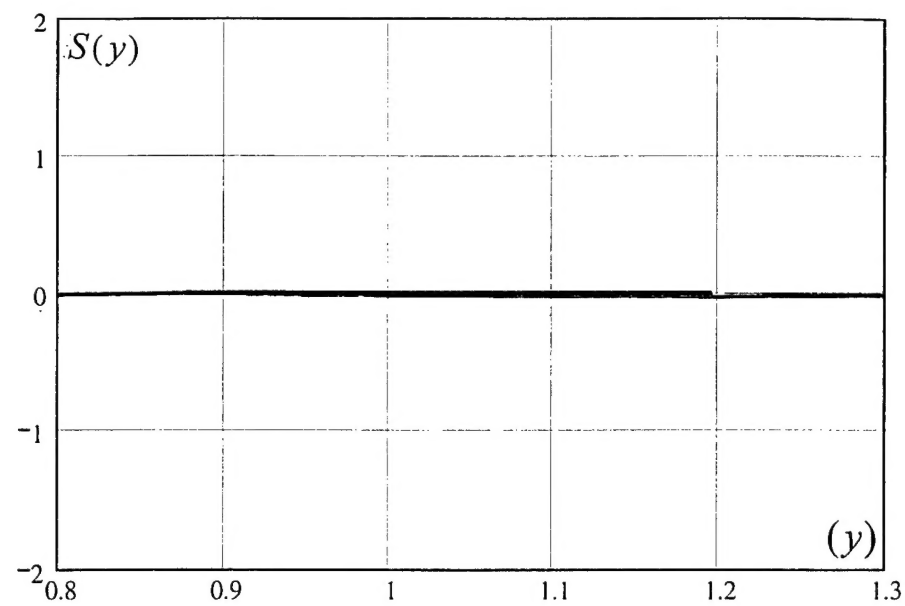


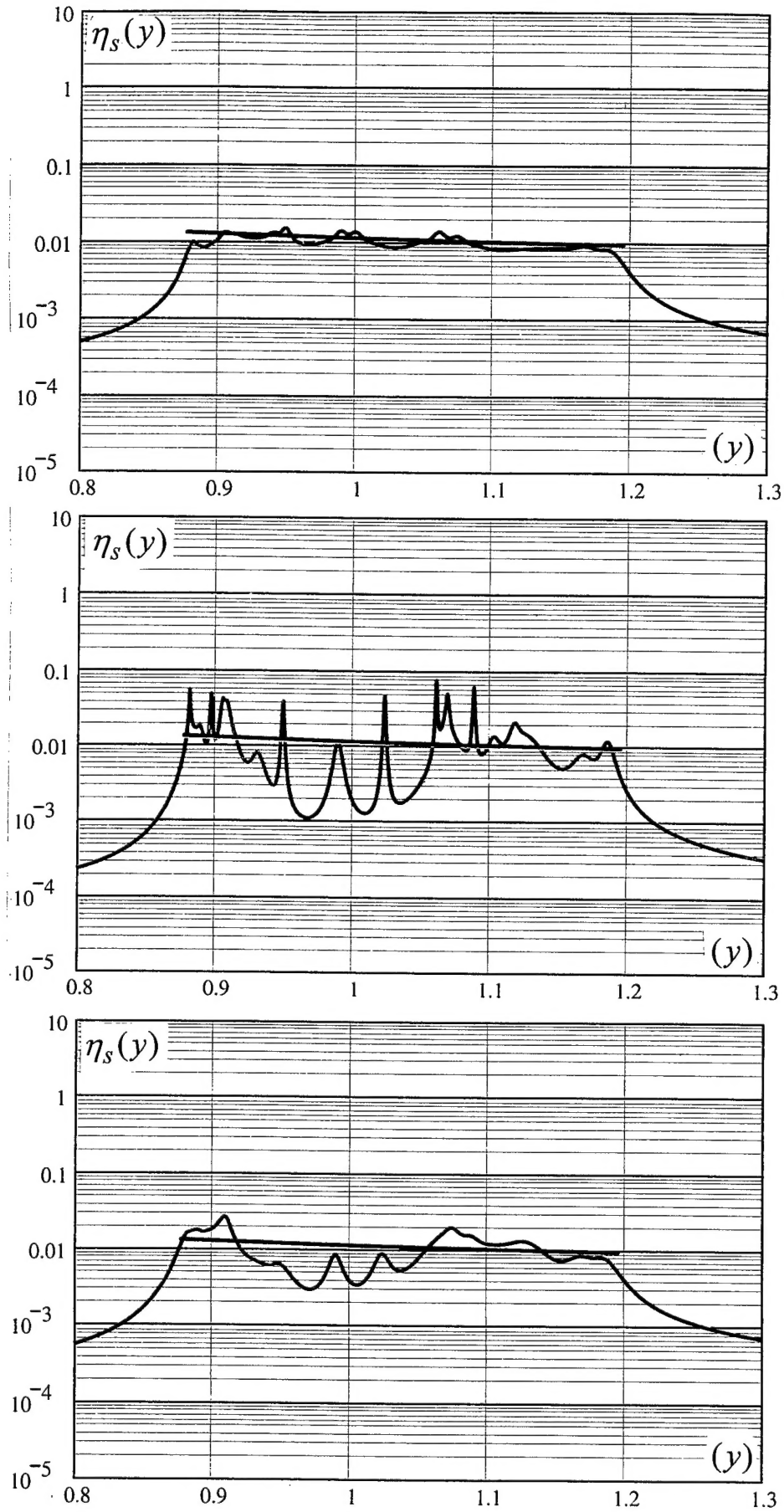
Fig. 11.2. As in Fig. 10.2, except that the coupling is a mix of stiffness and gyroscopic control: $\alpha_c = 0.1[\alpha=0.9.]$,

$\bar{g} = 0.11$, $\bar{m}_c = 0$. The coupling strength here is moderate.

f. As in 10f.

e. As in 10e.

d. As in 10d.



INITIAL DISTRIBUTION

Copies		Copies	Code	Name
3	NAVSEA 05T2	1	7020	Strasberg
1	Taddeo			
1	Biancardi	1	7030	Maidanik
1	Shaw			
		1	7203	Dlubac
2	ONR/ONT			
1	334 Couchman	1	7200	Shang
1	Library			
		1	7207	Becker
2	DTIC			
		1	7220	Niemiec
2	Johns Hopkins University			
1	Green	2	7250	Maga
1	Dickey			Diperna
3	ARL/Penn State University	3	3421	(TIC-Carderock)
1	Koopman			
1	Hwang			
1	Hambric			
1	R. H. Lyon, Corp.			
1	Lyon			
1	Cambridge Acoustical Associates			
1	Garrelick			
1	MIT			
1	Dyer			
1	Florida Atlantic University			
1	Cuschieri			
2	Boston University			
1	Pierce			
1	Barbone			

CENTER DISTRIBUTION

1	0112	Barkyoumb
2	7000	Dir. Head
1	7014	Fisher